

**MODELING NETWORK-WIDE IMPACTS OF TRAFFIC
BOTTLENECK MITIGATION STRATEGIES UNDER
STOCHASTIC CAPACITY CONDITIONS**

by

Mingxin Li

A dissertation submitted to the faculty of
The University of Utah
in partial fulfillment of the requirements for the degree of

Doctor of Philosophy

Department of Civil and Environmental Engineering

The University of Utah

May 2011

Copyright © Mingxin Li 2011

All Rights Reserved

The University of Utah Graduate School

STATEMENT OF DISSERTATION APPROVAL

The dissertation of Mingxin Li
has been approved by the following supervisory committee members:

<u>Xuesong Zhou</u>	, Chair	<u>10/28/2010</u> Date Approved
<u>Peter Martin</u>	, Member	<u>10/28/2010</u> Date Approved
<u>Richard J. Porter</u>	, Member	<u>10/28/2010</u> Date Approved
<u>Harvey J. Miller</u>	, Member	<u>10/28/2010</u> Date Approved
<u>Pedro Romero</u>	, Member	<u>10/28/2010</u> Date Approved

and by Paul Tikalsky, Chair of
the Department of Civil and Environmental Engineering

and by Charles A. Wight, Dean of The Graduate School.

ABSTRACT

Traffic congestion occurs because the available capacity cannot serve the desired demand on a portion of the roadway at a particular time. Major sources of congestion include recurring bottlenecks, incidents, work zones, inclement weather, poor signal timing, and day-to-day fluctuations in normal traffic demand.

This dissertation addresses a series of critical and challenging issues in evaluating the benefits of Advanced Traveler Information Strategies under different uncertainty sources. In particular, three major modeling approaches are integrated in this dissertation, namely: mathematical programming, dynamic simulation and analytical approximation. The proposed models aim to 1) represent static-state network user equilibrium conditions, knowledge quality and accessibility of traveler information systems under both stochastic capacity and stochastic demand distributions; 2) characterize day-to-day learning behavior with different information groups under stochastic capacity and 3) quantify travel time variability from stochastic capacity distribution functions on critical bottlenecks.

First, a nonlinear optimization-based conceptual framework is proposed for incorporating stochastic capacity, stochastic demand, travel time performance functions and varying degrees of traveler knowledge in an advanced traveler information provision environment. This method categorizes commuters into two classes: (1) those with access

to perfect traffic information every day, and (2) those with knowledge of the expected traffic conditions across different days. Using a gap function framework, two mathematical programming models are further formulated to describe the route choice behavior of the perfect information and expected travel time user classes under stochastic day-dependent travel time.

This dissertation also presents adaptive day-to-day traveler learning and route choice behavioral models under the travel time variability. To account for different levels of information availability and cognitive limitations of individual travelers, a set of “bounded rationality” rules are adapted to describe route choice rules for a traffic system with inherent process noise and different information provision strategies. In addition, this dissertation investigates a fundamental problem of quantifying travel time variability from its root sources: stochastic capacity and demand variations that follow commonly used log-normal distributions. The proposed models provide theoretically rigorous and practically usefully tools to understand the causes of travel time unreliability and evaluate the system-wide benefit of reducing demand and capacity variability.

To my wife Li Su and my daughter Vivian

TABLE OF CONTENTS

ABSTRACT.....	iii
LIST OF FIGURES	ix
LIST OF TABLES.....	xi
ACKNOWLEDGEMENTS.....	xii
CHAPTER	
1. INTRODUCTION	1
1.1 Background	1
1.2 Sources of Travel Time Uncertainty Distributions	3
1.3 Challenges and Motivations.....	5
1.3.1 Modeling challenges in static-state programming approach.....	5
1.3.2 Modeling challenges in dynamic traffic assignment approach	7
1.3.3 Modeling challenges in analytical approximation approach	8
1.4 Research Objectives	9
1.5 Overview of Approach and Organization of the Dissertation.....	12
2. LITERATURE REVIEW	14
2.1 Overview	14
2.2 Role of Traveler Information Systems and Travel Time Uncertainty Sources.....	14
2.3 Modeling Stochastic Capacity.....	17
2.3.1 Headway-based stochastic capacity models.....	17
2.3.2 Stochastic queue discharge rate model.....	19
2.3.3 Probability-based stochastic capacity models	20
2.4 Optimization Model for Static Network Equilibrium Analysis	21
2.5 Analytical Approach for Single Bottleneck Analysis	22
2.6 Simulation-based Approach for Network-wide Analysis	24
3. PLANNING-LEVEL METHODOLOGY FOR EVALUATING ATIS STRATEGIES UNDER STOCHASTIC CAPACITY CONDITIONS.....	28
3.1 Introduction	28
3.2 Conceptual Framework	29
3.2.1. Perfect information (PI) based user equilibrium	31
3.2.2 Expected travel time (ETT) knowledge-based user equilibrium.....	34
3.2.3. Quantification of the value of information.....	38
3.3 General Mathematical Problem Formulation	40

3.3.1 Formulation	41
3.3.2 Spreadsheet tool for calculating multiday user equilibrium.....	44
3.4 Solution Algorithm.....	46
3.5 Experimental Results.....	50
3.5.1 Measure of effectiveness (MOE)	53
3.5.2 Sensitivity analysis.....	54
3.5.3 Experiments on medium-scale networks.....	64
3.6 Summary	70
4. MULTIDAY STATIC TRAFFIC EQUILIBRIUM ANALYSIS UNDER STOCHASTIC DEMAND AND CAPACITY CONDITIONS	72
4.1 Introduction	72
4.2 Problem Statement and Illustrative Example.....	74
4.2.1 Traveler information (TI) users.....	78
4.2.2 Expected travel time (ETT) knowledge users	79
4.3 General Mathematical Problem Formulation.....	80
4.4 Solution Algorithm.....	86
4.5 Numerical Experiments.....	89
4.6 Summary	92
5. DAY-TO-DAY TRAVELER LEARNING FRAMEWORK.....	95
5.1 Introduction	95
5.2 Overall Modeling Framework.....	96
5.3 Day-To-Day Traveler Learning and Route Choice Model	98
5.3.1 Conceptual framework	99
5.3.2 Route choice utility function and simplified route switching rule.....	102
5.4 Conceptual Simulation Framework and System Implementation.....	106
5.5 Case Study.....	110
5.6 Summary	113
6. ANALYTICAL MODELS ON DERIVING TRAVEL TIME VARIABILITY DISTRIBUTIONS FROM STOCHASTIC CAPACITY DISTRIBUTIONS	115
6.1 Introduction	115
6.2 Review of Statistical Properties of Log-Normal Distribution.....	118
6.3 Deriving Travel Time Variability Distribution Based on BPR Function.....	120
6.4 Deriving Travel Time Variability Distribution Based on Point Queue Model.....	122
6.5 Deriving Time-Dependent Delay Variability Distribution	130
6.6 Calibrating Probability Distributions	133
6.7 Summary	139
7. CONCLUSIONS AND FUTURE RESEARCH NEEDS.....	141
7.1 Overall Conclusions	141
7.2 Research Contributions	144
7.2.1 Theoretical Contributions.....	144
7.2.2 Practical Contributions.....	145
7.3 Future Research Needs.....	146

APPENDIX: LIST OF TERMS.....	148
REFERENCES	150

LIST OF FIGURES

<u>Figure</u>	<u>Page</u>
1.1- Illustrates the percentage of each congestion source in the nation.....	2
1.2- Prebreakdown Headway Distribution for I-880.	5
1.3- Four main areas of interest.	13
2.1- Distribution of lane capacity converted from headway.....	20
3.1- Simple network used as an illustrative example of the framework.....	30
3.2- Equilibrium solutions with 100% PI users.	33
3.3- Solutions with 100% ETT information users.	37
3.4- Solutions on a reduced-capacity day.	39
3.5- Day-dependent travel times on different routes.	40
3.6- Spreadsheet-based calculation model.....	45
3.7- Solution algorithm for static traffic assignment with both PI and ETT users.	47
3.8- Histogram of 100 stochastic capacity samples.	52
3.9- Effectiveness of information provision at varying demand levels.	55
3.10- Effectiveness of information provision with different market penetration rate.	56
3.11- Effectiveness of information provision with varying toll.....	58
3.12- Effectiveness of information provision for different routes with varying toll.	61
3.13- Value of information as a function of FFFT difference and demand level.....	63
3.14- Chicago sketch network (left) and Anaheim, California network (right).....	67

3.15- Convergence patterns on Chicago sketch network.....	68
4.1- Simple network used as an illustrative example.....	77
4.2- Time-dependent capacity, demand and travel time patterns under different vehicle information market penetration rates.....	77
4.3- Travel flow split solution on four different types of days.....	85
4.4- Histogram of 100 stochastic demand flow rate samples.....	91
4.5- Effectiveness of information provision under stochastic capacity with different market penetration rate.....	93
5.1- Capacity-Enhancing Strategy Evaluation Framework.....	97
5.2- Comprehensive conceptual simulation framework.....	107
5.3- Portland network study area.....	111
5.4- Network-wide simulation results.....	112
6.1- Local link marginal delay evaluation method for vehicle entering at time t.....	124
6.2- Local marginal delay evaluation method for one unit of departure flow change at time t.....	125
6.3- Total delay change for one unit of discharge rate change for the entire congestion duration.....	126
6.4- Waiting time variability in different queue duration cases.....	129
6.5- Time-dependent queuing evolution diagram.....	131
6.6- Log-normal probability density function for queue discharge rate.....	135
6.7- Shifted Log-normal probability density function for queue discharge rate.....	135
6.8- Log-normal probability density function for demand flow rate distributions.....	136
6.9- Log-normal probability density function for travel time index distribution.....	137
6.10- Complete PDF for predicted travel time variations.....	138

LIST OF TABLES

<u>Table</u>	<u>Page</u>
3.1- Day-dependent path demand, capacity and travel time values.....	31
3.2- Test network characteristics and computational performance.	67
3.3- Value of traveler information under different peak-hour capacity approximation schemes.....	70
4.1- Sample solution for 5% TI users and 95% ETT users.....	84
4.2- Representative traveler information provision and traffic management strategies. . .	90
6.1- Summary of calibration results.....	136

ACKNOWLEDGEMENTS

I gratefully acknowledge the support of a great number of people who offered support, advice, inspiration and friendship throughout my time at the University of Utah.

First of all, I would like to express my sincerest gratitude to my advisor, Dr. Xuesong Zhou for his support and guidance throughout my Ph.D. study. I could not have completed my graduate work without his kind guidance. My thanks also goes to Dr. Harvey J. Miller for his willingness to serve as a member of my committee and his invaluable help and insightful comments on many parts of my dissertation. I am also grateful to Dr. Richard J. Porter and Dr. Pedro Romero for their constructive comments. I must include a special word of thanks to Dr. Martin for his advice and care. He has encouraged me to clarify the scope of this dissertation, which proved to be a great piece of advice. Thanks are also extended to Dr. Nagui M. Roupail at the North Carolina State University. His professional insights and constructive comments on the research methodology have significantly improved the quality of this dissertation.

This research was conducted under the sponsorship of the Strategic Highway Research Program (SHRP2) as part of C05: Understanding the Contribution of Operations, Technology, and Design to Meeting Highway Capacity Needs. I would like to thank Dr. Billy M. Williams, Anxi Jia, Wayne Kittelson and Brandon Nevers and other team members for their valuable contributions and insight throughout the development of this research project.

In closing, I am deeply grateful for love and support by my wife, Li Su, who sacrificed a lot in my pursuit of this Ph.D. Ultimately, I must acknowledge and thank my mom, dad for their love and endless support. There are just not enough words to express my gratitude to my family.

CHAPTER 1

INTRODUCTION

1.1 Background

Traffic congestion problems lead to a wide range of adverse consequences such as traffic delays, travel time unpredictability, and increased noise pollution as well as deterioration of air quality. Broadly speaking, traffic congestion occurs because the available capacity cannot serve the desired demand on a portion of roadway at a particular time. As shown in Figure 1.1, Major sources of congestion include physical bottlenecks, incidents, work zones, bad weather, poor signal timing, special events and day-to-day fluctuations in normal traffic (Cambridge Systematics, 2005).

Considerable research efforts have been devoted to understanding and quantifying the effectiveness of different traffic mitigation strategies in addressing various sources of delay. For instance, recurring congestion due to physical bottlenecks can be mitigated through road capacity enhancement. Real-time traffic information dissemination can reduce negative impacts of disruptions of nonrecurring congestion due to traffic incidents and special events. The success of advanced traveler information systems depends on careful planning and an integrated system-level perspective, which calls for advanced transportation analysis tools to estimate how effective information provision and tolling

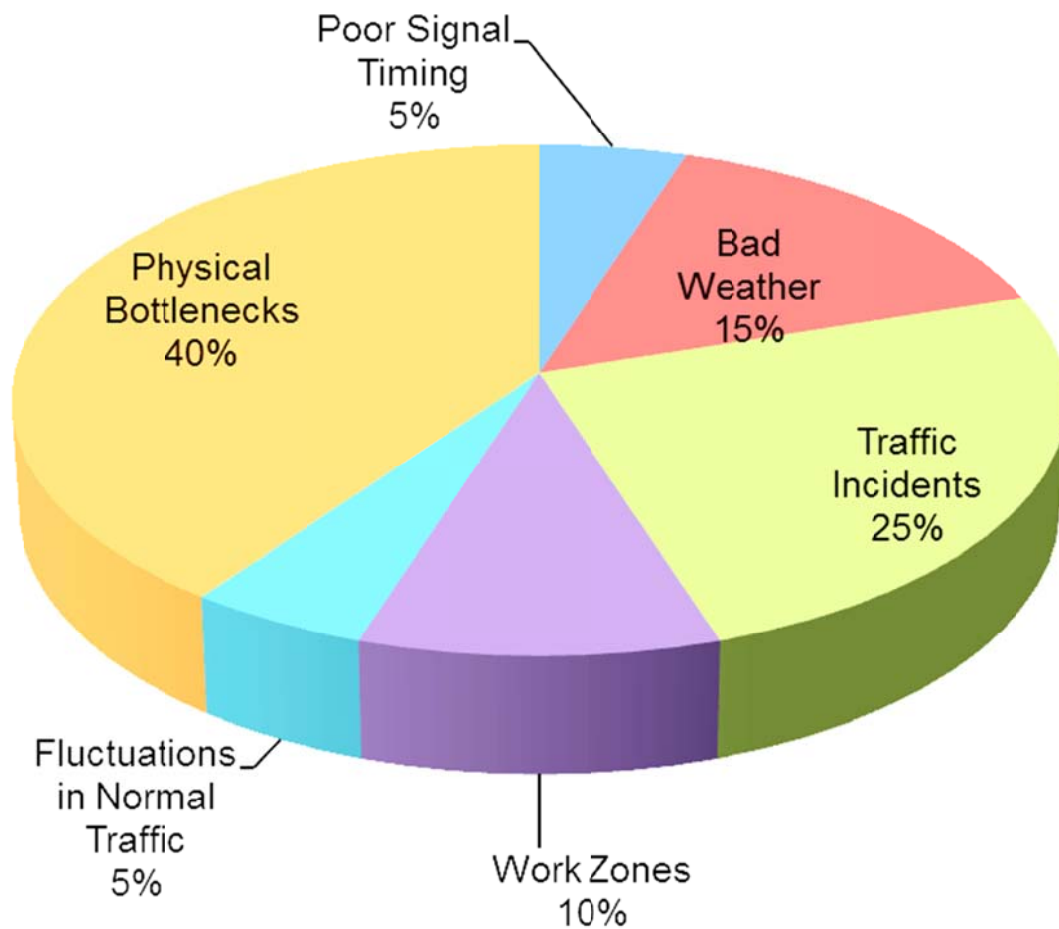


Figure 1.1- Illustrates the percentage of each congestion source in the nation. Adapted from data in Cambridge Systematics (2005), *Traffic Congestion and Reliability: Trends and Advanced Strategies for Congestion Mitigation*, Federal Highway Administration. http://www.ops.fhwa.dot.gov/congestion_report/index.htm (Accessed on March 12, 2010)

strategies can encourage route/departure time/mode switching to more effectively utilize network-wide capacity. This requires adopting and integrating various models that have evolved over the past decade, such as stochastic capacity analysis and dynamic traveler behavior modeling, within the classical user equilibrium analysis framework.

Traffic congestion mitigation strategies may include, but are not limited to, road capacity enhancement, and technological solutions, such as traffic signal optimization, incident management on freeways and arterials, Advanced Traveler Information Systems (ATIS), and pricing, etc. As one of the critical parts of implementing Intelligent Transportation Systems (ITS) infrastructures, ATIS is intended to inform travelers of unusual traffic congestion to allow users to make better route/departure time and mode decisions under uncertain conditions. Quantifying the effectiveness of those ATIS strategies is a theoretically challenging and practically important question, because the actual assessment of the system benefits can facilitate public transportation agencies to effectively design, deploy and use the traveler information systems within funding constraints. Given the emerging availability of private-sector traffic data and services, transportation system planners and managers are extremely interested in how different sources of traffic information with different degrees of data quality, coverage, and accessibility influence travelers' decisions and in terms of decreased congestion or improved travel time reliability provides benefits to transportation system users.

1.2 Sources of Travel Time Uncertainty Distributions

To systematically evaluate the benefits of traveler information provision strategies in a realistic stochastic environment, a reliable modeling tool needs to consider various

sources of travel time uncertainties. Generally, inherent travel time uncertainty stems from the following sources:

(1) The first source of uncertainty has a bearing on **system demand input**, primarily caused by day-to-day variations, seasonal variations and special events.

(2) The second uncertainty is due to **system throughput variation**, which results from stochastic capacity or incidents, work zones, and weather conditions. Under stochastic capacity and new ATIS strategies, a more dynamic learning model is needed to balance the two different sources - available information and personal experience.

For example, an empirically-observed distribution of stochastic capacity (Jie, et al. 2010) is illustrated in Figure 1.2. It shows that the 50th percentile capacity on I-880 is 1,976 passenger cars per hour per lane, while the 85th percentile capacity is 1,778 passenger cars per hour per lane. Thus, 15 percent of the time, the I-880 bottleneck breaks down after only 1,778 passenger cars per hour per.

(3)The third uncertainty is further compounded by **the absence of precise traffic information** due to inadequate sensor coverage or limited traveler knowledge and experience, which can further compound the issue of travel time uncertainty.

(4) The fourth uncertainty is **traveler perception errors**, which is typically modeled in a stochastic traffic assignment framework to capture unbiased random noises (with a mean of zero) associated with drivers' socio-economic characteristics, personal observations, as well as the quality of traveler information.

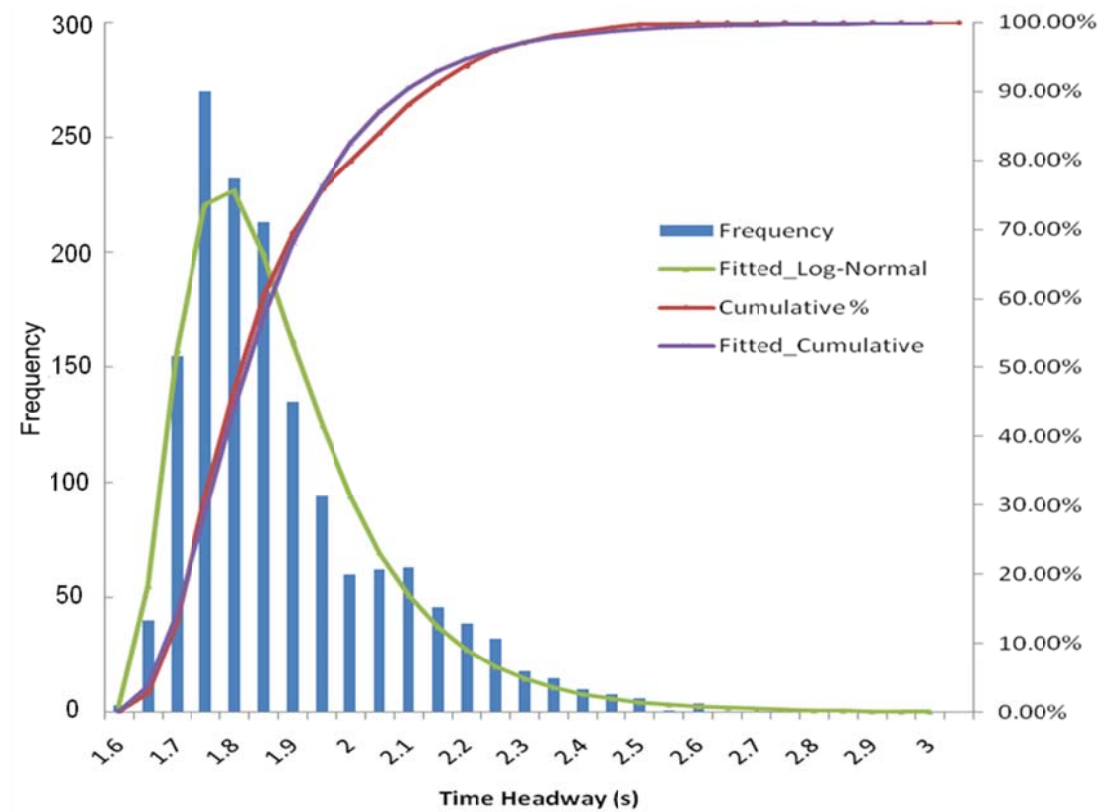


Figure 1.2- Prebreakdown Headway Distribution for I-880.

1.3 Challenges and Motivations

1.3.1 Modeling challenges in static-state programming approach

To evaluate traffic mobility impacts under user equilibrium conditions, a static traffic assignment approach is typically used for estimating link flows and travel times (Sheffi, 1985). Conventional static traffic assignment approaches generally assume users have perfect knowledge of network conditions, and that link capacities are fixed or deterministic. However, this perfect information assumption does not allow modelers to realistically evaluate the longer-term benefits of real-time traveler information provision strategies.

Capturing stochastic capacity at the critical points of networks (such as bottlenecks) which suffer from queue and congestion more frequently, e.g., freeway bottlenecks and signalized intersections, enables reasonable and realistic modeling of travel time variability and the concept of sustainable flow rates. Without taking into account this feature, it is impossible to fully consider the variability in the transportation system due to one of its critical sources, stochastic capacity. Moreover, travel times would be stochastic on different days, which further motivate the development of day-to-day learning and route updating models to be discussed in this dissertation.

In order to incorporate stochastic capacity in a user equilibrium framework and study the impact of information on drivers who tend to maximize their expected utility, de Palma, et al. (2005) used a graphical method to compare two extreme information user classes which govern day to day traffic conditions. This early investigation provides great theoretical insights in analyzing the travelers' behavior under stochastic capacity. However a more rigorous mathematical programming model and efficient solution algorithms are critically needed to describe the steady-state user equilibrium conditions on a general traffic network.

Although a variety of network analysis tools are currently available to assess different traffic operations and control strategies, two challenging theoretical research questions remain for characterizing steady-state conditions under stochastic capacity:

1. How to develop mathematical models that describe realistic user behavior under stochastic capacity?
2. How to develop efficient and operational algorithms to find multiday user equilibrium solutions under stochastic capacity on a large-scale network?

1.3.2 Modeling challenges in dynamic traffic assignment approach

To describe the dynamic traveler behavior over multiple days, a day-to-day learning model is required to describe the nonequilibrium state of traffic patterns. Dynamic Traffic Assignment (DTA) methodologies uniquely address these modeling needs, and a variety of models have been developed to represent the time-dependent route choice behavior (Mahmassani, 2001; Ben-Akiva, 2001). Most day-to-day learning models focus on long-term planning applications with stable road capacity. For instance, in the day-to-day learning frameworks proposed by Hu and Mahmassani (1997), Jha et al. (1998), and Chen and Mahmassani (2004), day-to-day traffic evolution and stochasticity are mainly due to route and departure time choices. Additionally, these models mainly study the learning behavior based on *historical* personal traveling experiences and real-time *snapshot* information. In reality, travelers are more likely to utilize various information sources, before their trips and en-route, to find the most reliable routes.

Three major limitations exist in past studies in terms of traveler's learning behavior. First, most of these models only consider the day-to-day travel choice dynamic represented under deterministic capacity, rather than considering stochastic and sustainable service rate (SSR). As a result, most research on DTA models has been based only on within-day dynamics, where all parameters associated with the system (such as supply and demand) are time-dependent but still under a deterministic framework. Additionally, under stochastic capacity, travel time experience on a single day can be dramatically affected by the underlying capacity, which in turn influences drivers' travel choices. Second, drivers only utilize the experienced travel times on the latest days to reach convergence, e.g., myopic adjustment model (Hatcher and Mahmassani, 1992).

Third, users are assumed to have complete network knowledge and perfect information regarding the time dependent system conditions and are able to make optimal route choices to minimize their travel times. However, these models ignore the multiple user classes (MUC) with different information availability.

In this context, the primary challenging research questions considered are:

3. How to update variability of travel time estimates due to stochastic capacity for different information groups?

4. How to model predictive information and day-to-day evolution which result from user decision and network dynamics?

1.3.3 Modeling challenges in analytical approximation approach

Substantial development attention has been given to both the traffic network modeling and traffic flow theory fields in an effort to quickly estimate and predict travel time variability from its underlying uncertainty sources, because traffic systems can be viewed as stochastic processes with nondeterministic demand and capacity inputs. Focusing on analytical travel time performance functions, e.g., widely used U.S. Bureau of Public Roads (BPR) functions, a number of studies have developed various numerical approximation methods to characterize travel time variability distributions as a result of stochastic capacity and stochastic demand. A well recognized limitation of the BPR function and other static travel time functions is that it cannot effectively describe the dynamic buildup and dissipation of traffic system congestion. Consequently, the travel time variability estimation methods from the above studies are more suitable for analyzing long-term steady-state traffic equilibrium results; dynamic traffic-oriented

models are still critically needed for quickly estimating path travel time variability distributions, especially under heavy congestion conditions.

Given a set of observed or simulated traffic conditions, e.g., traffic flow and queue profiles on a link or a corridor, this dissertation provides efficient analytical approximation methods to specify the Probability Density Function (PDF) of travel time distributions as a result of stochastic capacity and demand distributions. This study aims to address the following two research questions:

5. For planning-level applications, how can a quick characterization of travel time reliability statistics be used without resorting to the comprehensive but computationally challenging day-to-day simulation or numerical approximation approaches?

6. For real-time traffic prediction applications, how can an analytical relationship be derived and constructed between the capacity change and the waiting time change on a bottleneck?

1.4 Research Objectives

To meet the six research questions described previously, this research introduces and extends the following research methodologies.

To address research questions (1-2), this research will first focus on modeling and solving the steady-state user equilibrium problem with stochastic capacity, to find a single path flow pattern that satisfies the generalization of Wardrop's first principle: travelers with the same OD and departure time experience the same and minimum expected travel time along any used paths on different days, with no unused path offering a lower expected travel time. A new model will be developed to explicitly address the

stochastic nature of network capacity and represents travelers' imperfect route choice in response to capacity fluctuation in a day-to-day learning framework. The resulting problem is an expected utility-based dynamic user equilibrium problem that is formulated using a gap function approach, based on the gap function-based terminology given by Smith (1993) and a recent paper by Lu et al. (2009).

To address research question (3), the traveler decision will be simulated in a day-to-day learning behavioral framework. This task will adapt the empirically calibrated choice model by Noland et al. (1998) to explicitly account for travel times, early and late schedule delays, and travel time reliability. The utility function will therefore take into account the essential traffic attributes, such as alternative travel time and travel time reliability. The underlying travel behavior model in the enhanced traffic simulator should be able to (1) combine multiple data sources to make travelers' own "predictions"; (2) dynamically adjust travelers' confidence levels on different information sources, based on experienced travel times.

To address research question (4), this research will formalize a new theoretical traffic estimation-prediction framework that considers a variety of information sources and can quantify the impact of information accuracy. Essentially, the travel behavior model will consider three major information sources: historical/experienced, pretrip, and en-route information. This research aims to seamlessly incorporate stochastic capacity models at freeway bottlenecks and signalized intersections, and develop adaptive day-to-day traveler learning and route choice behavioral models under the travel time variability introduced by random capacity variations. The model will adaptively recognize and

capture the systematic day-to-day traffic evolution, and also maintain robustness under disruptions as a result of unexpected incidents and random weather conditions.

To address research questions (5-6), this study will utilize several key statistical properties of the log-normal distribution, which is a state-of-practice distribution used in many empirical studies for describing travel time variability. By assuming log-normal distributions for stochastic demand and capacity, and in the context of the BPR function as travel time performance functions, this study proves that the resulting travel time follows a log-normal distribution, so the travel time variability can be analytically derived from the variation parameters in demand and capacity. Furthermore, this research considers a more realistic point queue model. Under an assumption of log-normal distributions for stochastic capacity variations, the corresponding total waiting time will be characterized through log-normal distributions. This dissertation then plans to use simplified peak-hour demand profiles to derive time-of-day travel time variability functions at a traffic bottleneck.

Additionally, this dissertation provides theoretical investigation results for the following emerging practical questions from ATIS planning and deployment applications.

(1) Given low-resolution traffic information freely available from radio stations and freeway Variable Message Signs (VMS), can additional high-quality traffic information provision services, such as Internet-connected GPS navigation devices, improve the system-wide average travel time or travel time reliability?

(2) Typically, travelers do not have full knowledge of historical traffic patterns for each link in a transportation network, and they acquire and update their own network knowledge based on their past experienced travel time. Recently, many websites, such as

Google Maps, have begun to provide free color-coded maps for displaying historical regional travel time patterns. This source provides additional opportunities for commuters to learn the traffic conditions and enhance their network knowledge beyond their own experienced routes. Can the improved network knowledge quality improve the overall system performance?

(3) In addition to many real-time ATIS strategies that focus on informed route switching, many traffic management strategies, such as telecommuting and flexible working hours, aim to reduce and smooth the overall day-to-day travel demand variations. Transportation agencies need to quantify the benefit and then prioritize various potential congestion mitigation solutions: With limited funding constraints, should the transportation agencies increase ATIS market penetration rates, improve real-time data quality, or reduce day-to-day traffic demand variations?

1.5 Overview of Approach and Organization of the Dissertation

This dissertation has seven chapters. The comprehensive evaluation framework in Figure 1.3 indicates the structure of this dissertation. Aiming to provide a comprehensive review on various traffic bottlenecks and congestion modeling elements, Chapter 2 discusses several topics pertaining to ATIS, stochastic capacity modeling, optimization approach for equilibrium analysis, analytical approach for a single bottleneck analysis and simulation-based approach for dynamic traffic travel time analysis. Focusing on steady-state static user equilibrium analysis, Chapter 3 considers stochastic capacity and travel time performance functions in an advanced traveler information provision environment. Chapter 4 further considers the steady-state evaluation of traveler

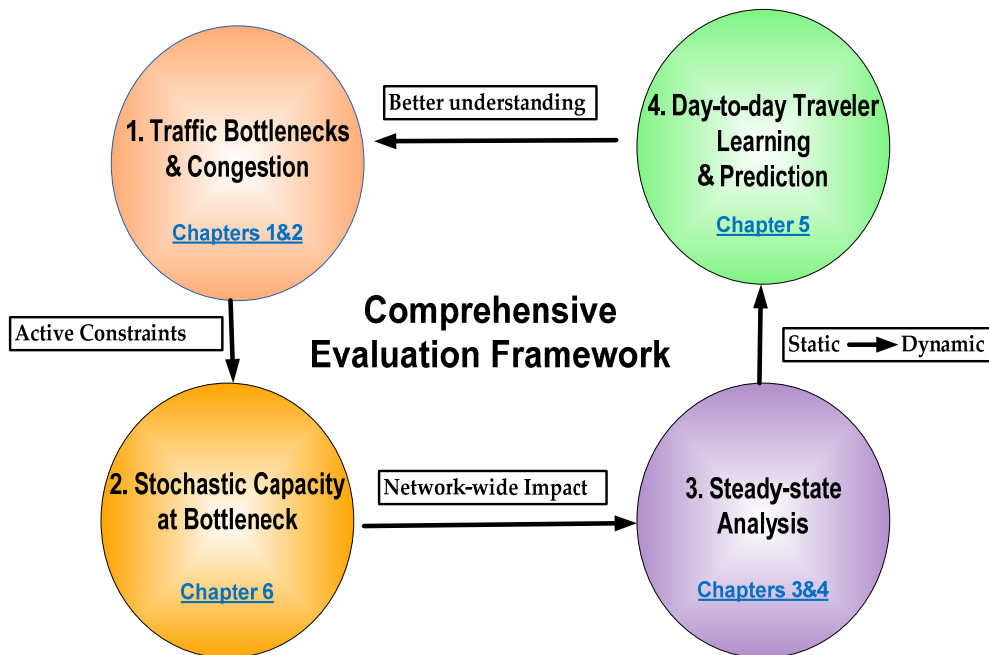


Figure 1.3- Four main areas of interest.

information provision strategies with stochastic traffic demand, stochastic road capacity, and different degrees of traffic information provision quality. Chapter 5 presents a simulation-based method to seamlessly incorporate stochastic capacity models at freeway bottlenecks and signalized intersections, and develops adaptive day-to-day traveler learning and route choice behavioral models under the travel time variability introduced by random capacity variations. With a focus on a single bottleneck with stochastic demand/supply distributions, a volume-to-capacity ratio-based travel time function and a point queue model are used in Chapter 6 to demonstrate how day-to-day travel time variability can be explained from the underlying stochastic demand and capacity distributions. Concluding remarks and future research extensions are given in Chapter 7.

CHAPTER 2

LITERATURE REVIEW

2.1 Overview

This chapter reviews topics relevant to modeling stochastic capacity and three categories of analysis approaches associated with travel time uncertainty, network equilibrium and single bottleneck issue. After a short introduction to the role of ATIS and the sources of network evolution uncertainty, section 2.3 highlights three approaches for modeling stochastic capacity, namely headway-based stochastic capacity models, stochastic queue discharge rate model and probability-based stochastic capacity models. Section 2.4 reviews the literature pertaining to optimization model for static network equilibrium analysis. Section 2.5 overviews major analytical approaches for single bottleneck analysis. Finally, the literature on simulation-based approach for network-wide dynamic traffic evolution analysis is reviewed in section 2.6.

2.2 Role of Traveler Information Systems and Travel

Time Uncertainty Sources

Advanced Traveler Information Systems (ATIS) is intended to inform travelers of unusual traffic congestion, and further allow users to make better route/departure time

and mode decisions under uncertain conditions. How to quantify the effectiveness of those ATIS strategies is a theoretically challenging and practically important question, as the actual assessment of the system benefits can facilitate public transportation agencies to effectively design, deploy and use the traveler information systems within funding constraints. Given the emerging availability of private-sector traffic data and services, transportation system planners and managers are extremely interested in how different sources of traffic information with different degrees of data quality, coverage, and accessibility influence travelers' decisions and provide benefits to transportation system users, e.g., in terms of decreased congestion or improved travel time reliability.

Generally, inherent travel time uncertainty stems from the following sources:

(1) The first source of uncertainty has a bearing on **system demand input** and is primarily caused by day-to-day variations, seasonal variations and special events. Another level of traveler decision uncertainty is related to random departure times and route choice, which can lead to uncertain demand input for a certain set of links (Noland and Polak, 2002).

(2) The second uncertainty is due to **system throughput variation**, which results from stochastic capacity (Brilon et al., 2005, Chen et al., 2002), incidents, work zones, or weather conditions (Srinivasan and Guo, 2004). Under stochastic capacity and new ATIS strategies, a more dynamic learning model is needed to balance the two different sources-available information and personal experience. Past studies focusing on sources of day-to-day variation and capacity reliability for a road network do not fully consider uncertainty related to alternative route, which should have different features compared with the current selected route.

(3) The third uncertainty is further compounded by the **absence of precise traffic information** due to inadequate sensor coverage or limited traveler knowledge and experience, which can further compound the issue of travel time uncertainty. In fact, there are only a small fraction of travelers who currently have full access to or are willing to always retrieve pretrip or en-route traveler information through web-based traveler information sites, car radio, dynamic message signs or Internet-connected navigation devices. When making route choices, the majority of travelers still rely on their personal knowledge and driving experiences that have been gained over a long time period of time, which can be described as the expected travel time (caused by stochastic demand and capacity). When there is a significant variation in capacity, the resulting network conditions could deviate considerably from the average traffic pattern. In this case, the expected value-based travel knowledge should be treated as a biased estimate to the current traffic state.

(4) The fourth uncertainty is **traveler perception errors**, which is typically modeled in a stochastic traffic assignment framework to capture unbiased random noises (with a mean of zero) associated with drivers' socio-economic characteristics, personal observations, as well as the quality of traveler information.

To systematically evaluate the benefits of traveler information provision strategies in a realistic stochastic environment, various sources of travel time uncertainties have to be considered. In studies by Mahmassani (1984) and Chen et al. (2002), uncertainties in transportation network analysis are summarized as: variations in link capacities and travel demands, the imperfect parameter estimation for link travel time functions and route choice behaviors. In a study by Nakayama (2007), stochastic demand is characterized

through a negative-binomial distribution, as the number of trips can be viewed as the collective result of individual trip-making decisions. Weijermars (2007) used traffic volume data to identify and estimate the magnitude of systematic and random variations in traffic flow patterns. Many researchers have studied how to reformulate the traditional static traffic assignment problem under stochastic capacity and demand conditions, and different numerical approximation methods have been proposed to describe the travel time variability due to different underlying random sources, for a single-day traffic equilibrium solution. Zhou and Chen (2008) presented analytical models to derive travel time distributions based on log-normally distributed stochastic demand distributions. Lam et al. (2009) and Sumalee et al. (2009) further highlighted the correlation between link travel time distributions due to variations in origin-destination demand, as an OD flow change can impact flow and travel time on those links along its passing paths simultaneously. Recently, a number of mathematical models are presented to describe equilibrium conditions under reliability-related utility functions and stochastic demand and capacity, e.g., a variational inequality model by Lam et al. (2009), a fixed point model by Sumalee et al. (2009).

2.3 Modeling Stochastic Capacity

2.3.1 Headway-based stochastic capacity models

Consistent with the current practice, the flow rates just preceding the breakdown condition are used to analyze the stochastic capacity for the freeway bottlenecks. Based on the sensor data aggregated at 15-minute intervals, Jia et al. (2010) found that

prebreakdown headways followed a shifted log-normal distribution with the following probability density function:

$$(f_x = (x; \mu, \sigma) = \frac{1}{(x-c)\sigma\sqrt{2\pi}} e^{-\frac{[\ln(x-c)-\mu]^2}{2\sigma^2}}, x > 0 \quad (2.1)$$

where

x is the average prebreakdown headway (in seconds) for 15-minute interval,

c is the minimum prebreakdown headway (in seconds),

μ is the mean of the variable's natural logarithm, and

σ is the standard deviation of the variable's natural logarithm.

Based on the traffic measurement data from PeMS (2009) and TransGuide (2009) systems, the corresponding parameters for Equation 2.1 are calibrated as: $c=1.5$ seconds, $\mu=-0.97$, and $\sigma=0.68$.

Turning to signalized intersections, traffic engineers have long known that saturation flow rates fluctuate over time and that this fluctuation can be observed even from cycle to cycle at the same intersection. Similar to the calibration procedure for the prebreakdown headway distribution on freeway bottlenecks, a stochastic model was developed for predicting saturation headways at signalized intersections. The model was based on a saturation headway database developed by the Florida Department of Transportation (Bonneson et al. 2005). Extensive investigation of candidate distributions revealed that the shifted Log-Normal probability distribution model again provides an

acceptable fit to the empirical data. The corresponding fitted probability density function is:

$$f_x = (x; \mu, \sigma) = \frac{1}{(x-1.9) \times 0.2 \sqrt{2\pi}} e^{-\frac{[\ln(x-1.9)+1.14]^2}{2 \times (0.2)^2}}, x > 0 \quad (2.2)$$

2.3.2 Stochastic queue discharge rate model

Similar to the conventional definition of capacity in the HCM, the queue discharge flow rate is also typically characterized in a deterministic manner. However, the empirical study by Lorenz and Elefteriadou (2000) has clearly demonstrated that the queue discharge flow rate at freeway bottlenecks is also stochastic in nature. Dong and Mahmassani (2009) suggested and calibrated a linear relationship between queue discharge rates and prebreakdown flow rates. The most recent study, Jia et al. (2010) concluded that the queue discharge rate series are strongly time-correlated and developed the following recursive queue discharge model.

$$C_t = C_{t-1} + \gamma(\mu_c - C_{t-1}) + \delta_t, t \geq 1 \quad (2.3)$$

where

C_t is the queue discharge rate at time interval t (in pc/h/ln),

γ is a linear parameter that models the strength of regression to the mean,

μ_c is the average discharge rate (in pc/h/ln) and

$\delta_i \sim N(0, \sigma^2)$ is the random error.

When $t=1$, C_0 is the prebreakdown flow rate.

Calibrated with the sensor data from a study site on I-880 in the Bay Area of California, the fitted parameters for equation 2.3 are: $\gamma = 0.2$, $\mu_c = 1850$ pc/h/ln, and $\sigma = 100$ pc/h/ln.

2.3.3 Probability-based stochastic capacity models

The statistical analysis in some existing empirical studies (e.g., Brilon et al., 2005 and 2007) indicated that the probability of freeway breakdown follow a Weibull distribution (equation 2.4). The stochastic capacity across the time horizon is illustrated in Figure 2.1.

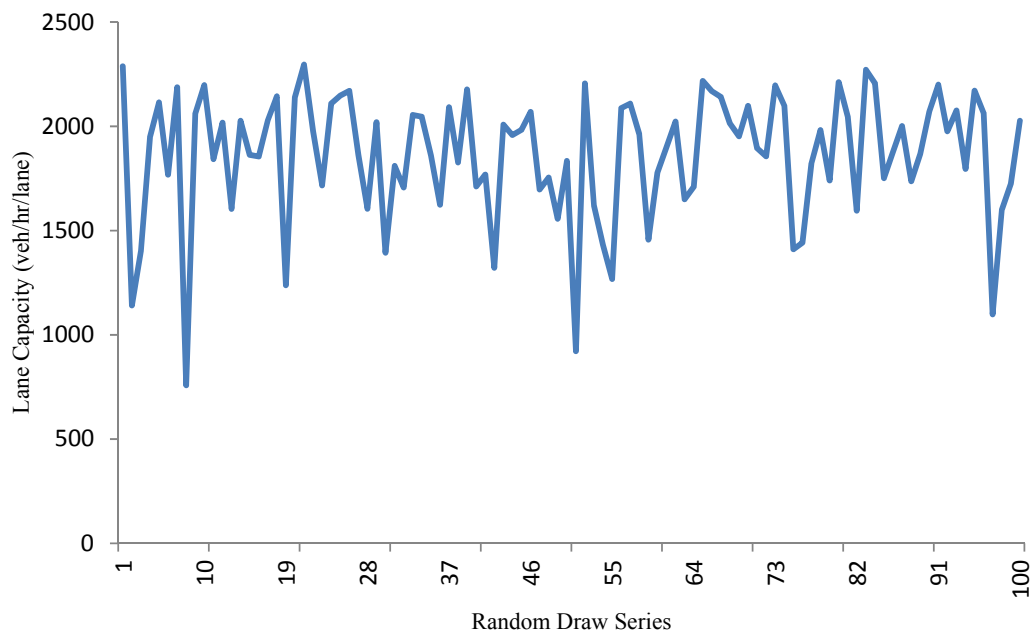


Figure 2.1- Distribution of lane capacity converted from headway.

$$F(x) = 1 - e^{-\left(\frac{x}{b}\right)^a} \quad (2.4)$$

where

a = shape parameter

b = scale parameter

x = flow rate (veh/h)

F(x) = (cumulative) probability of freeway breakdown at flow rate x

2.4 Optimization Model for Static Network Equilibrium Analysis

To achieve the objective of user equilibrium or system-optimum strategy for traffic mobility, static traffic assignment approaches were used for estimating link flows and travel times (Sheffi, 1985). A wide range of studies have been devoted to modeling the impact to traveler information provision strategies in the last two decades. A majority of the existing models (e.g., Yang, 1998; Yang and Meng, 2001; Yin and Yang, 2003) are based on networks with deterministic demand and road capacity, and they typically consider the perception errors in a stochastic user equilibrium (SUE)-based framework, in which the information quality issues can be modeled through the “perception error” term of a discrete choice model. For example, In many SUE-based models along this line, all travelers are assumed to have unbiased network knowledge/information about the equilibrium condition, and equipped users have less travel time perception errors compared to nonequipped users, thanks to external traffic information provision. Chorus et al. (2006) presented a comprehensive review of both the empirical and the conceptual literature concerning the use of travel information and effects on travelers’ choices.

Based on the classical gap function-based framework for user equilibrium by Smith (1993), Lo and Chen (2000) reformulated the nonlinear complementarity problem for traffic user equilibrium with fixed demand and fixed capacity to a route flow-based mathematical program through a convex and smooth gap function. A recent study by Lu et al. (2009) further extended Lo and Chen's model to general dynamic traffic networks with a route swapping rule, which is based on a first-order gradient descent algorithm for solving convex optimization problems. In this dissertation, the gap-function based equilibrium model proposed by Lu et al. (2009) will be extended to consider multiple user information classes under stochastic demand and capacity conditions.

2.5 Analytical Approach for Single Bottleneck Analysis

Analytical DUE models typically propagate traffic flows and link performance functions at a single bottleneck to determine path travel costs. To evaluate the impact of flow switching strategies in the dynamic traffic assignment process, a variety of studies have been conducted for computing local link marginals due to adding or deleting a vehicle from a link. Ghali and Smith (1995) used a deterministic point queue model to describe traffic flows and gave analytical formula to quantify the marginal impact of total link travel time due to a small change in incoming flow. Peeta and Mahamssani (1995) proposed the first path-based formulation and simulation-based Dynamic SO model, in which the path marginal is the sum of the constituent local link marginal. This dissertation focuses on how to quantify the system-wide impact of a major traffic improvement strategy (e.g., adding one lane, route switch), rather than the small change in the traffic flow.

Focusing on analytical travel time performance functions, e.g., widely used Bureau of Public Roads (BPR) (1964) functions, a number of studies have developed various numerical approximation methods to characterize travel time variability distributions as a result of stochastic capacity and stochastic demand. Lo and Tung (2003) presented a Mellin transforms-based method to estimate the mean and variance of travel time distribution for a given stochastic capacity probability distribution function. By performing a sensitivity analysis on a multivariate normal distribution-based link representation in a network, Clark and Watling (2005) proposed a computational procedure to construct the probability density function (PDF) of link travel times under stochastic demand conditions. Recently, a Fourier transformation approach was introduced by Ng and Waller (2010) to approximate the probability density function of travel time from underlying stochastic capacity distributions, for a given set of traffic flow assignment results.

In order to distinguish different system throughput states (e.g., stochastic capacity) in a user equilibrium framework, de Palma and Picard (2005) used a graphical method to consider two types of information user classes, including (1) those with perfect information on good days and bad days (e.g., under normal and reduced capacity); and (2) those with information on expected travel times on different days. Their pioneering investigation provides great theoretical insights into analyzing traveler behavior under stochastic capacity. Along these lines, this research has focused on developing a rigorous mathematical programming model and efficient solution algorithms for general traffic networks with continuous stochastic capacity distributions.

2.6 Simulation-based Approach for Network-wide Analysis

The simulation-based approach produces trip itineraries based on traveler inputs, e.g., origin, destination, desired arrival/departure times, traveler preferences etc., and determines link and path travel costs through traffic simulation instead of analytical evaluation. Depending on the level of representation detail, flow models embedded in traffic simulators can be classified as macroscopic, mesoscopic or microscopic. In macroscopic models (e.g., the classical first-order model by Lighthill and Whitham (1955) and Richards (1956)), traffic flow is described as one-dimensional compressible fluid using partial differential equations, and the vehicular flow on discretized highway segments are moved according to a speed-density relationship. Microscopic models, on the other hand, offer a more detailed representation by considering stimuli and responses among individual drivers, including both car-following and lane changing behavior.

Focusing on the effect of commuter route choice decisions, Chang, Mahmassani and Herman (1985) developed an early mesoscopic simulation model to characterize traffic flow as discrete vehicle groups/particles, and individual vehicle positions are updated by a macroscopic flow-density relationship. Compared to the fluid-based representation in macroscopic models, mesoscopic models keep track of individual vehicles, their origin-destination, and path trajectory data to better simulate travelers' behavior in a network. Without considering a sophisticated lane-changing mechanism, mesoscopic models are able to use a longer simulation time interval than microscopic models, for example, 6 seconds vs. 0.1 seconds. This leads to significant computational savings, especially when searching for dynamic traffic user equilibrium or day-to-day learning solutions on large-scale regional networks.

Through a simulation-based modeling framework, Nakayama (2007) incorporated stochastic demand and stochastic route choice components in a day-to-day simulation model to examine network reliability on linear corridors. Obviously, a day-to-day modeling framework is suitable for studying medium-term transitions and within-day dynamics in traveler decisions and the resulting traffic flow patterns. On the other hand, the simulation-based modeling approach requires a sufficiently long period (e.g., many days of simulation) to stabilize traffic conditions and it does not have well-accepted converge criteria to describe steady-state conditions (as a traffic user equilibrium model does).

To better describe adaptive traveler behavior and simulate the resulting travel flow pattern in an environment where roadway capacity varies within a single day and over multiple days, a day-to-day learning framework is needed to allow a realistic consideration and evaluation of different capacity-enhancing and traffic management scenarios. A wide variety of day-to-day learning models have been proposed to understand and simulate the medium-term traffic evolution process under various advanced traveler information provision strategies. An early study by Hu and Mahmassani (1997) took into account both route and departure time choices as the sources of day-to-day traffic dynamics. Srinivasan and Guo (2004) examined network evolution and user response characteristics under varying market penetration levels of traveler information. Jha et al. (1998) adapted a Bayesian framework to model the traveler perception updating process. Chen and Mahmassani (2004) further studied triggering mechanism and termination conditions for the travel time learning process. However, existing day-to-day learning frameworks assume a constant road capacity, and

the variability sources considered in those models are limited to route and departure time choices.

What assignment/simulation tools can be considered as the prime evaluation tool is an important question, because DTA models consist of a great number of parameters and inputs that must be calibrated to accurately reflect field conditions. Another question that should be answered is whether the transportation system analysts and planners can make the most of the potential of the simulation package that supports Advanced Traveler Information Systems (ATIS) and Advanced Traffic Management Systems (ATMS) strategies for road capacity enhancement, such as traffic signal optimization and incident management on freeways and arterials. As shown below, a variety of network analysis tools are currently available to assess the impacts of ITS technologies and different traffic operations and control strategies.

- DYNASMART-P, developed at UT at Austin, UMD, and Northwestern University by Mahmassani et al.
- DYNAMIT, developed at MIT by Ben-Akiva et al.
- EMME/3, developed by INRO
- IDAS, developed by Cambridge Systematics, Inc.
- Integration, developed by M. Van Aerde& Assoc.
- Paramics, developed by QuadstoneParamics
- SCRITS, initially developed for FHWA by SAIC
- TRANSIMS developed by Los Alamos National Laboratory
- VISSIM, developed by PTV AG

With its current ability to model buildup and dissipation of traffic congestion on a large-scale network, DYNASMART-P is considered a good analysis tool for assessing the capacity impacts of various types of traveler information (historical, pretrip, en-route information, VMS), ramp metering, and road-pricing strategies. DYNASMART-P has been used for region-wide transportation operations planning to (1) address operational issues in the transportation planning process; and (2) develop and evaluate traffic management and control strategies, particularly in the ITS context. More importantly, DYNASMART-P provides a unique system-optimization capability, which can be used to quantify the maximum network-flow rate under different traffic conditions. The benchmark set by system-optimal assignment will be used to assess the effectiveness of capacity enhancement strategies and to further provide useful guidance on how to design management strategies that will optimize the network route flow pattern.

It is also important to recognize the use of a single model in evaluating traffic network capacity is not sufficient to meet different needs in both operational and planning applications. For example, dynamic assignment tools require accurate time-dependent OD demand matrices as fundamental input, and the complex traffic flow and route choice models should be carefully calibrated to provide reliable assessment results. DYNASMART-P can offer a rapid analysis framework that can estimate/approximate the magnitude and probabilistic upper bound of the network capacity at peak hours.

CHAPTER 3

PLANNING-LEVEL METHODOLOGY FOR EVALUATING ATIS STRATEGIES UNDER STOCHASTIC CAPACITY CONDITIONS

3.1 Introduction

In this chapter, a nonlinear optimization-based conceptual framework is proposed for incorporating stochastic capacity, travel time performance functions and varying degrees of traveler knowledge in an advanced traveler information provision environment. The proposed method categorizes commuters into two classes: (1) those with access to perfect traffic information every day, and (2) those with knowledge of the expected traffic conditions across different days. With a special focus on formulating and solving the steady-state user equilibrium problem with stochastic capacity, this research aims to find a network flow pattern that satisfies a generalization of Wardrop's first principle: travelers with the same origin-destination pair experience the same and minimum expected travel time along any used paths on different days, with no unused path offering a shorter expected travel time. Through the gap function-based reformulation for user equilibrium, the proposed model explicitly considers the stochastic

nature of network capacity over different days and represents travelers' imperfect information and general knowledge about the random travel time variations. A mathematical programming model is formulated to describe the route choice behavior of the perfect information (PI) and expected travel time (ETT) user classes under stochastic day-dependent travel time. Driven by an operational algorithm suitable for large-scale networks, the model was applied to a simple corridor and a medium-scale network to illustrate the effectiveness of traveler information under stochastic capacity conditions. A solution method is developed to find the equilibrium path flow distribution, while stochastic travel times on different days are generated from a sampling-based simulation framework.

3.2 Conceptual Framework

The conceptual modeling framework is illustrated in Figure 3.1 using a simple corridor with a single origin-to-destination pair and two paths $p=1$ for the primary path, $p=2$ for the alternative path, where p is the path index. As each path only has one link, path 1 is denoted as link $a=1$ with a free-flow travel time of 20 minutes, and path 2 is denoted as link $a=2$ with a free-flow travel time of 30 minutes, where a is the link index. This example considers five different days $d = 1, 2, 3, 4$ and 5 , and the peak hour demand is $Q=8000$ vehicles per hour on each day.

Following a similar analysis setting in the study by De Palma and Picard (2005), the first illustrative example considers day 1 as the “bad” day on path 1, with a reduced capacity for the primary route, and days 2, 3, 4, and 5 as good days with the full capacity available. As detailed in Table 3.1, the primary path has the following capacity values:

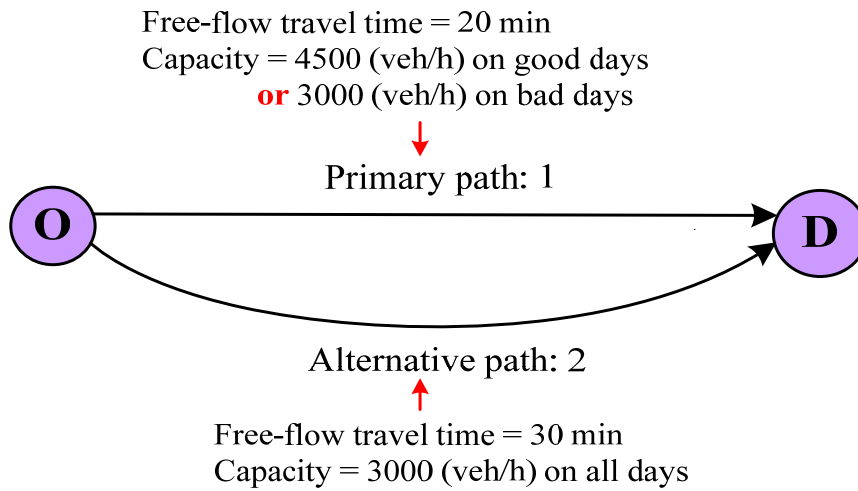


Figure 3.1-Simple network used as an illustrative example of the framework.

- On the bad day ($d=1$) it is 3,000 vehicles per hour (vph) per link.
- On the good day ($d=2, 3, 4, 5$) it is 4,500 vph per link.

The alternative path is assumed to have a fixed capacity of $c_{a,d} = 3,000$ on days $d=1, 2, 3, 4$ and 5 , where $c_{a,d}$ is defined as the capacity of link a on day d .

To setup a mathematical programming model for steady-state traffic equilibrium, the nonnegative flow variables $f_{p,d}$ is considered as the traffic flow using path p on day d . Obviously, the path flow distribution should ensure the total demand constraint on each day:

$$f_{1,d} + f_{2,d} = Q \quad \forall d \quad (3.1)$$

Let $T_{p,d}$ be defined as the travel time on path p on day d , which can be calculated from the BPR function such as

Table 3.1-Day-dependent path demand, capacity and travel time values.

		Day 1	Day 2	Day 3	Day 4	Day 5	Avg.	
Day-Dependent Capacity	Daily Capacity on Path/Link 1 (veh/h) $C_{a=1,d}$	Path 1	3000*	4500	4500	4500	4500	4200
	Daily Capacity on Path/Link 2 (veh/h) $C_{a=2,d}$	Path 2	3000	3000	3000	3000	3000	3000
PI-Based User Equilibrium	Flow (Veh/hour/link)	Path 1	4636	6172	6172	6172	6172	5865
		Path 2	3364	1828	1828	1828	1828	2135
	Travel Time (min)	Path 1	37.1	30.6	30.6	30.6	30.6	31.9
		Path 2	37.1	30.6	30.6	30.6	30.6	31.9
ETT-Based User Equilibrium	Flow (Veh/hour/link)	Path 1	5503	5503	5503	5503	5503	5503
		Path 2	2497	2497	2497	2497	2497	2497
	Travel Time (min)	Path 1	54.0	26.7	26.7	26.7	26.7	32.2
		Path 2	32.2	32.2	32.2	32.2	32.2	32.2

*reduced capacity

$$T_{p,d} = FFTT_a \times \left(1 + \alpha \times \left[\frac{f_{a,d}}{C_{a,d}} \right]^\beta \right) \quad (3.2)$$

where $FFTT_a$ is the free-flow travel time of link a . Coefficients α and β are set to commonly used default values 0.15 and 4, respectively. Now the two different degrees of traveler knowledge can be examined.

3.2.1. Perfect information (PI) based user equilibrium

Every day, perfect travel time estimates (i.e. zero prediction error) for all links are available to travelers to make route decisions, and travelers can switch routes every day. This perfect and complete information assumption for each day is consistent with

deterministic static traffic assignment, which usually considers a typical weekday. It should be cautioned that this assumption might not be realistic from a dynamic traffic assignment perspective, as both pretrip and en-route traveler information available to commuters are essentially forecasted estimates of traffic conditions unfolding in the future, with always some degree of prediction errors. According to Wardrop's first principle of user equilibrium, for a specific origin-destination pair, travelers with perfect information experience the same and minimum travel time along any used paths on each day d , with no unused path offering a shorter travel time.

To construct the objective function in the optimization model, the following gap function (for each day d) can be used to characterize the Karush-Kuhn-Tucker optimality conditions required for reaching the user equilibrium for perfect information users.

$$gap_d^{PI} = f_{1,d}^{PI} \times (T_{1,d} - \pi_d) + f_{2,d}^{PI} \times (T_{2,d} - \pi_d) = 0, \forall d \quad (3.3)$$

where $f_{1,d}^{PI}$ and $f_{2,d}^{PI}$ are path flow rate of PI users on paths 1 and 2, respectively, on day d , where π_d is minimum path travel time on day d

$$\pi_d = \min(T_{1,d}, T_{2,d}), \forall d \quad (3.4)$$

For the illustrative simple corridor, Table 3.1 shows the traffic assignment results when all the travelers in the network have access to perfect information, and a standard deterministic user equilibrium state is reached every day. See also Figure 3.2 for a graphical representation of the flows and travel times for PI users.

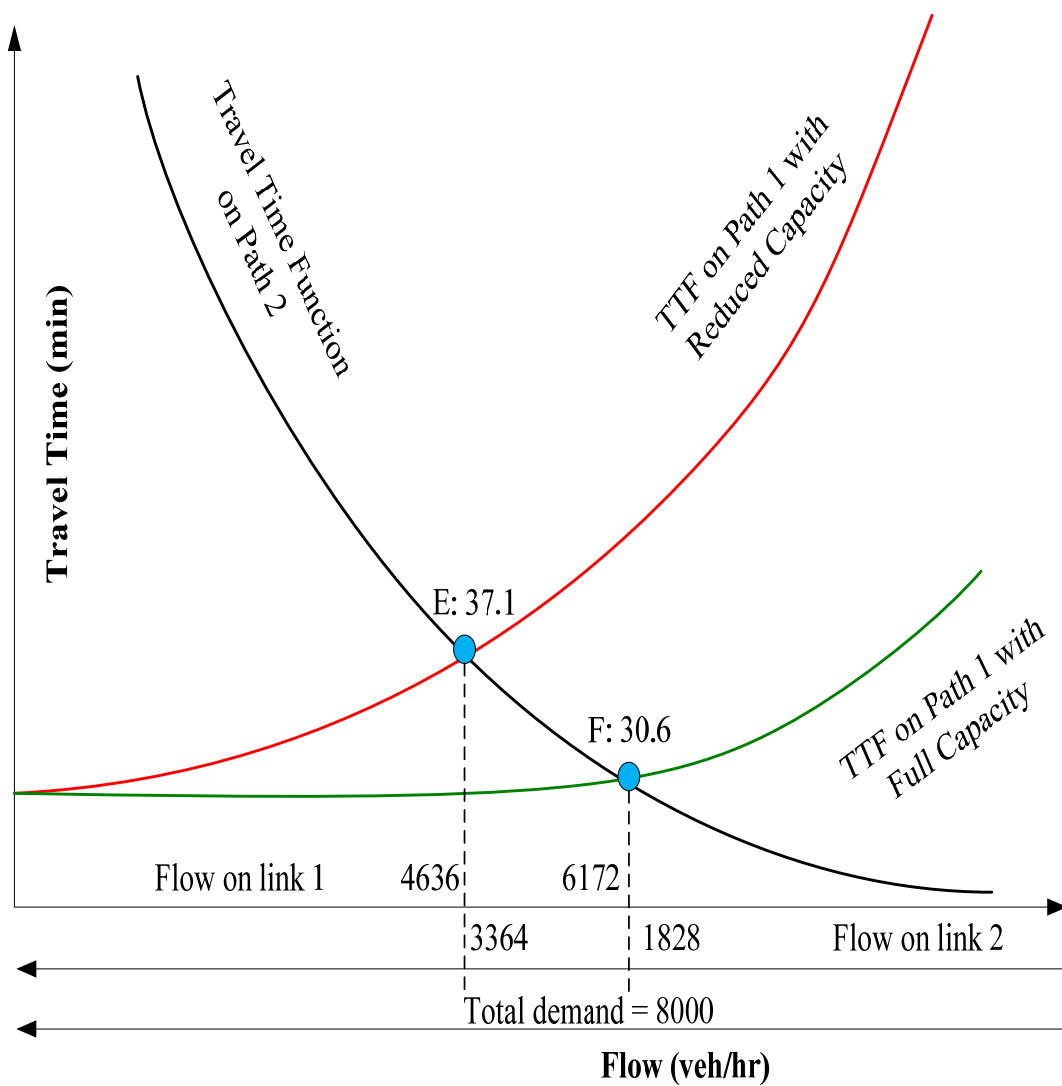


Figure 3.2-Equilibrium solutions with 100% PI users.

Point E: reduced-capacity days, equilibrated travel times = 37.1 min, 4636 vehicles on link 1 and 3364 vehicles on link 2;

Point F: full-capacity days, equilibrated travel times = 30.6 min with 6172 vehicles on link 1 and 1828 vehicles on link 2.

3.2.2 Expected travel time (ETT) knowledge-based user equilibrium

As there are different realized capacity values on different days, the travel times on different links can be viewed as a set of random variables. In reality, most travelers are not equipped with advanced traveler information systems, so they rely on their expected travel times (based on their knowledge and experience) over different days to make route choices. The expected travel time can be considered as the long-run average, or more precisely, the probability-weighted sum of the possible travel time values from different days. Under a user equilibrium condition with ETT users, the expected travel times on used routes in the network are assumed to be the same, and accordingly, an ETT user selects the same route every day, regardless of the actual traffic conditions.

The expected travel time for link a with random capacity \tilde{c}_a over different days can be represented as

$$\bar{T}_a(f_a, \tilde{c}_a) = \frac{\sum_d T_{a,d}(f_{a,d}, c_{a,d})}{|d|}, \quad (3.5)$$

where travel time on each day d for link a $T_{a,d}(f_{a,d}, c_{a,d})$ is a function of the prevailing flow and capacity on that particular day. For link $a=1$ in the illustrative example,

$$\begin{aligned} \bar{T}_a(f_a, \tilde{c}_a) &= 0.2 \times \bar{T}_a(f_a, c_a^R) + 0.8 \times \bar{T}_a(f_a, c_a^F) \\ &= 0.2 \times FFFT_a \times \left(1 + \alpha \times \left[\frac{f_a}{c_a^R} \right]^\beta \right) + 0.8 \times FFFT_a \times \left(1 + \alpha \times \left[\frac{f_a}{c_a^F} \right]^\beta \right) \\ &= FFFT_a \times \left(1 + 0.2 \times \alpha \times \left[\frac{f_a}{c_a^R} \right]^\beta + 0.8 \times \alpha \times \left[\frac{f_a}{c_a^F} \right]^\beta \right) \end{aligned} \quad (3.6)$$

where c_a^R and c_a^F corresponds to the reduced and full capacity on link a .

Note that \bar{T}_a is different from the expected value (EV) solution $T_a(f_a, \bar{c}_a)$ typically used in the context of stochastic optimization, which can be calculated using the expected value of capacity on link a , \bar{c}_a .

$$T_a(f_a, \bar{c}_a) = FFTT_a \times \left(1 + \alpha \times \left[\frac{f_a}{\bar{c}_a} \right]^\beta \right) = FFTT_a \times \left(1 + \alpha \times \left[\frac{f_a}{0.2 \times c_a^R + 0.8 \times c_a^F} \right]^\beta \right) \quad (3.7)$$

In this study, we generalize Wardrop's first principle to describe the equilibrium conditions for travelers relying on their expected travel time to make route decisions: travelers with the same origin-destination pair experience the same and minimum expected travel time along any used paths on different days, with no unused path offering a shorter expected travel time. Obviously, when there is a single capacity value, then the above conditions are consistent with the standard user equilibrium with deterministic capacity, as the expected travel time devolves to the travel time on the single day.

The corresponding KKT condition can be re-written as

$$gap^{ETT} = f_1^{ETT} \times (\bar{T}_1 - \bar{\pi}) + f_2^{ETT} \times (\bar{T}_2 - \bar{\pi}) = 0 \quad (3.8)$$

where $\bar{\pi}$ is the least expected travel time between the given OD pair over a multiday horizon satisfies

$$\bar{\pi} = \min(\bar{T}_1, \bar{T}_2) \quad (3.9)$$

An ETT knowledge-user uses the same route on different days, which leads to a day-invariant ETT flow pattern:

$$f_a^{ETT} = f_{a,d=1}^{ETT} = f_{a,d=2}^{ETT} = f_{a,d=3}^{ETT} = f_{a,d=4}^{ETT} = f_{a,d=5}^{ETT} \quad \forall a \quad (3.10)$$

When $gap^{ETT} = 0$, it can be shown that if $f_a^{ETT} > 0$, then $\bar{T}_a = \bar{\pi}$. That is, the selected routes by expected travel time information users between an OD pair have equal and minimum costs. On the other hand, if $f_a^{ETT} = 0$, then $\bar{T}_a \geq \bar{\pi}$, which indicates that all unused routes by ETT users have greater or equal costs (compared to the used path costs). These two conditions further imply that no individual trip maker with expected travel time information can reduce his/her expected path costs by switching routes on any given day, under a user equilibrium condition.

If it is assumed that all users rely on ETT information in the simple corridor, then the ETT-based user equilibrium assigns about 5503 vehicles on path 1, and about 2497 vehicles on path 2, leading to different travel time on 5 different days shown in Table 3.1. The relative travel time savings were examined under different market penetration rates of perfect information users shown in Figure 3.3. As both paths carry positive flows, their average travel times over the 5-day horizon are the same at 32.2 min.

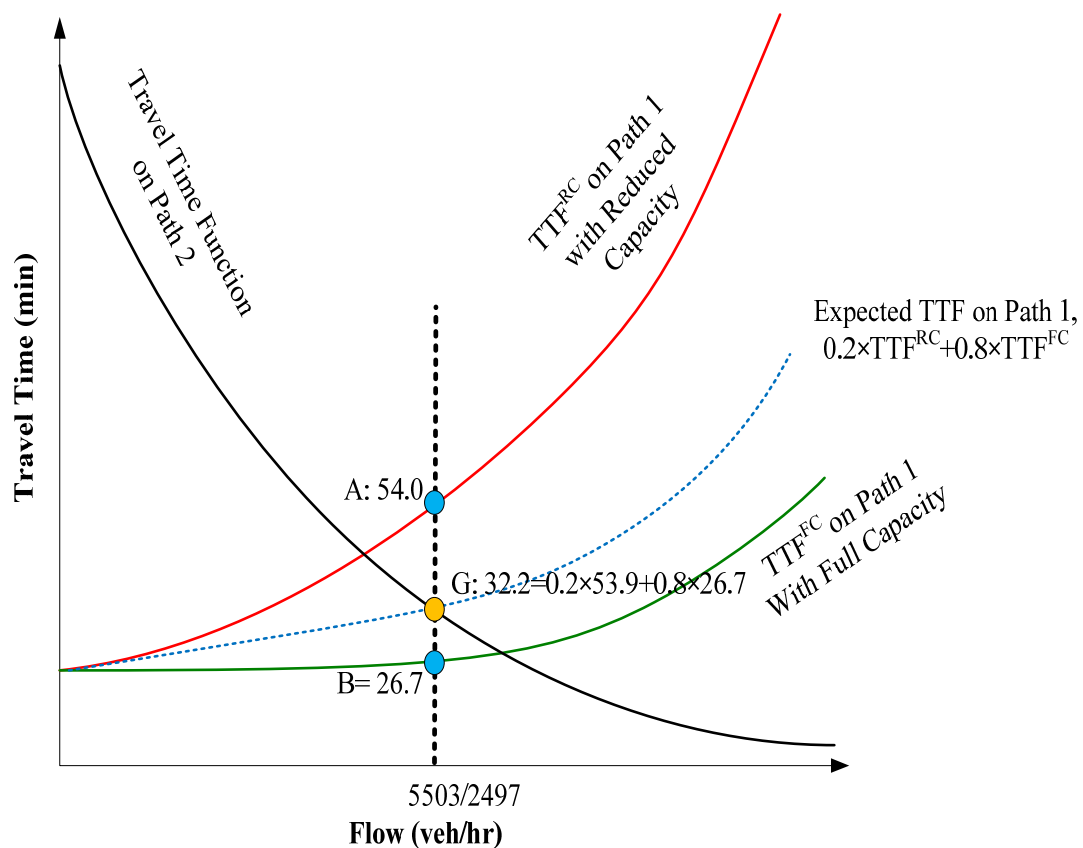


Figure 3.3-Solutions with 100% ETT information users.

The expected travel time function (TTF) is generated by assigning a 20% weight to TTF with reduced-capacity (RC) days and an 80% weight to TTF with full-capacity (FC). The ETT-based user equilibrium corresponds to the intersection (in orange) of expected TTF on path 2 and path 1. 5503 vehicles are using link 1 and 2497 vehicles are using link 2 each day.

Point A: travel time = 54.0 min on link 1, reduced-capacity days,

Point B: travel time = 26.7 min on link 1, full-capacity days.

Point G: travel time = 32.2 min on link 2 every day, and the expected travel time on link 1 is the same 32.2 min.

3.2.3. Quantification of the value of information

In Figure 3.4, the relative travel time savings were examined under different market penetration rates of perfect information users when there are both PI and ETT users. Denote the amount of PI users as f^{PI} , and denote the flow volume at points A, B, C, D and E as f^A, f^B, f^C, f^D, f^E . Obviously, $f^A = f^B$. If f^{PI} is less than $f^A - f^E$, then those PI travelers enjoy a travel time saving from point C to point D with $T_{a=1}(f^A - f^{PI}, c_{a=1}^R) - T_{a=2}(Q - f^A + f^{PI}, c_{a=2})$.

The travel time saving ($T_C - T_D$) diminishes as the flow of PI users increases, where T_C and T_D correspond to the travel time at points C and D. When f^{PI} further increases and reaches the value $f^A - f^E$, both paths have the same equilibrated travel time of 37.1 min. If f^{PI} exceeds $f^A - f^E$, none of the PI users is able to reduce his/her travel time by switching routes and the equilibrium point remains the same as the equilibrium point (E) for 100% PI users with reduced capacity shown in Figure 3.5.

As the proposed model approximates a long-term stochastic steady state under stochastic capacity, Figure 3.5 further shows a possible sequence of the corresponding travel times on 2 different routes over a 20-day horizon. Note that, even though there still exists a 5-day cycle with 4 good days and 1 bad day with reduced capacity, the impaired capacity conditions occur on day 1, day 7, day 11 and day 19 in this example. This irregularity, which is permitted by the model, shows the unpredictability of stochastic travel times, so the ETT knowledge users simply consider the average travel time on path 1 (with a 20% chance or risk of severe traffic congestion) in their long-term route choice decisions.

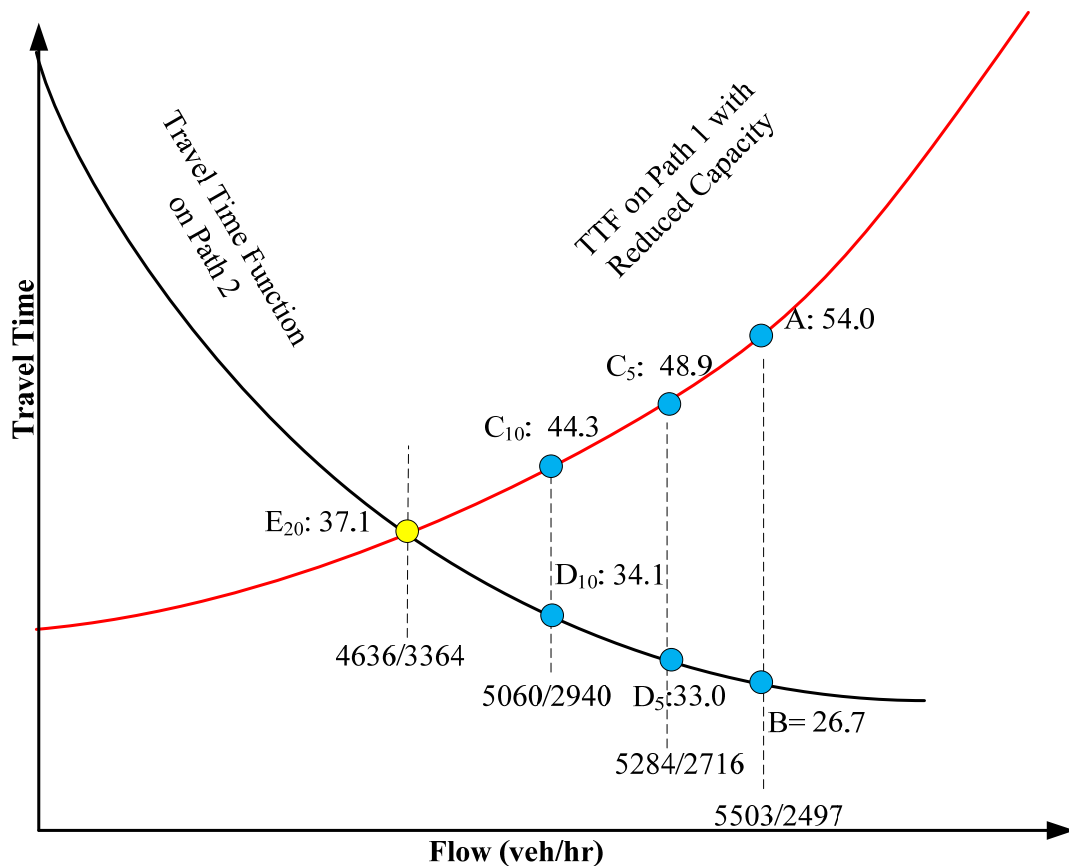


Figure 3.4-Solutions on a reduced-capacity day.

5% PI users (400 vehicles) and 95% ETT users (7600 vehicles),

Point C₅: 5284 ETT vehicles on link 1, travel time = 48.9 min.

Point D₅: 2716 vehicles (2316 ETT users + 400 PI users) on link 2, travel time = 33.0 min.

PI users travel time saving = $44.0 - 33.0 = 11.0$ min, where 44.0 min is the average travel time for ETT users = $(5284 \cdot 48.9 + 2316 \cdot 33.0) / 7,600$.

10% PI users (800 vehicles) and 90% ETT users (7200 vehicles)

Point C₁₀: 5060 ETT vehicles on link 1, travel time = 44.3 min

Point D₁₀: 2940 vehicles (2140 ETT users + 800 PI users) on link 2, travel time = 34.1 min,

PI users travel time saving = $41.3 - 34.1 = 7.1$ min, where 43.1 min is average travel time for ETT users

20% PI users (1600 vehicles) and 80% ETT users (6400 vehicles)

Point E₂₀: 64 PI, 4572 ETT, and 4636 vehicles in total on link 1, travel time = 37.1 min

1536 PI, 1828 ETT, and 3364 vehicles in total on link 2, travel time = 37.1 min

PI users travel time saving = 0 min

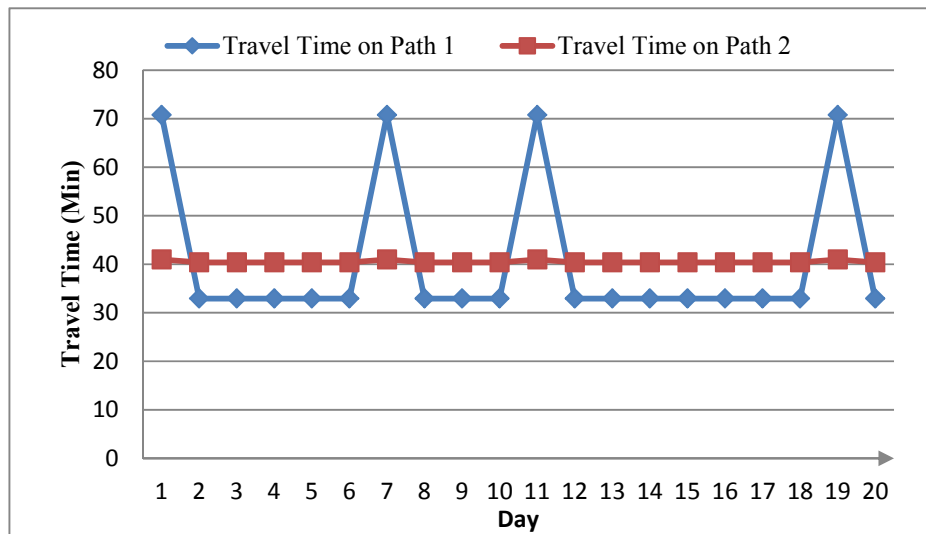


Figure 3.5-Day-dependent travel times on different routes.

It should also be noted that the behavioral model used here is structurally different from the commonly used day-to-day learning model in a DTA framework, even though the underlying traffic states are represented within the same multiday structure. In a day-to-day dynamic learning model, the perceived travel time on day $d + 1$ is updated using experienced travel times from previous days d , $d - 1$, $d - 2$ and so on, and the path can also be changed on a daily basis. In comparison, the ETT knowledge users consider average traffic conditions over all the days as a whole, and always stick to the same route.

3.3 General Mathematical Problem Formulation

This section extends the above conceptual framework to a general network with multiple origin-destination pairs and with road pricing strategies.

3.3.1 Formulation

The sets and subscripts, parameters and decision variables in the proposed flow assignment model are introduced as follows:

Indices:

i = index of origins, $i = 1, \dots, I$, where I is the number of origins

j = index of destinations, $j = 1, \dots, J$, where J is the number of destinations

p = index of paths, $p=1, \dots, P$, where P is the number of paths between an OD pair i and j

a = index of links, $a=1, \dots, A$, where A is the number of links in networks

d = index of days, $d=1, \dots, D$, where D is the number of days over analysis horizon

Input Parameters:

$c_{a,d}$ = capacity of link a on day d

$s_{a,d}$ = toll value charged on link a on day d

$q^{i,j}$ = OD demand volume between an OD pair i and j

$\delta_{p,a}$ = path-link incidence coefficient, $\delta_{p,a}=1$, if path p passes through link a , and 0 otherwise

γ = market penetration rate of the perfect information (PI) users as a function of the total OD demand

VOT = value of time in dollars per minute

Decision variables:

- $f_{p,d}^{PI,i,j}$ = flow of PI users on path p for OD pair (i,j) on day d
- $f_p^{ETT,i,j}$ = flow of ETT users on path p for OD pair (i,j) (flow rates are the same across different days)
- $v_{a,d}$ = total flow on link a on day d
- $T_{a,d}$ = travel time on link a on day d
- $U_{a,d}$ = generalized disutility on link a on day d , which is a function of capacity $c_{a,d}$ and link flow $v_{a,d}$
- $U_{p,d}^{i,j}$ = generalized disutility of path p between OD pair (i,j) on day d
- $\overline{U}_p^{i,j}$ = expected disutility of path p between OD pair (i,j) over the multiday horizon
- $\pi_d^{i,j}$ = day-dependent least path disutility between OD pair (i,j) on day d
- $\overline{\pi}^{i,j}$ = least expected disutility between OD pair (i,j) over the multiday horizon

The proposed model incorporates the two user classes into a static traffic assignment framework under stochastic capacity that varies on a daily basis during the peak hour. The objective function aims to minimize the total gap for users with perfect traffic information and users with imperfect information based on expected travel times.

Objective function:

$$\min Gap = \sum_d \sum_i \sum_j \sum_p \left[f_{p,d}^{PI,i,j} \times (U_{p,d}^{i,j} - \pi_d^{i,j}) + f_p^{ETT,i,j} \times (\overline{U}_p^{i,j} - \overline{\pi}^{i,j}) \right] \quad (3.11)$$

PI flow constraints:

$$\gamma \times q^{i,j} = \sum_p f_{p,d}^{PI,i,j} \quad \forall i, j, d \quad (3.12)$$

ETT flow constraints

$$(1 - \gamma) \times q^{i,j} = \sum_p f_p^{ETT,i,j} \quad \forall i, j \quad (3.13)$$

Path - link flow balance constraints

$$v_{a,d} = \sum_i \sum_j \sum_p (f_{p,d}^{PI,i,j} \cdot \delta_{p,a}) + \sum_i \sum_j \sum_p (f_p^{ETT,i,j} \cdot \delta_{p,a}) \quad \forall a, d \quad (3.14)$$

Path- link cost connection

$$U_{a,d} = T_{a,d}(v_{a,d}, c_{a,d}) + \frac{S_{a,d}}{VOT} \quad \forall a, d \quad (3.15)$$

$$U_{p,d}^{i,j} = \sum_a (U_{a,d} \cdot \delta_{p,a}) \quad \forall i, j, d, p \quad (3.16)$$

Average disutility definitional constraint:

$$\bar{U}_p^{i,j} = \frac{1}{D} \sum_d U_{p,d}^{i,j} \quad \forall i, j, p \quad (3.17)$$

Least disutility definitional constraints:

$$\pi_d^{i,j} \leq U_{p,d}^{i,j} \quad \forall i, j, p, d \quad (3.18)$$

$$\bar{\pi}^{i,j} \leq \bar{U}_p^{i,j} \quad \forall i, j, p \quad (3.19)$$

Constraints (3.12) and (3.13) show the relationship between OD demand and path flows for each information class. Equation (3.14) aggregates path flows from two different user classes to link flows. Equations (3.15-3.16) calculate the path disutility for each path on day d, where the dollar value of road toll is incorporated as equivalent travel time through value of time (VOT). Equation (3.17) defines the average disutility for each

path across different days, which will be used in the gap function for ETT users in objective function (3.11).

For comparison purposes, the system optimal benchmark can also be defined as:

$$\min z = \sum_d \sum_a [v_{a,d} \times T_{a,d}(v_{a,d}, c_{a,d})] \quad (3.20)$$

where the flow to be optimized $f_{a,d}$ can be day-varying.

Because the path utility function is convex and monotonic with respect to path flow and the expected travel time function is a convex combination of day-dependent travel times, the resulting gap function can be shown to be smooth, convex and bounded. Interested readers are referred to the paper by Lo and Chen (2000) for the detailed proof on a similar reformulation. These nice features allow a wide range of efficient nonlinear programming solution algorithms, such as gradient projection algorithms, to be applied to solve the proposed model.

3.3.2 Spreadsheet tool for calculating multiday user equilibrium

Considering the above simple corridor with two routes, a spreadsheet application is developed with the following input elements: (1) deterministic, fixed demand, (2) day-dependent capacity generated from a stochastic capacity distribution, and (3) static travel time functions. The proposed nonlinear model is formulated using the embedded optimization solver in Excel to bring the total gap function toward zero, while the traffic flow of PI and ETT users on different routes are considered as variables to be optimized (i.e., cells to be changed). A wide range of travel time statistics can be derived from the

traffic assignment results, such as the mean and variance of day-dependent travel times. Figure 3.6 demonstrates how the spreadsheet model is operated according to the following steps:

1. *Input data preparation.* Prepare the following input data:

- a. total demand;
- b. PI market penetration γ ;
- c. random capacity on different days; and
- d. BPR step function parameters

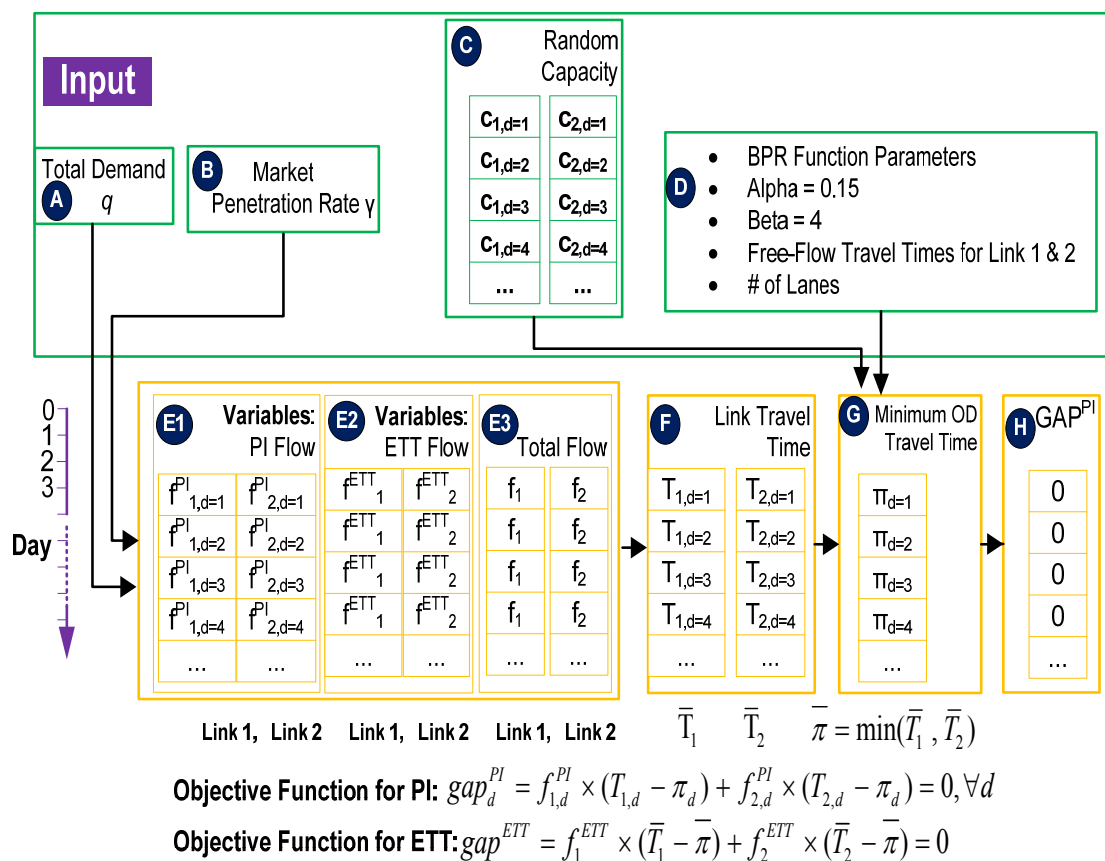


Figure 3.6-Spreadsheet-based calculation model.

2. *Volume calculation*: Corresponding to equation (3.1), the hourly traffic volume is distributed to different paths in block E1 and E2, which also contain variables to be optimized. The total hourly traffic volume is calculated paths in block E3.

3. *Link travel time calculation*: The day-dependent link travel times and the expected travel times are calculated using equations. (3.2) and (3.5) in block F, based on the link flow from block E1 and E2.

4. *Minimum travel time determination*: Find the minimum travel time π_d on each day and π for the average travel time in block G.

5. *Defining the objective function*: Define the objective function related to the gap functions in block H, corresponding to equations. (3.3) or (3.9) for PI and ETT users, respectively.

6. *Solving the optimization model*: Solve the optimization model and derive travel time statistics according to travel time data in block F.

3.4 Solution Algorithm

The solution algorithm executing the above steps is depicted in Figure 3.7. In order to iteratively reduce the overall gap in the proposed optimization problem for a general network with multiple origins and destinations, we extend a descent search solution framework developed by Lu et al. (2009), which also used a path-based gap function to describe the dynamic traffic equilibrium pattern. Figure 3.7 presents the iterative procedure for solving the multiclass static traveler assignment problem under stochastic capacity conditions.

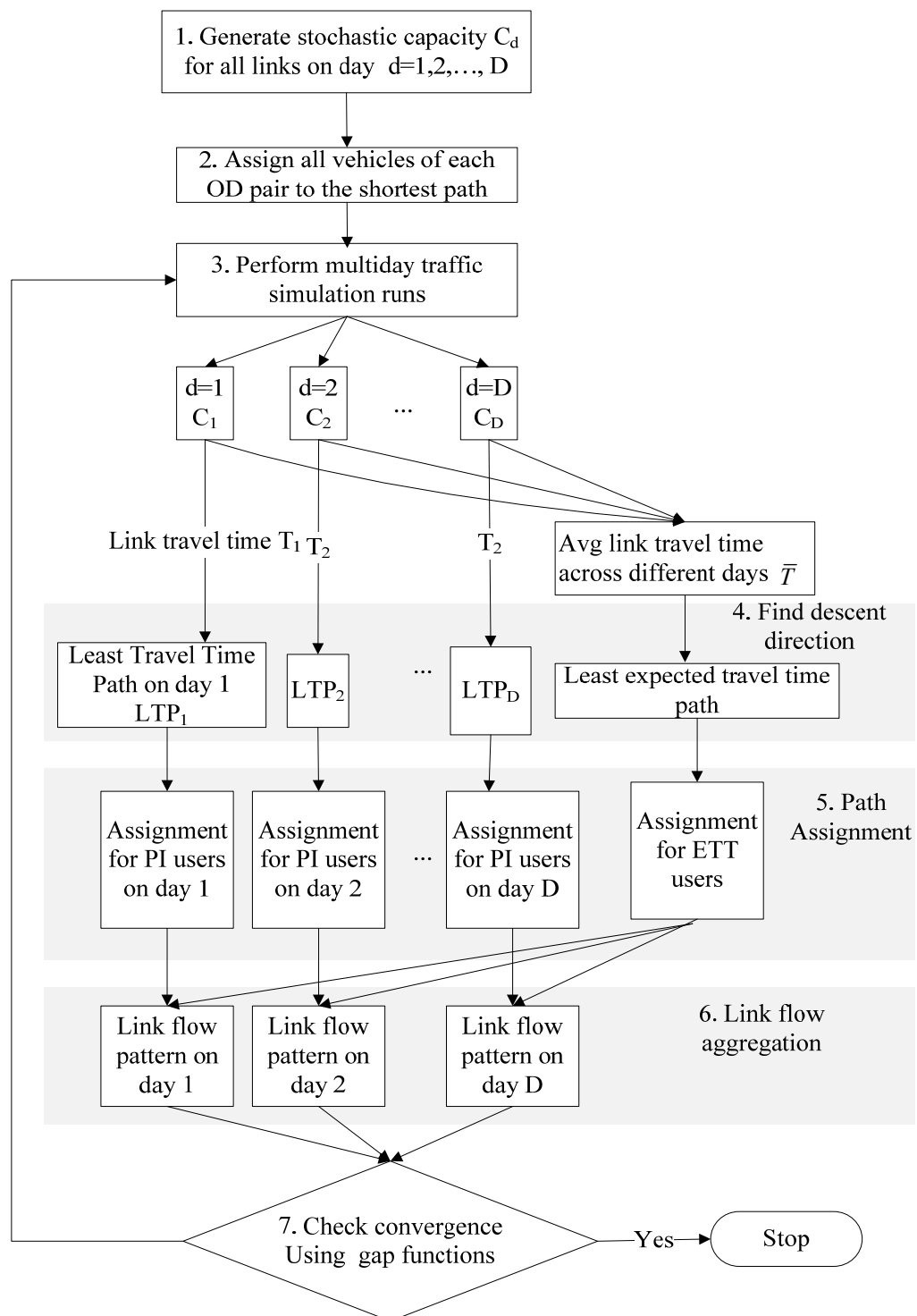


Figure 3.7-Solution algorithm for static traffic assignment with both PI and ETT users.

The proposed procedure adds day-dependent simulation, path finding and assignment dimensions to the existing static traffic assignment algorithm that typically assumes deterministic road capacity conditions. In this study, we implement the proposed algorithm within a mesoscopic traffic assignment framework, which represents flow as vehicles with origin, destination and path attributes. Recall that, in conventional assignment programs, a vehicle is associated with a single path. In the proposed multiday traffic assignment algorithm, an ETT vehicle still follows a single path across different days, but a PI vehicle can use and store different (day-dependent) paths on different days.

The main steps of the solution procedure are described as follows:

Step 1: Day-dependent capacity generation.

Generate road capacity vector $C_d = [c_{a,d}]$, for all link $a=1, 2, \dots, A$, on day $d=1, 2, \dots, D$, according to given stochastic capacity distributions.

Step 2: Initialization.

Let iteration number $n=0$. Generate PI and ETT vehicles according to given market penetration rate γ . For each OD pair, compute the shortest path (in distance) and assign both PI and ETT vehicles to the corresponding shortest path.

Step 3: Multiday traffic simulation with stochastic capacity.

On each day $d=1, 2, \dots, D$, for given link flow patterns, generate day-dependent link travel times according to stochastic capacity vector C_d . The simulation results generate link travel time $T_{a,d}$ for link $a=1, 2, \dots, A$, on day $d=1, 2, \dots, D$.

Step 4: Find descent directions for traffic assignment.

Find the Least Travel time Path (LTP) using day-dependent link travel time $T_{a,d}$ on each day d , for link $a=1, 2, \dots, A$.

Find the Least Expected Travel time Path (LETP) using average link travel time

$$\bar{T}_a = \frac{\sum_d T_{a,d}}{D}, \text{ for link } a=1, 2, \dots, A.$$

Step 5: Path assignment for PI and ETT vehicles.

For each day d , a certain percentage of PI vehicles are assigned to the least travel time path.

By adapting the path-swapping method proposed by Lu et al. (2009), this study uses the following probabilistic ratio for a vehicle on path p to switch to the least travel time path at iteration n :

$$\frac{1}{n+1} \times \frac{U_{p,d}^{i,j} - \pi_d^{i,j}}{U_{p,d}^{i,j}} \quad (3.21)$$

The first term $1/(n+1)$ is equivalent to the fixed step size in the Method of Successive Average (MSA). The second term ensures that the path swapping probability is proportional to the relative difference between the experienced path travel time $U_{p,d}^{i,j}$ and the minimum path travel time $\pi_d^{i,j}$. An intuitive interpretation for this heuristic swapping rule is that travelers on longer paths (i.e., farther from the equilibrium solution) are more likely to switch to the least travel time path than those on paths with travel cost closer to the least travel time path.

Similarly, a certain percentage of ETT vehicles are swapped to the least **expected** travel time path, the route swapping probability at iteration n can be determined by

$$\frac{1}{n+1} \times \frac{\bar{U}_p^{i,j} - \bar{\pi}^{i,j}}{\bar{U}_p^{i,j}} \quad (3.22)$$

As shown in Lu et al. (2009), search directions specified by equations (3.21-3.22) can be proven to be in the descent directions of the gap function in equation (3.11) for $f_{p,d}^{PI,i,j}$, $f_p^{ETT,i,j}$, respectively, at iteration n .

Step 6: Link flow aggregation.

For each day d , calculate the aggregated link volume $v_{a,d}$ using PI flow volume on day d and ETT flow (across every day), using equation (3.14).

Step 7: Convergence checking.

Calculate the gap function as shown in equation (3.11), if $Gap < \delta$ convergence is achieved, where δ is a prespecified parameter. If convergence is attained, stop. Otherwise, go to Step 3.

3.5 Experimental Results

The first set of experiments uses the simple corridor with two routes in the illustrative example, shown in Table 3.1. In this set of experiments, it is further assumed that links 1 and 2 have 3 and 2 lanes, respectively, and on this basis 100 days of random lane capacity are generated. The headway data used in this analysis were obtained from a recent research effort by Jia et al. (2010). In their study, the prebreakdown time headways are found to follow a shifted log-normal distribution with the following probability density function:

$$f_X = (x; \mu, \sigma) = \frac{1}{(x-c)\sigma\sqrt{2\pi}} e^{-\frac{(\ln x - \mu)^2}{2\sigma^2}}, \quad x > 0 \quad (3.23)$$

where

x is the average prebreakdown headway (in second) for 15-minute interval,

c is the minimum prebreakdown headway (in second),

μ is the mean of the variable's natural logarithm, and

σ is the standard deviation of the variable's natural logarithm.

Their calibration results based on data from several bottleneck locations in the Bay Area, California show that $c=1.5$ seconds, $\mu=-0.97$, and $\sigma=0.68$. To convert 15-minute breakdown flow rates to hourly capacity, we take an average value of 4 samples from the above random distribution. The histogram in Figure 3.8 shows the probabilistic distribution of 100 lane capacity samples on link 1. The stochastic distribution of hourly capacity has a sample mean of 1837 vehicles/hour/lane and a coefficient of variation of 0.064.

In Figure 3.8, most of samples range from 1700 to 2100 vehicles/hour/lane, which reveals the inherent randomness of road capacity. The hourly lane capacity is multiplied by the number of lanes to generate link capacity, and the resulting average total capacity of both links is 9,298 vehicles per hour.

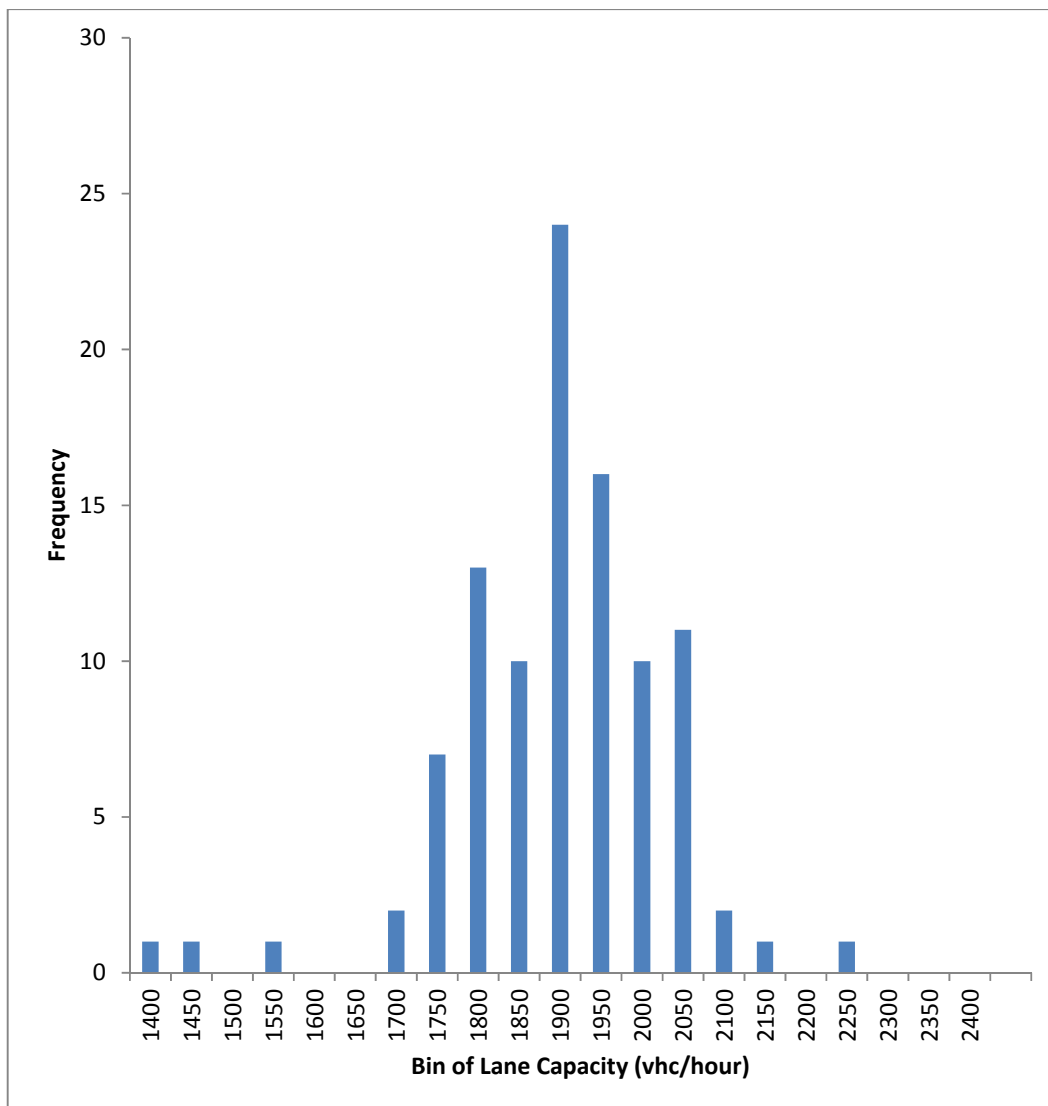


Figure 3.8-Histogram of 100 stochastic capacity samples.

3.5.1 Measure of effectiveness (MOE)

Mean travel time for users using ETT knowledge over different days can be represented as

$$\bar{T}^{ETT} = \frac{1}{|d|} \times \sum_d T_d^{ETT} \quad (3.24)$$

and the average travel time for ETT users on day d is

$$T_d^{ETT} = \frac{\sum_p \sum_{i,j} (f_p^{ETT} \times T_{p,d}^{ETT,i,j})}{q \times (1 - \gamma)} \quad (3.25)$$

where $T_{p,d}^{ETT,i,j}$ is the travel time experienced by ETT users on day d along path p for OD pair (i,j).

Travel time standard deviation is used to represent day-to-day travel time variability:

$$STD^{ETT} = \sqrt{\frac{\sum_d (T_d^{ETT} - \bar{T}^{ETT})^2}{(|d| - 1)}} \quad (3.26)$$

Similarly, \bar{T}^{PI} , \bar{T}_d^{PI} and STD^{ETT} can be calculated for PI users and \bar{T} , \bar{T}_d , STD for different classes of users.

Relative travel time improvement is defined as an indicator of the value of information:

$$\frac{\bar{T}^{ETT} - \bar{T}^{PI}}{\bar{T}^{ETT}} \quad (3.27)$$

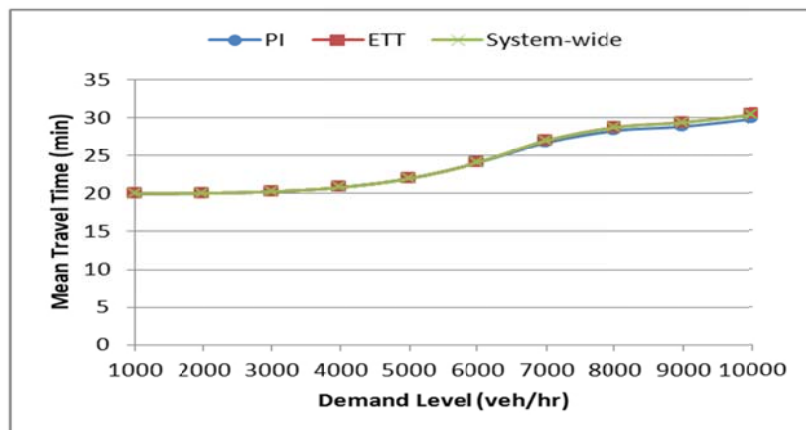
This measure compares the relative difference of mean travel time savings between PI and ETT users across all days.

3.5.2 Sensitivity analysis

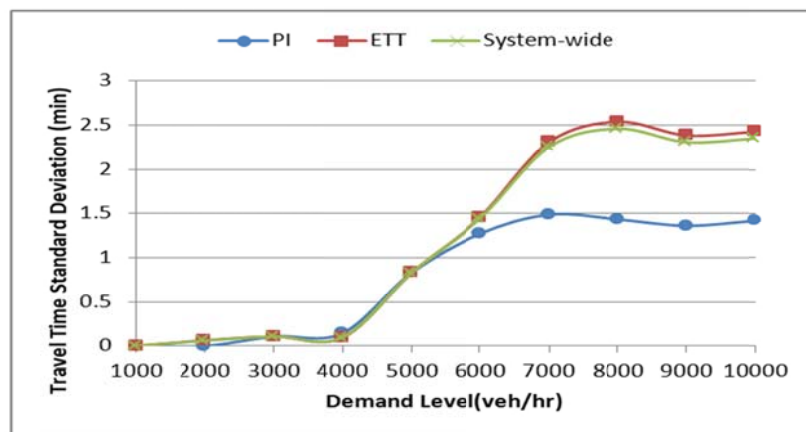
The following experiments describe the results of a sensitivity analysis for three major inputs: the total demand q , the market penetration rate of PI users, and the toll values imposed on the primary route. In the baseline configuration, $q = 8,000$ vehicle/hour, $\gamma = 0.05$ and there is no tolling on the primary routes.

3.5.2.1 MOE at varying demand levels

Figure 3.9 shows the different MOEs, when the total demand level q is varied between 1,000 and 10,000 vehicles per hour. Figure 3.9a shows that the average travel time dramatically increases after the total demand is raised above 4,000 vehicles per hour, which is close to the capacity of the primary route. Interestingly, Figure 3.9b shows that PI users experience significantly lower travel time variability compared to ETT users.



(a)

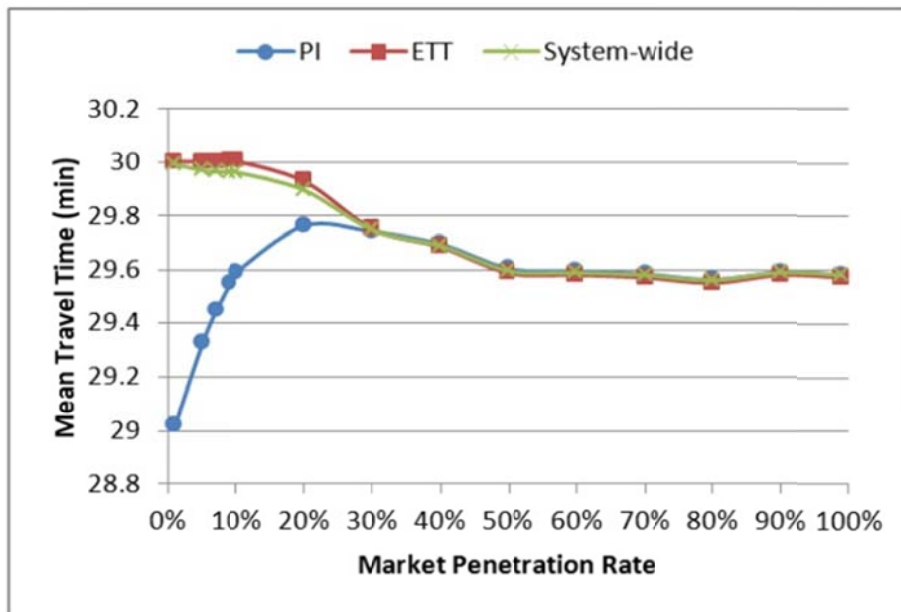


(b)

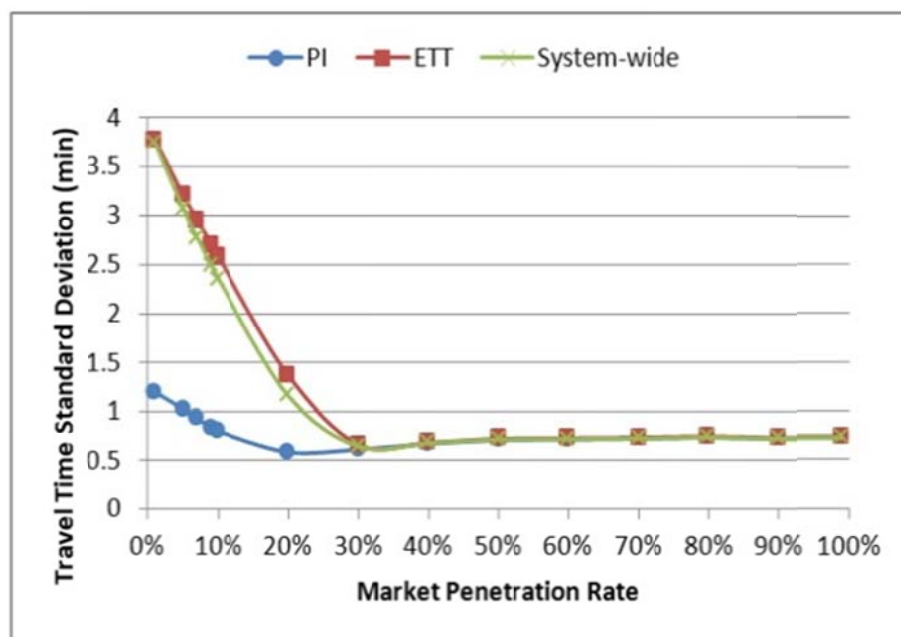
Figure 3.9-Effectiveness of information provision at varying demand levels.

3.5.2.2 MOE's at different market penetration rates

Figure 3.10 shows the sensitivity analysis results of travel time under different PI users market penetration rates. In many previous studies, the proposed models' aim was to evaluate the effect of varying market penetration rates and identify the saturation level of market penetration of ATIS services. In this research the objective is to understand the relationship between market penetration rate and the value of information.



(a)



(b)

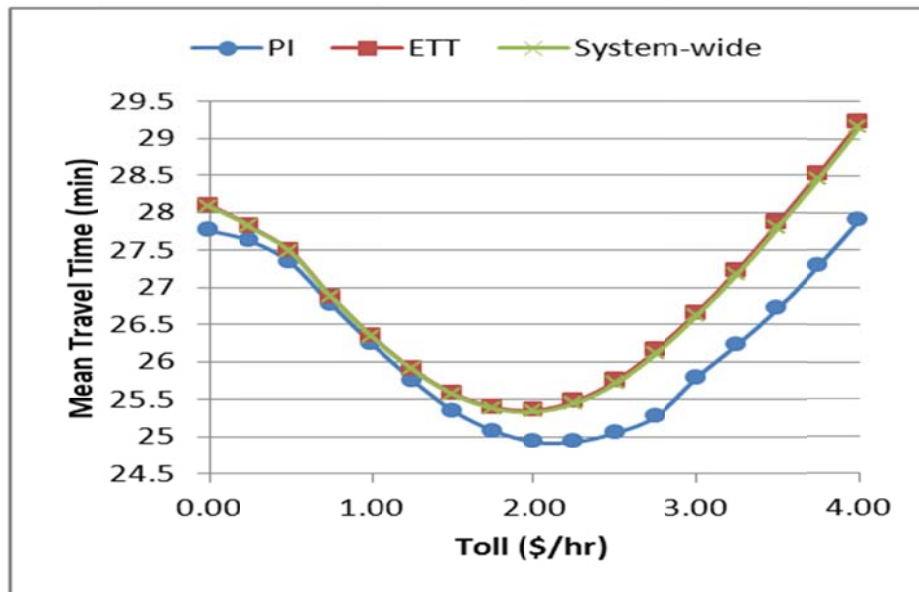
Figure 3.10-Effectiveness of information provision with different market penetration rate.

When the market penetration rate is below 30%, all PI users are able to switch from a congested route (typically route 1) to a less congested route (typically route 2), so that travel information provision strategies yield meaningful savings in terms of mean travel time and travel time variability (Figure 3.10a, Figure 3.10b). However, when the market penetration rate exceeds a certain threshold (30% in our example), a large number of PI users can take the detour, so the previously less congested route becomes crowded. Under the assumption of user equilibrium with perfect information, both routes at this point should have the same travel time so that no PI user can reduce his/her travel time by switching routes. This implies no additional benefit is available by using traveler information strategies.

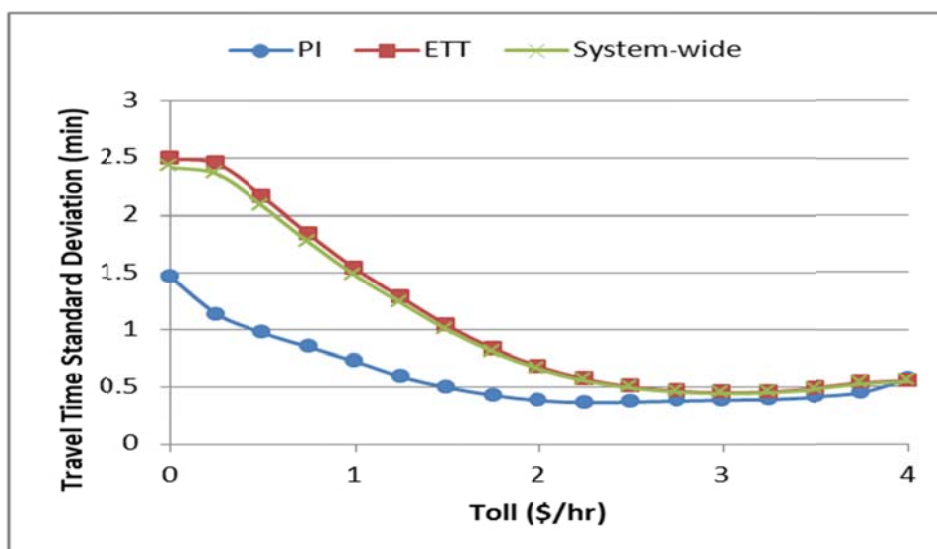
Although the finding on the diminishing value of information as a function of market penetration rate is similar to a number of previous studies (for example, Yang et al., 1993; Yang, 1999), those findings are based on two fundamentally different settings. Thus, for travelers not equipped with ATIS, previous studies have considered different levels of perception errors under deterministic capacity for a single day, while this proposed approach assumes no perception error on the expected travel time of multiple days with stochastic capacity.

3.5.2.3 MOE's at different tolling rates

Figure 3.11 shows the results with 5% PI users, with a static toll being imposed on route 1 to encourage route switching to route 2. The value of time is set to \$15 per hour, so each dollar is equivalent to 4 minutes of travel time.

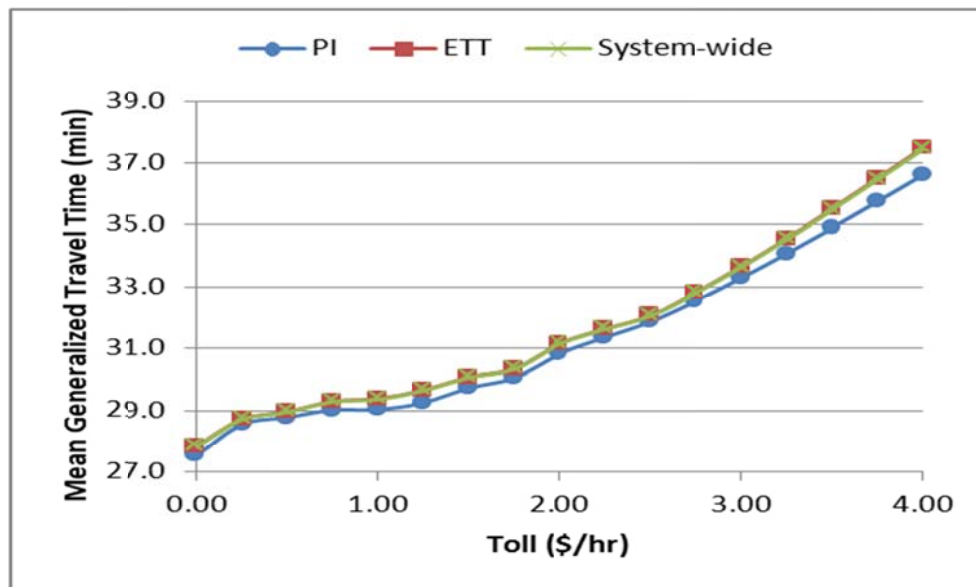


(a)



(b)

Figure 3.11- Effectiveness of information provision with varying toll.



(c)

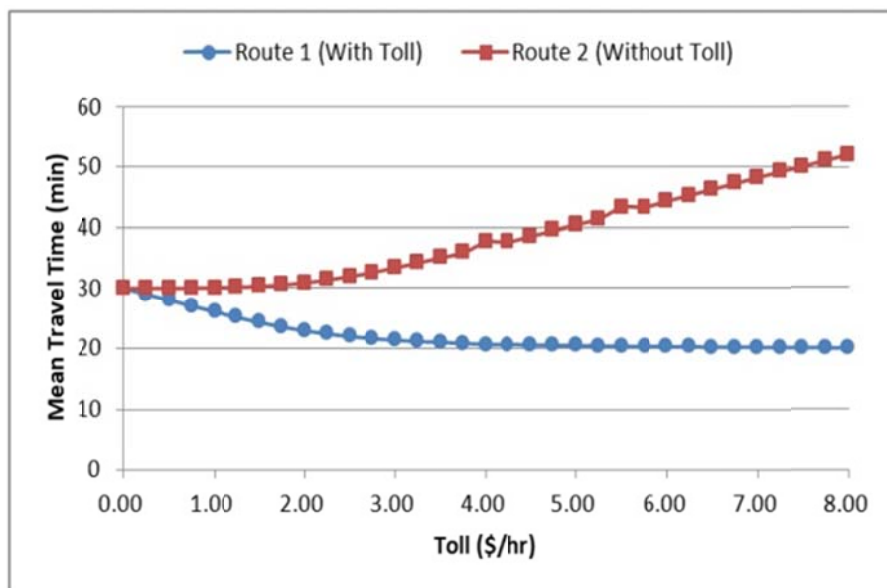
Figure 3.11- Continued

Figure 3.11a shows strong bowl-shaped curves, indicating an optimal toll value of \$2 in order to reduce the average (experienced) travel time to about 25.5-min for all users. This shows that the ideal system-optimal state can be approached using tolled user equilibrium patterns.

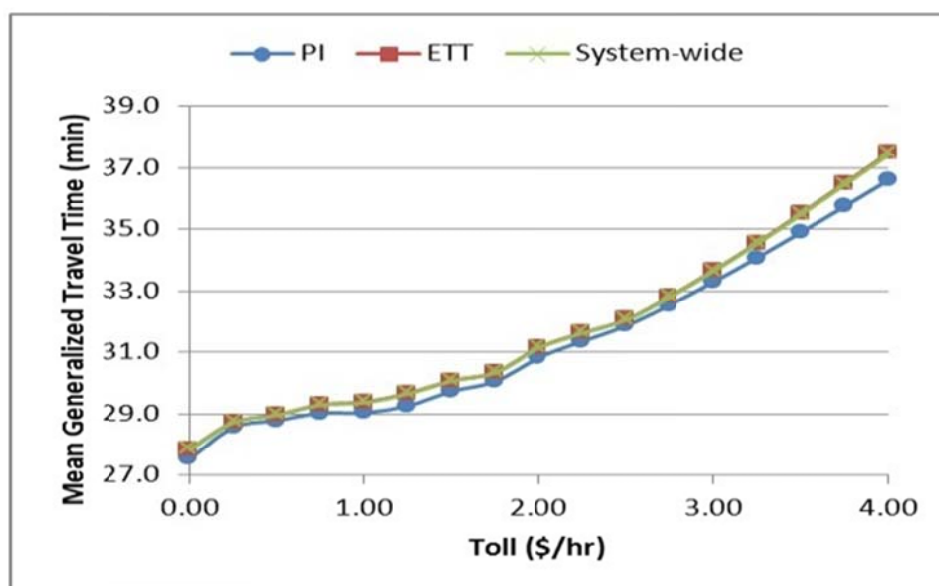
Figure 3.11b demonstrates another benefit of the toll strategy as it can dramatically reduce the travel time variability for all users. If the generalized travel time is considered (including both pure travel time and equivalent travel time associated with tolls), the mean generalized travel time in Figure 3.11c of all the solution strategies grows gradually with increasing toll values.

Road pricing is an effective instrument for mitigating congestion. Ideally, road pricing rate is calculated based on 1) marginal social cost due to congestion (usually not perceived by the users) and 2) the private cost (perceived by the users). But applying this theory is very difficult due to the unclear relationship between the demand function and the cost function.

One key assumption in this model is that a for-pay service can advise users about the best route (with lower travel time) as shown in Figure 3.12a, in spite of the fact that both routes have the same disutility (travel time/VOT + toll) in Figure 3.12b. Comparison of the path travel time standard deviation without tolls on route 2 and with the varying toll level on route 1 is shown in Figure 3.12c. Without tolls, path travel time distributions show large standard deviations. With the toll, the path travel time distributions reveal much smaller variations depending on the toll level. Because the flow on route 1 is reduced (due to the imposed toll), travel time reliability has been decreased accordingly by charging a toll on route 1.

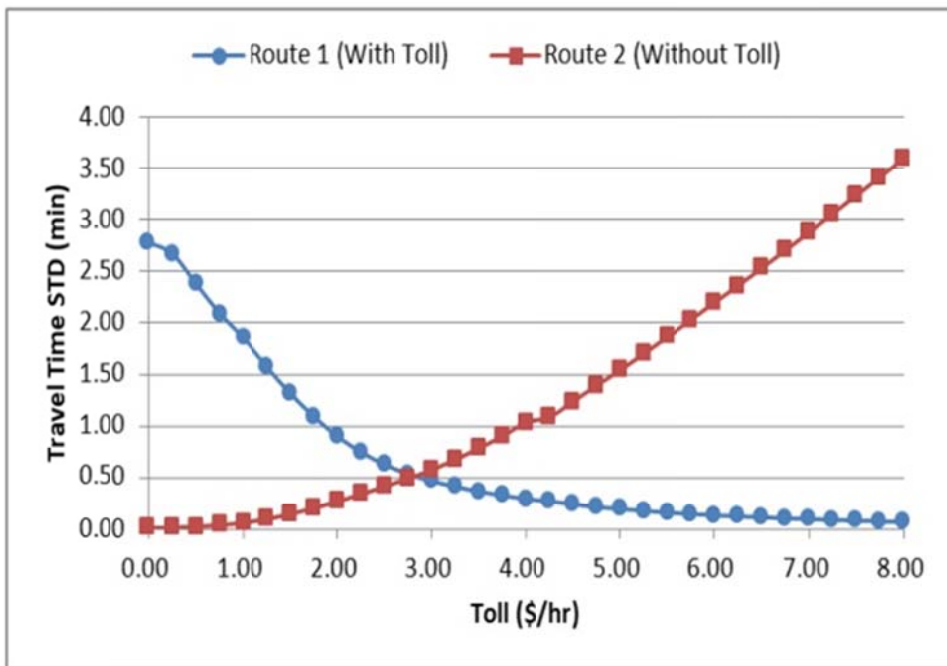


(a)

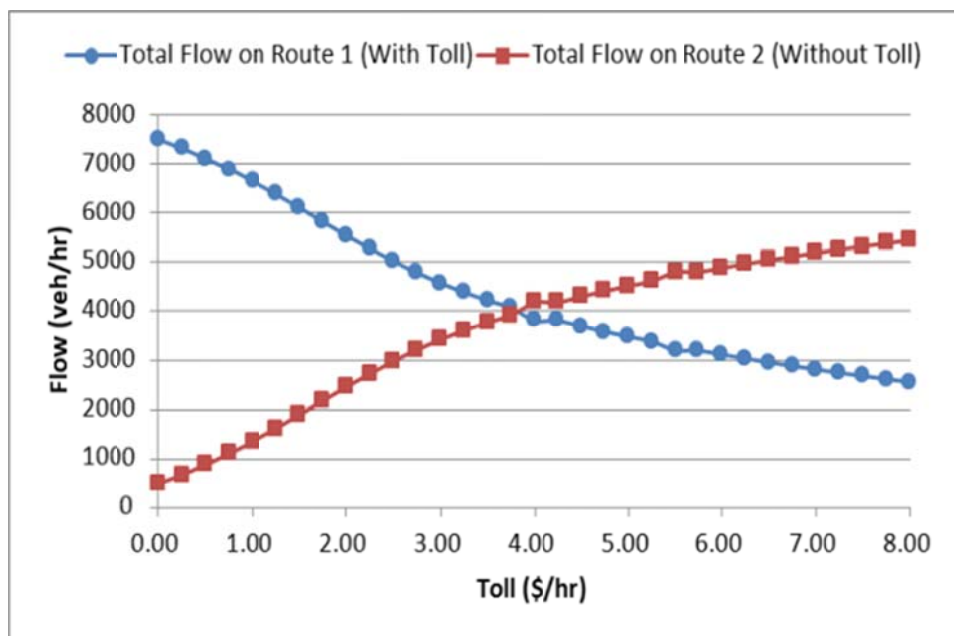


(b)

Figure 3.12- Effectiveness of information provision for different routes with varying toll.



(c)



(d)

Figure 3.12- Continued

As shown in Figure 3.12d, the proposed model has the potential to hold the traffic flow within a given capacity or desirable level by applying varying tolling levels and illustrates more clearly the potential of these tolling strategies for congestion mitigation purposes when it comes to “paying” for reduced travel time.

3.5.2.4 Impact of FFTT difference and demand level on value of information

Figure 3.13 shows how the free-flow travel time (FFTT) difference between the primary and second routes affects the computed value of travel information at different demand levels ranging from 5000 to 9000 veh/h.

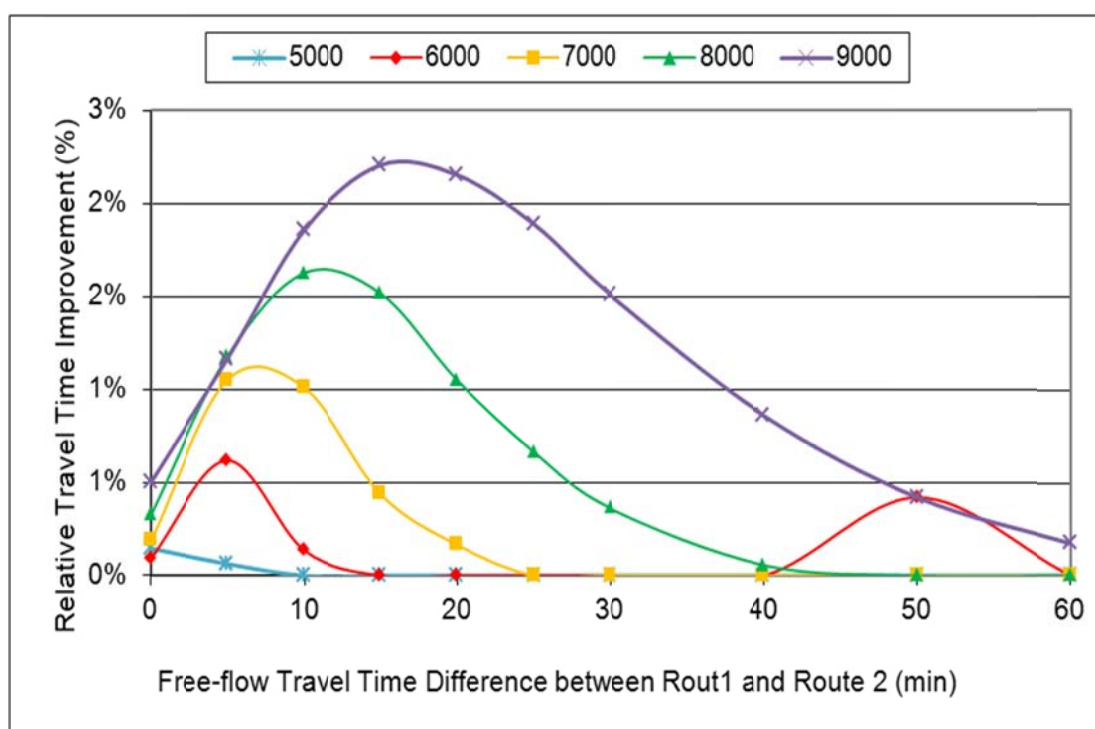


Figure 3.13- Value of information as a function of FFTT difference and demand level.

The plot demonstrates that for a fixed 5% PI market penetration rate and certain demand level (say 8000 veh/h), if both routes have similar free-flow travel times, then the value of information is not too significant. When the free-flow travel time difference increases (that is, the alternative route becomes less attractive compared to the primary route), the benefit of information provision grows steadily and reaches a maximum value. Beyond that, the value of information begins to drop, as the free-flow travel time difference is too large to generate meaningful route switching opportunities under a user equilibrium condition. By comparing the curves associated with different demand levels, the peaks of the value of information function shift to the right. Also, higher demand levels (i.e., a more congested system) yield significantly higher value of travel information at the same free-flow travel time difference.

3.5.3 Experiments on medium-scale networks

The following numerical experiments are performed on two medium-scale network data sets, which are publicly available at a website maintained by Bar-Gera (2001). The proposed algorithm is implemented in C++ on the Windows Vista 64-bit platform and evaluated on a computer with an Intel Xeon CPU with 4 2.33 GHz processors and 9 GB memory.

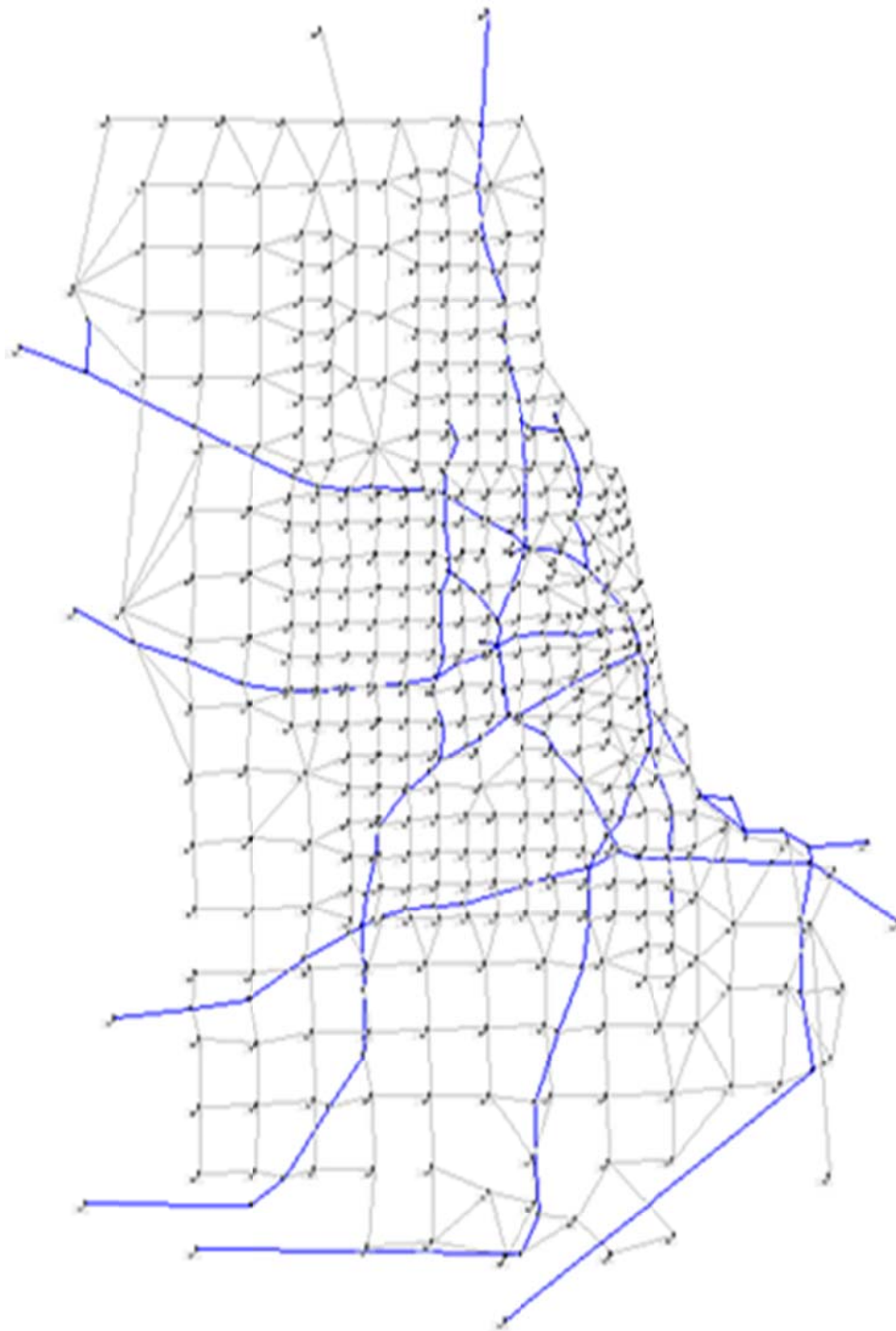
To fully utilize the available parallel computing capability, all the shortest path calculations and path assignment computations for different origin zones (at steps 4 and 5) are migrated to different processors. The above parallelization scheme is implemented through an Open Multi-Processing (OpenMP) shared-memory parallel programming interface. As shown in Figure 3.7, the parallelization of shortest path calculation can be also carried out for different days.

As shown in Figure 3.14 and Table 3.2, the Anaheim, California network contains about 38 zones, and 0.1 million vehicles, and the Chicago sketch network, an aggregated representation of the Chicago region, has 387 zones with 1.2 million vehicles.

Under a setting of 10% PI users, 20 assignment iterations and 30 days of random road capacity, the Anaheim network uses about 30 minutes, and the Chicago sketch network takes about 8 hours of CPU time and 2.6G memory. There are three major factors affecting the computational complexity of the proposed algorithm: (1) the number of OD zones, (2) the number of days in the random capacity representation, and (3) the number of PI vehicles. Specifically, the first two factors are related to the number of path finding calculations, as the algorithm must find the least travel time routes using day-dependent travel time for PI vehicles originating from each origin zone. The other two factors, namely the number of days and the number of PI vehicles, jointly determine the complexity of path swapping operations, as each PI vehicle must carry and update individual paths on different days in the proposed path-based and mesoscopic representation. In addition, as steps 4 and 5 are the most computationally intensive in the proposed algorithm, additional CPU cores can also accordingly speed up the overall computational process through parallel computing.

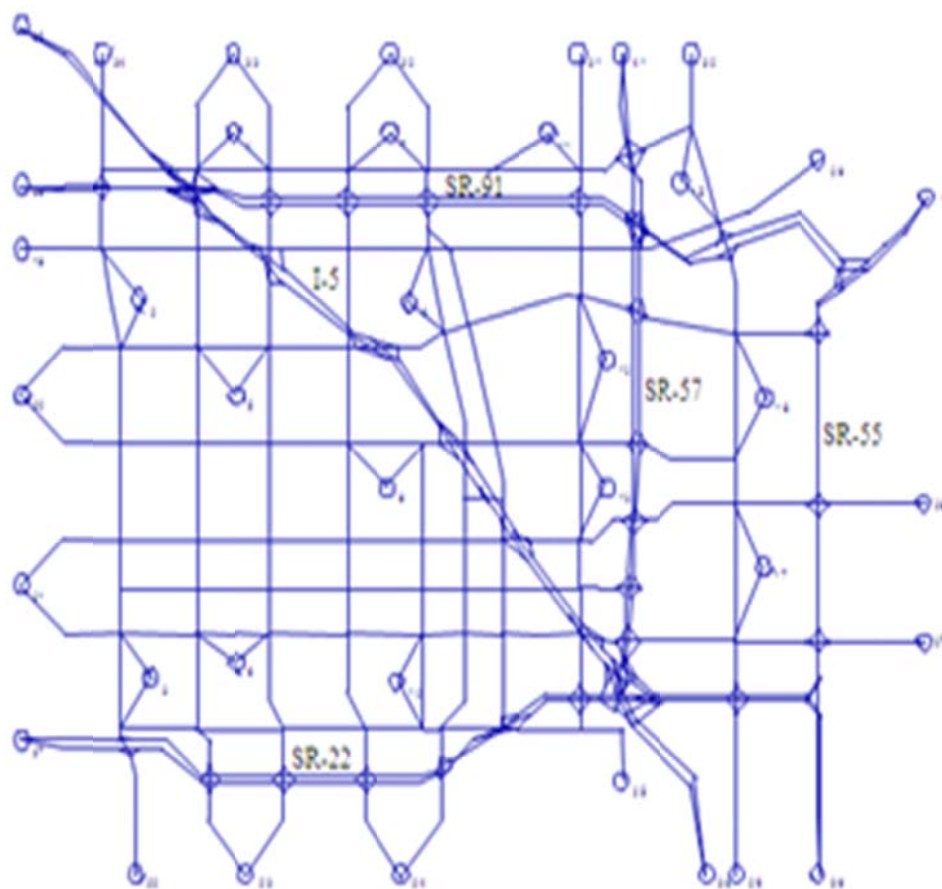
To measure the convergence of the proposed algorithm, we use the following average optimality gap as the solution quality indicator:

$$AvgGap = \frac{1}{D \times \sum_{i,j} q^{i,j}} \times \sum_d \sum_i \sum_j \sum_p \left[f_{p,d}^{PI,i,j} \times (U_{p,d}^{i,j} - \pi_d^{i,j}) + f_p^{ETT,i,j} \times (\bar{U}_p^{i,j} - \bar{\pi}^{i,j}) \right]. \quad (3.28)$$



(a)

Figure 3.14-Chicago sketch network (a) and Anaheim, California network (b).



(b)

Figure 3.14-Continued

Table 3.2- Test network characteristics and computational performance.

	Anaheim, California	Chicago Sketch Network
# of nodes	416	933
# of links	914	2950
# of OD zones	38	387
Total OD Volume	104K	1,261K
Computational time	34 min	8 h 16 min
Average optimization Gap(min)	0.289	0.344

With 30 day samples, 20 iterations and 10% PI vehicles.

Figure 3.15 compares the convergence of two algorithms in the Chicago sketch network: (i) the proposed route-swapping algorithm that uses the swapping ratio in equation (3.22), (ii) the algorithm uses the conventional MSA method with a fixed step size of $1/(n+1)$, where n is the iteration counter. Both algorithms can steadily reduce the optimality gap toward zero, and the average gap measures reach within 0.5 minutes per vehicles within the first 10 iterations. In comparison, the proposed route swapping rule is able to more quickly decrease the optimality gap within first 5-7 iterations. Shown in Table 3.2, the two test networks have quite small optimality gaps at iteration 20, namely 0.289 and 0.344 minutes. To reduce the overall computational efforts, one might consider using fewer iterations as long as the solution quality reaches an acceptable level.

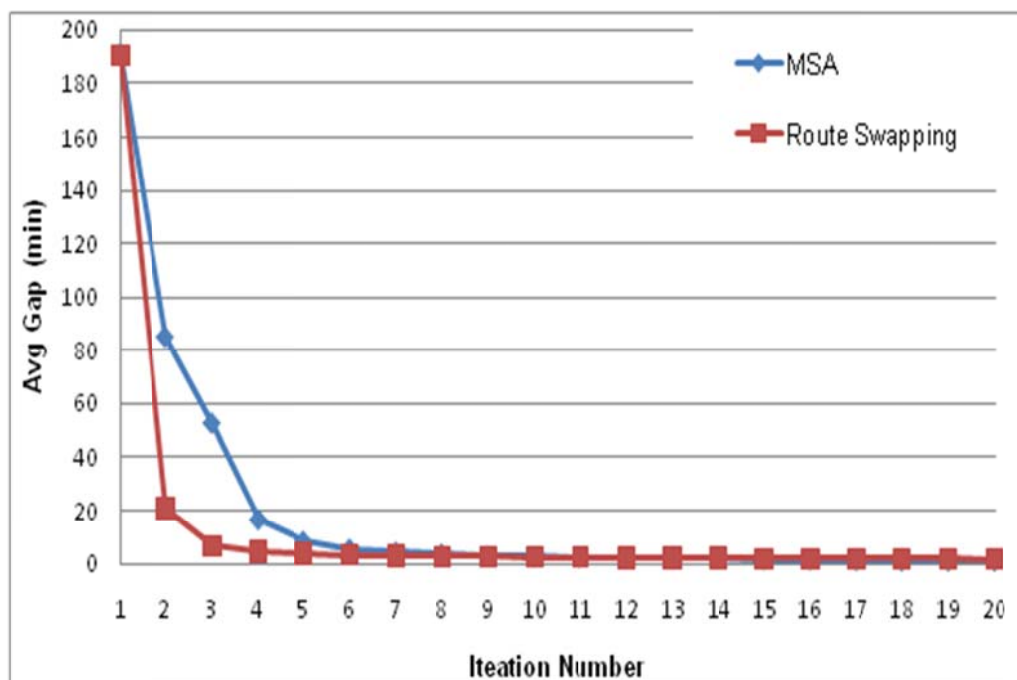


Figure 3.15- Convergence patterns on Chicago sketch network.

The original data sets use the BPR function to describe travel time performance, and a single valued mean capacity is specified for each link. To generate random road capacity samples, we use the prebreakdown headway distribution in equation (3.23) to generate multiple samples of 15-minute prebreakdown capacity first. To approximate the peak-hour capacity values used in the BPR function, we evaluate the impact of two alternative schemes:

(i) Possible multiple congestion periods within a peak hour, so we use the average of 4 prebreakdown capacity values as the peak hour capacity, leading to a Coefficient of Variation (CV) = 6.4%.

(ii) Single congestion period, where a single value of 15-minute prebreakdown capacity becomes the dominating factor for the whole peak hour, leading to CV = 12.8%.

As shown in Table 3.3, the single valued prebreakdown capacity implies larger variations compared to the average (aggregated) prebreakdown capacity, so it slightly increases the average travel time for PI and ETT travelers on both networks. However, according to the above experimental results, the travel time savings obtainable for PI users seem to be not too significant even under the large link travel time variations. Similarly, for the hypothetical network in Figure 3.2, the capacity variations also only lead to less than 1-minute travel time savings due to traveler information provision, shown in Figure 3.10 (a).

To fully understand the benefit of traffic information provision, an analyst needs to better characterize travel time dynamics/variability, which is caused by a wide range of recurring and nonrecurring delay sources, such as incidents, work zones, and random fluctuations in road capacity.

Table 3.3- Value of traveler information under different peak-hour capacity approximation schemes.

Peak-hour Capacity Approximation Scheme	Anaheim network			Chicago Sketch Network		
	ETT Travel Time	PI Travel Time	Average Relative Travel Time Saving (%)	ETT Travel Time	PI Travel Time	Average Relative Travel time Saving (%)
Average Prebreakdown Capacity with CV= 0.064	12.903	12.864	0.302%	17.348	17.242	0.611%
Single-valued Prebreakdown Capacity with CV= 0.128	13.233	13.157	0.574%	17.794	17.469	1.827%

Although the proposed framework allows and is naturally suited to consider any given random capacity distributions with a multiday or sample-based representation scheme, the calibrated capacity distribution used in our study in fact only focuses on “normal” random capacity perturbations, while the “outliers” in the capacity distribution due to nonrecurring events such as incidents, work zone, severe weather, are not explicitly modeled in the given capacity distribution and should also be integrated in the future research to fully account for the benefits of traveler information provision strategies under random capacity breakdowns and “unplanned” events.

3.6 Summary

In this chapter, a novel nonlinear optimization-based analysis method is proposed along with related modeling components pertaining to stochastic capacity, travel time performance functions and different degrees of traveler knowledge in an ATIS

environment. Within a multiday analysis framework, this proposed method categorizes commuters into two classes: (1) travelers with access to perfect traffic information every day, and (2) travelers with some degree of knowledge of average traffic conditions across different days. Within a gap function framework (for describing the user equilibrium under different information availability), a mathematical programming model is formulated to describe the route choice behavior of the perfect information (PI) and expected travel time (ETT) user classes under stochastic day-dependent travel time. The model was applied to a simple corridor and two medium-scale networks to illustrate the effectiveness of traveler information under stochastic capacity.

CHAPTER 4

MULTIDAY STATIC TRAFFIC EQUILIBRIUM ANALYSIS UNDER STOCHASTIC DEMAND AND CAPACITY CONDITIONS

4.1 Introduction

In addition to systematic variations due to seasonal and weekly patterns, the stochasticity in traffic demand can be caused by special events, severe weather conditions and random variations. In reality, in response to variations of stochastic and day-variant travel time, a majority of commuters only have knowledge about the average traffic conditions across different days, and accordingly make their habitual route choice decisions to minimize the expected path travel time. Travelers who are equipped with advanced traveler information can select different routes on different days, depending on prevailing traffic conditions. In comparison, although end-to-end travel time variability measures might be approximated through numerical perturbation or statistical inference methods around the single steady-state solution, the single-day equilibrium representation has two limitations: First, it is unable to capture the day-variant route choice behavior by equipped travelers in an environment with stochastic capacity and demand. Second, its underlying Logit model typically assumes the perception error has a mean of zero and the

perceived travel time is an unbiased estimate of the actual travel time. However, for any given day, the information, (i.e. average travel time perception) used by unequipped travelers becomes biased travel time estimates toward prevailing traffic conditions on a particular day. A “day” in this multiday model can be viewed as a random sample or realization from a stochastic programming perspective.

This chapter aims to systematically evaluate benefits of traveler information provision strategies in a realistic environment with stochastic traffic demand, stochastic road capacity, and different degrees of traveler knowledge and traffic information provision quality. Based on a stochastic user equilibrium modeling framework, the proposed model uses a multiday representation scheme to describe stochastic samples of uncertain demand and capacity supply, as well as day-dependent travel time. Two classes of travelers are considered: travelers who have knowledge on average traffic conditions and select single paths over different days, and travelers who can make day-varying route choice decisions based on prevailing traffic information available every day. A gap-function based optimization model is further developed to find equilibrium solutions, and a number of representative examples are used to illustrate how the proposed method can systematically evaluate the travel time reliability-related benefit of traffic information quality improvement and demand smoothing strategies.

The remainder of this chapter is organized as follows. The second section provides a conceptual framework and then discusses the related modeling components. The third section presents a gap function-based mathematical programming formulation. A graphical method and illustrative examples are used in the fourth section to describe equilibrium solutions for different representative cases with stochastic demand and

stochastic capacity. The solution algorithm for a general large-scale network is presented in the last section, followed by numerical experimental results.

4.2 Problem Statement and Illustrative Example

The sets and subscripts, parameters and decision variables in the proposed stochastic flow assignment model are introduced as follows:

Indices:

- i = index of origins, $i = 1, \dots, I$, where I is the number of origins
- j = index of destinations, $j = 1, \dots, J$, where J is the number of destinations
- p = index of paths, $p=1, \dots, P$, where P is the number of paths between an OD pair i and j
- a = index of links, $a=1, \dots, A$, where A is the number of links in networks
- d = index of days, $d=1, \dots, D$, where D is the number of days over analysis horizon

Input Parameters:

- $c_{a,d}$ = realized capacity value of link a on day d from a stochastic distribution
- $q_d^{i,j}$ = OD demand volume between an OD pair i and j on day d from a stochastic distribution.
- $\delta_{p,a}$ = path-link incidence coefficient, $\delta_{p,a}=1$, if path p passes through link a , and 0 otherwise
- γ = market penetration rate of the travel information (TI) users as a function of the total OD demand

a positive unit scaling parameter between travel time units and utility units

ρ^{TI}, ρ^{ETT} = for TI and ETT users, respectively, related to the quality of information/knowledge

Decision variables:

$f_{p,d}^{TI,i,j}$ = flow of TI users on path p for OD pair ij on day d

$y_{p,d}^{TI,i,j}$ = flow ratio of TI users on path p for OD pair ij on day d

$f_{p,d}^{ETT,i,j}$ = flow of ETT users on path p for OD pair ij on day d

$y_p^{ETT,i,j}$ = flow ratio of ETT users on path p for OD pair ij (flow rates are the same across different days)

$v_{a,d}$ = total flow on link a on day d

$T_{a,d}$ = travel time on link a on day d

$T_{p,d}^{i,j}$ = travel time of path p between OD pair ij on day d

$\overline{T_p^{i,j}}$ = expected travel time of path p between OD pair ij over the multiday horizon

$\pi_d^{i,j}$ = day-dependent reference path disutility between OD pair i and j on day d

$\overline{\pi^{i,j}}$ = least reference expected disutility between OD pair i and j over the multiday horizon

To illustrate the mathematic formulation to be introduced later, let us start with a simple network with two nodes, two links, and one OD pair, as shown in Figure 4.1. As each path only has one route, we denote primary path $p=1$ as link $a=1$ with a free-flow travel time of 20 minutes, and denote alternative path $p=2$ as link $a=2$ with a free-flow travel time of 30 minutes. This example considers 25 different days $d = 1, 2, \dots, D$, where the number of days $D=25$.

The alternative path is assumed to have a fixed capacity of $c_{a,d}=3000$ vehicles per hour per lane for all days. The primary path has an 80% probability to have a full 4500 veh/h capacity and has a 80% chance to have a reduced 3000 veh/h capacity. Our example considers a high demand level as 9600 veh/h with a 20% probability, and a low demand level as 7600 veh/h with a 80% probability. The distributions of stochastic demand and capacity are assumed to be independent. Shown in the bottom part of Figure 4.2, days 1, 6, 11, 16 are 21 have a reduced capacity on link 1, and days from 21 to 25 have a high demand level. The day-by-day travel time pattern changes when changing the market penetration rate from 0% to 5%, and the latter case demonstrates reduced travel time variability on different demand/supply combinations.

Obviously, the sum of path flows on this corridor equals to the total OD demand,

$$f_{1,d} + f_{2,d} = q_d \quad \forall d \quad (4.1)$$

Without loss of generality, this study uses the widely used Bureau of Public Road (BPR) function as the link performance function.

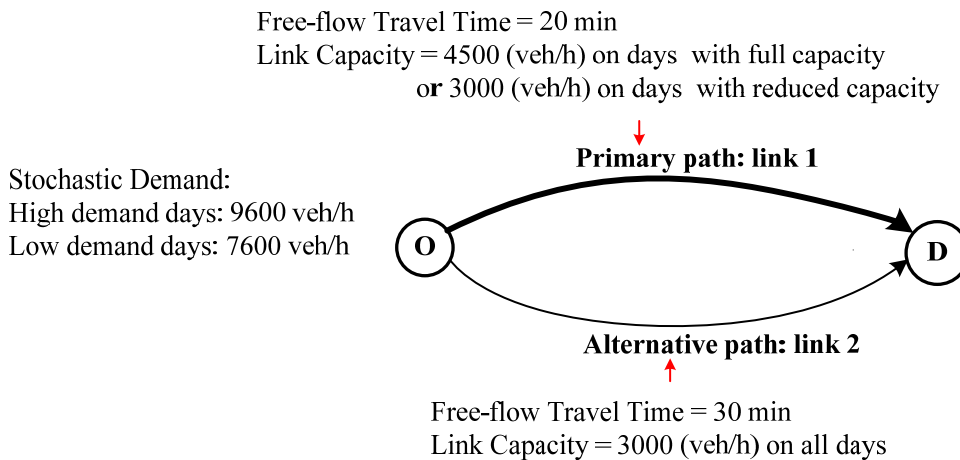


Figure 4.1- Simple network used as an illustrative example.

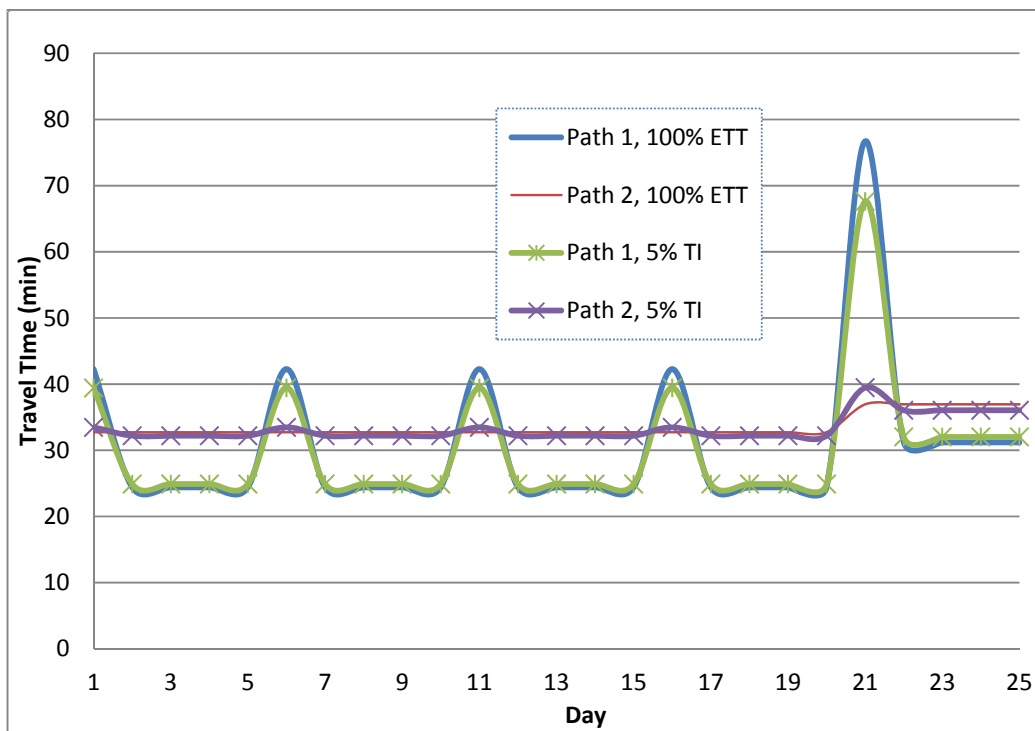


Figure 4.2- Time-dependent capacity, demand and travel time patterns under different vehicle information market penetration rates.

$$T_{a,d} = FFTT_a \times \left(1 + \alpha \times \left[\frac{f_{a,d}}{c_{a,d}} \right]^\beta \right) \quad (4.2)$$

where $FFTT_a$ are the travel time and free-flow travel time of link a . In the following examples, the common values of parameters $\alpha = 0.15$ and $\beta = 4$ were used.

This study considers two different information user classes with different degrees of traveler information accessibility.

4.2.1 Traveler information (TI) users

Every day, link travel time estimates with a certain level of prediction errors are available for TI traveler to make route decisions, and a TI traveler can select a route on each day to minimize their perceived path disutility. Within a discrete choice modeling framework, the utility for a TI user to travel over a given path p equals the negative path travel time $T_{p,d}$ on day d

$$U_{p,d}^{TI} = V_{p,d}^{TI} + \varepsilon_{p,d} = -\frac{T_{p,d}}{\rho^{TI}} + \varepsilon_{p,d} \quad p = 1, 2, \forall d \quad (4.3)$$

where ρ is a positive unit scaling parameter between travel time units and utility units, and $\varepsilon_{p,d}$ is a random error term, independent and identically distributed (iid) for all routes. The perception error term $\varepsilon_{p,d}$ is assumed to follow a Gumbel distribution, which leads to a commonly used multinomial logit model. Scaling parameter ρ reflects

the level of information quality, a very small ρ indicates a low-error and high-quality information source. If ρ converges to zero, then perfect information is available to TI users.

4.2.2 Expected travel time (ETT) knowledge users

In response to random day-to-day travel time variations, unequipped travelers rely on their expected travel times (based on their network knowledge and past experience) over different days to make route choices. The expected travel time can be considered as the probability-weighted sum of the possible travel time values in the analysis time horizon. Under a steady-state multiday user equilibrium condition, the expected travel times on used routes in the network are assumed to be the same, and an ETT user always chooses the same route every day according to the following utility function.

$$U_p^{ETT} = V_p^{ETT} + \varepsilon_p = -\frac{\bar{T}_p}{\rho^{ETT}} + \varepsilon_p \quad p = 1, 2. \quad (4.4)$$

where $\bar{T}_p = \frac{1}{D} \sum_d T_{p,d}$

For link a , the expected travel time is

$$\bar{T}_a = \frac{1}{D} FFFT_a \times \sum_d \left(1 + \alpha \times \left(\frac{f_{a,d}}{c_{a,d}} \right)^\beta \right) = FFFT_a \times \left(1 + \frac{1}{D} \sum_d \left[\alpha \times \left(\frac{f_{a,d}}{c_{a,d}} \right)^\beta \right] \right) \quad (4.5)$$

As the BPR function is a convex function, one can easily prove that, through Jensen's inequality and by considering the flow-to-capacity ratio as a random variable, the average travel time obtained from equation (4.5) is greater than the value calculated based on the average flow-to-capacity ratio.

$$\begin{aligned} \bar{T}_a &= FF\bar{T}T_a \times \left(1 + \frac{1}{D} \sum_d \left[\alpha \times \left(\frac{f_{a,d}}{c_{a,d}} \right)^\beta \right] \right) \\ &\geq T_a \left(E \left(\frac{f_{a,d}}{c_{a,d}} \right) \right) = FF\bar{T}T_a \times \left(1 + \alpha \times \left[E \left(\frac{f_{a,d}}{c_{a,d}} \right) \right]^\beta \right), \end{aligned} \quad (4.6)$$

where $E \left(\frac{f_{a,d}}{c_{a,d}} \right)$ is the mean ratio of flow and capacity on link a over different days, respectively. This indicates that, using the mean volume-to-capacity ratio, in a single-day equilibrium representation, to calculate the expected travel time under stochastic demand and capacity distributions could underestimate the actual expected congestion level.

4.3 General Mathematical Problem Formulation

We first list all the constraints in the proposed optimization model that aims to incorporate two user classes (in terms of day-dependent flow $f_{p,d}^{TI,i,j}$ and $f_{p,d}^{ETT,i,j}$) into a stochastic traffic assignment framework under day-dependent capacity $c_{a,d}$ and day-dependent demand $q_d^{i,j}$ during the peak hour. Specifically, constraints (4.7) and (4.8) show the relationship between OD demand and path flows for each information class. Equation (4.9) aggregates path flows from two different user classes to link flows.

Equations (4.10-4.11) calculate the path disutility for each path on day d . Equation (4.12) defines the average disutility for each path across different days.

TI flow constraints:

$$\gamma \times q_d^{i,j} = \sum_p f_{p,d}^{TI,i,j} \quad \forall i, j, d \quad (4.7)$$

ETT flow constraints

$$(1 - \gamma) \times q_d^{i,j} = \sum_p f_{p,d}^{ETT,i,j} \quad \forall i, j, d \quad (4.8)$$

Path - link flow balance constraints

$$v_{a,d} = \sum_{i,j,p} \left[\left(f_{p,d}^{TI,i,j} + f_{p,d}^{ETT,i,j} \right) \times \delta_{p,a} \right] \quad \forall a, d \quad (4.9)$$

Path- link cost connection

$$T_{a,d} = BPR(v_{a,d}, c_{a,d}) \quad \forall a, d \quad (4.10)$$

$$T_{p,d}^{i,j} = \sum_a (T_{a,d} \cdot \delta_{p,a}) \quad \forall i, j, p, d \quad (4.11)$$

Average disutility definitional constraint:

$$\bar{T}_p^{i,j} = \frac{1}{D} \sum_d T_{p,d}^{i,j} \quad \forall i, j, p \quad (4.12)$$

Definitional constraints:

$$0 < y_{p,d}^{TI,i,j} \leq 1, 0 < y_p^{ETT,i,j} \leq 1, f_{p,d}^{ETT,i,j} > 0, f_{p,d}^{TI,i,j} > 0, \forall i, j, p, d \quad (4.13)$$

To construct an optimization model of a stochastic traffic assignment program, we define the following gap function for TI users, in a general network.

Objective function:

$$\begin{aligned} \min Gap = & \sum_{d,i,j,p} \left[y_{p,d}^{TI,i,j} \times \left(\rho^{TI} \ln y_{p,d}^{TI,i,j} + \Gamma_{p,d}^{i,j} - \pi_d^{i,j} \right) \right]^2 \\ & + D \times \sum_{i,j,p} \left[y_p^{ETT,i,j} \times \left(\rho^{ETT} \ln y_p^{ETT,i,j} + \overline{\Gamma}_p^{i,j} - \overline{\pi}^{i,j} \right) \right]^2 \end{aligned} \quad (4.14)$$

Since $y_{p,d}^{TI,i,j}$ and $y_p^{ETT,i,j}$ are always positive for feasible paths in a logit model, the optimal solution of the proposed mathematical program reduces the gap to zero, leads to equations (4.15 - 4.16),

$$\rho^{TI} \ln y_{p,d}^{TI,i,j} + \Gamma_{p,d}^{i,j} - \pi_d^{i,j} = 0 \quad \forall i, j, p, d \quad (4.15)$$

$$\rho^{ETT} \ln y_p^{ETT,i,j} + \overline{\Gamma}_p^{i,j} - \overline{\pi}^{i,j} \quad \forall i, j, p \quad (4.16)$$

In this study, we extend the gap-function reformulation method developed by Zhou et al. (2007) (for modeling stochastic time-dependent user equilibrium conditions) to describe the day-dependent statistic user equilibrium conditions. Essentially, we want to show equation (4.15) is equivalent to the logit route choice model used in a stochastic path assignment function as

$$y_{p,d}^{TI,i,j} = \frac{\text{Exp}\left(-\frac{\Gamma_{p,d}^{i,j}}{\rho^{TI}}\right)}{\sum_p \text{Exp}\left(-\frac{\Gamma_{p,d}^{i,j}}{\rho^{TI}}\right)}, \quad \forall i, j, p, d \quad (4.17)$$

In addition, equation (16) is equivalent to equation (18).

$$y_p^{ETT,i,j} = \frac{\text{Exp}\left(-\frac{\overline{\Gamma_p^{i,j}}}{\rho^{ETT}}\right)}{\sum_p \text{Exp}\left(-\frac{\overline{\Gamma_p^{i,j}}}{\rho^{ETT}}\right)}, \forall i, j, p, d \quad (4.18)$$

Obviously, equation (15) can be re-expressed as

$$y_{p,d}^{TI,i,j} = \text{Exp}\left(\frac{-T_{p,d}^{i,j} + \pi_d^{i,j}}{\rho^{TI}}\right) = \text{Exp}\left(\frac{-T_{p,d}^{i,j}}{\rho^{TI}}\right) \times \text{Exp}\left(\frac{\pi_d^{i,j}}{\rho^{TI}}\right) \quad (4.19)$$

Since $\sum_p y_{p,d}^{TI,i,j} = 1$, we can derive that

$$\text{Exp}\left(\frac{\pi_d^{i,j}}{\rho^{TI}}\right) = \frac{1}{\sum_p \left[\text{Exp}\left(\frac{-T_{p,d}^{i,j}}{\rho^{TI}}\right) \right]}. \quad (4.20)$$

Substituting equation (4.20) into equation (4.19) leads to equation (4.17).

Similarly, we can prove the equation (4.16) and equation (4.18) are equivalent.

In the objective function equation (4.14), we can view $\rho^{TI} \ln y_{p,d}^{TI,i,j} + \overline{\Gamma_{p,d}^{i,j}}$ and $\rho^{ETT} \ln y_p^{ETT,i,j} + \overline{\Gamma_p^{i,j}}$ as generalized path disutility, and then view $\pi_d^{i,j}$ and $\overline{\pi^{i,j}}$ as reference path disutility. The overall objective function aims to minimize the total gap (as squared deviations between generalized path utility and reference utility) to zero, in order to ensure the stochastic user equilibrium conditions for users with traveler traffic

information and users with imperfect network knowledge based on expected travel times. Note that, we also add a constant weight of D (i.e., the number of days) for the subgap function for ETT users, in order to appropriately scale two subgap functions with day-invariant and day-dependent dimensions. With the proposed objective function, we can quantify the optimality gap of a feasible solution and further determine if the solution reaches the convergence within limited iterations. In addition, we can use an efficient convex programming technique to solve a restricted subproblem.

A survey by Ban et al. (2009) shows the majority of surveyed commuters trust the estimates if the perceived accuracy is within 5 minutes. In this study, $\rho^{ETT}=5$ minutes as the default perception error scale for ETT users, and $\rho^{TI}=3$ minute as the information accuracy scale for TI users. By setting TI market penetration rate $\gamma=5\%$, we can obtain the solution shown in Table 4.1.

These 25 days can be categorized into four different states, where RC and FC represent reduced and full capacity, and HD and LD represent high demand and low demand, respectively.

Table 4.1- Sample solution for 5% TI users and 95% ETT users.

Demand/supply combinations	ETT flow split $y_{p=1}^{ETT}$	TI flow split $y_{p=1,d}^{TI}$	Combined flow split on link 1	Travel time on link 1 (min)	Travel time on link 2 (min)
A: RC+HD	65.7%	0.008%	62.4%	67.6	42.3
B: RC+LD	65.7%	12.1%	63.0%	46.7	39.4
C: FC+HD	65.7%	79.3%	66.3%	32.0	36.0
D: FC+LD	65.7%	91.9%	67.0%	24.9	32.2

Under a multiday steady-state equilibrium condition, ETT users keep the same route selection ratio even under different demand levels. On every day, TI path flow ratios are changing, and a less congested path received high TI path selection probability. The multiday assignment results can be further visualized in Figure 4.3. The horizontal axis is the flow ratio on link 1 (i.e., variable $y_a = \frac{f_{a,d}}{q_d}$), and the link travel time function can be rewritten as

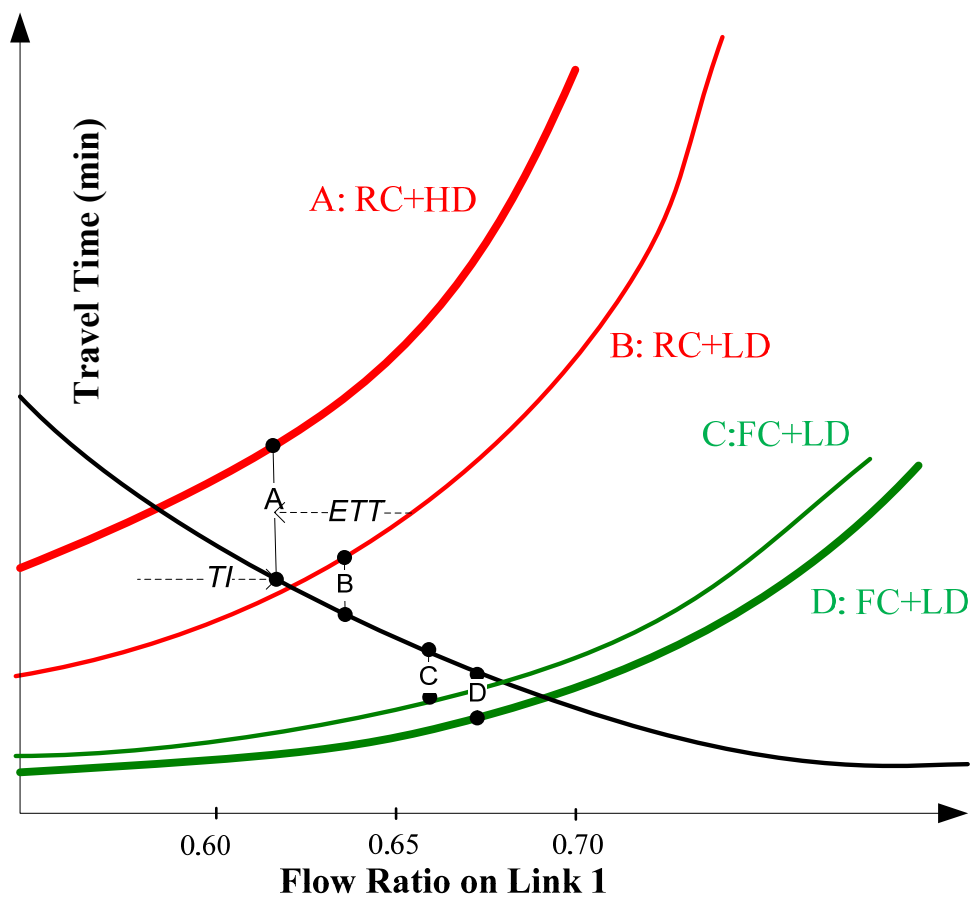


Figure 4.3- Travel flow split solution on four different types of days.

$$T_{a,d} = FTT_a \times \left(1 + \alpha \times \left(\frac{q_d}{c_{a,d}} \right)^\beta \times (y_{a,d})^\beta \right). \quad (4.21)$$

There are four curves on path 1 to represent four different states A, B, C and D, and curve E represents travel time function on path 2 as a function of $y_{a=1}$. The solutions on four different stages are shown as four vertical lines marked with A, B, D and D, with different route/link split ratios. Their upper and lower end points on the lines of travel time functions on paths 1 and 2 correspond to the actual travel time on different links. For vertical line A, two horizontal arrows point to the average travel time experienced by TI and ETT users, which are determined by the path flow splits of those two different information user classes. Obviously, with the access to the traveler information every day, TI users are more likely select the least travel time route and obtain better average travel time. On the other hand, there are always a small percentage of TI users still selecting congested route(s) due to perception errors.

4.4 Solution Algorithm

In order to iteratively reduce the overall gap in the proposed optimization problem for a general network with multiple origins and destinations, we extend a descent search solution framework developed by Lu et al. (2009), which also used a path-based gap function to describe the dynamic traffic equilibrium pattern. The proposed procedure adds day-dependent simulation, path finding and assignment dimensions to the existing static traffic assignment algorithm that typically assumes deterministic road capacity conditions. In this study, we implement the proposed algorithm within a mesoscopic

traffic assignment framework, which represents flow as vehicles with origin, destination and path attributes. The solution procedure is described as follows:

Step 1: Initialization.

Generate demand vector $q_d = [q_d^{i,j}]$ and road capacity vector $C_d = [c_{a,d}]$ on day $d=1, 2, \dots, D$, according to given stochastic demand and capacity distributions. Let iteration number $n=0$. Generate TI and ETT vehicles according to the maximum number of vehicles per OD pair $Q^{i,j} = \max_d \{q_d^{i,j}\}$ and given market penetration rate γ . To simulate stochastic demand effect, on each day d , a vehicle has a probability of $q_d^{i,j} / Q^{i,j}$ to make a trip. For each OD pair, compute the shortest path (in distance) and assign both TI and ETT vehicles to the corresponding shortest path.

Step 2: Multiday traffic simulation with stochastic capacity.

On each day $d=1, 2, \dots, D$, for given link flow patterns, generate day-dependent link travel times according to stochastic capacity vector C_d . The simulation results generate link travel time $T_{a,d}$ for link $a=1, 2, \dots, A$, on day $d=1, 2, \dots, D$.

Step 3: Find descent directions for stochastic traffic assignment

Find the Least Travel time Path (LTP) using day-dependent link travel time $T_{a,d}$ on each day d , for link $a=1, 2, \dots, A$.

Find the Least Expected Travel Time Path (LETP) using average link travel time

$$\bar{T}_a = \frac{\sum_d T_{a,d}}{D}, \text{ for link } a=1, 2, \dots, A.$$

Step 4: Path assignment for PI and ETT vehicles

For each day d , a certain percentage of TI vehicles are assigned to the least travel time path. By adapting the path-swapping method proposed by Lu et al. (2009), this study uses the following probabilistic ratio for a vehicle on path p to switch to the least travel time path at iteration n :

$$\frac{1}{n+1} \times \frac{U_{p,d}^{i,j} - \pi_d^{i,j}}{U_{p,d}^{i,j}} \quad (4.22)$$

The first term $1/(n+1)$ is equivalent to the fixed step size in the Method of Successive Average (MSA). The second term ensures that, the path swapping probability is proportional to the relative difference between the experienced path disutility $U_{p,d}^{i,j}$ and the minimum path disutility $\pi_d^{i,j}$, where $U_{p,d}^{i,j} = \rho^{TI} \ln y_{p,d}^{TI,i,j} + T_{p,d}^{i,j}$ and $\pi_d^{i,j} = \min_p U_{p,d}^{i,j}$.

Similarly, a certain percentage of ETT vehicles are swapped to the least expected travel time path, the route swapping probability at iteration n can be determined by

$$\frac{1}{n+1} \times \frac{\bar{U}_p^{i,j} - \bar{\pi}^{i,j}}{\bar{U}_p^{i,j}} \quad (4.23)$$

where $\bar{U}_p^{i,j} = \rho^{ETT} \ln y_p^{ETT,i,j} + \bar{T}_p^{i,j}$ and $\bar{\pi}_d^{i,j} = \min_p \bar{U}_{p,d}^{i,j}$.

Step 5: Link flow aggregation

For each day d , calculate the aggregated link volume $v_{a,d}$ using TI flow volume on day d and ETT flow (across every day), using equation (4.9).

Step 6: Convergence checking

Calculate the gap function as shown in equation (4.14), if $Gap < \delta$ convergence is achieved, where δ is a prespecified parameter. If convergence is attained, stop. Otherwise, go to Step 2.

4.5 Numerical Experiments

In the first set of experiments using the two-route corridor and 25-day representation, we are interested in the following emerging questions:

1) Given low-resolution traffic information freely available from radio stations and freeway Variable Message Signs (VMS), can additional high-quality traffic information provision services, such as Internet-connected GPS navigation devices, improve the system-wide average travel time or travel time reliability?

2) Typically, travelers do not have full knowledge of historical traffic patterns for each link in a transportation network, and they acquire and update their own network knowledge based on their past experienced travel time on travelled routes. Recently, many websites, such as Google Maps, start to provide free color-coded maps for displaying historical regional travel time patterns. This source provides additional opportunities for commuters to better learn the traffic conditions and enhance their network knowledge beyond their daily commuting routes. Can the improved network knowledge quality necessarily improve the overall system performance? (A more comprehensive discussion on network knowledge can be found in the dissertation by Ramming, 2002).

3) In addition to many real-time ATIS strategies that target on informed route switching, many traffic management strategies, such as telecommuting, flexible working hours, aim to reduce and smooth the overall day-to-day travel demand variations. Transportation agencies need to quantify the benefit and then prioritize various potential congestion mitigation solutions: increasing ATIS market penetration rates, improving real-time data quality, or reducing day-to-day traffic demand variations?

Table 4.2 shows experimental results for the above three different strategies from the base case with a market penetration rate of 5%, $\rho^{ETT}=5$ min and $\rho^{TI} = 3$ min. It is interesting to observe that all scenarios do not significantly reduce the average traffic congestion, but they can improve the travel time reliability to different degrees.

Table 4.2- Representative traveler information provision and traffic management strategies.

		Mean travel time (min)	STD (Min)
Base case		31.06	11.81
Improve traveler information accessibility	Improve market penetration rate to 7.5%	30.93	10.6
	Improve market penetration rate to 10%	30.83	9.6
Improve network knowledge quality	Reduce ρ^{ETT} to 4 min	31.20	12.34
	Reduce ρ^{ETT} to 2 min	31.03	11.71
Improve information quality	Reduce ρ^{TI} to 2 min	31.03	11.71
	Reduce ρ^{TI} to 1 min	30.83	10.72
Demand Smoothing	Pr(7800) =0.8 Pr(8800) =0.8	30.75	8.53
	Constant Demand: 8000 veh/h	30.65	6.01

Demand smoothing strategies produce the most effective variability reductions, followed by traveler information accessibility enhancement strategies. Improved knowledge quality strategies (e.g., $\rho^{ETT} = 4$ min) might not improve system-wide performance, as the better information allows more ETT users to use the congested route 1 due to reduced perception errors in the average travel time.

In the second set of experiments, we use a realistic demand pattern on the two-route corridor with a 100-day representation. The I80-E corridor is one of the major freeways through Bay Area, California, and has been chosen for the numerical example. Using measured traffic flow data from 03/02/2009 to 07/21/2009 between 8AM and 9AM (AM peak hours over 100 nonholiday weekdays).

Figure 4.4 displays the probabilistic distribution of 100 lane flow rate samples at Sycamore Ave.

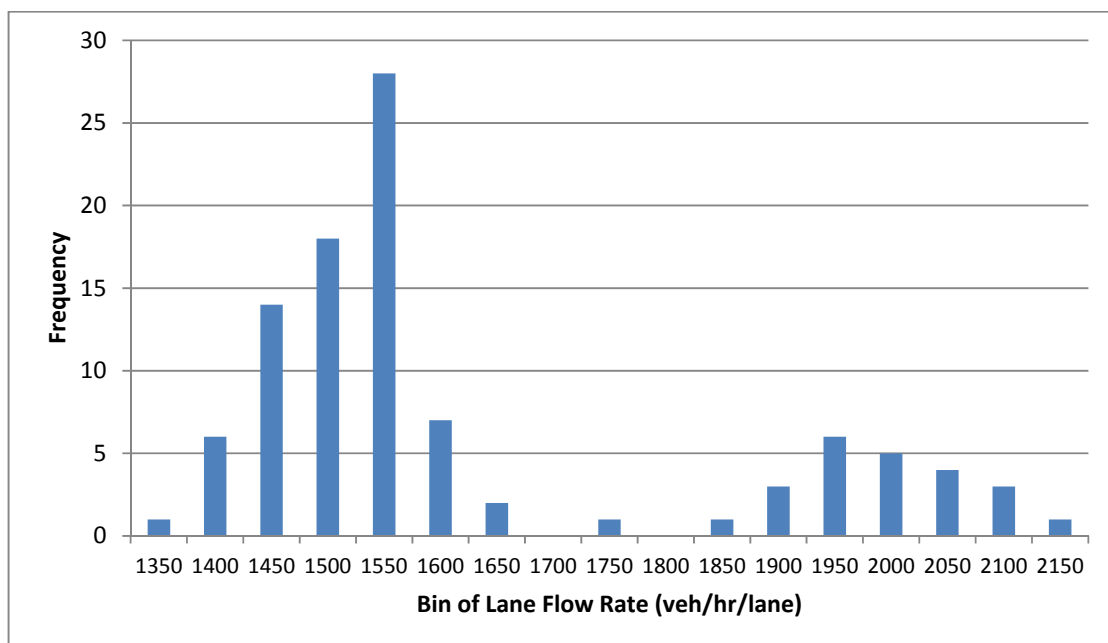


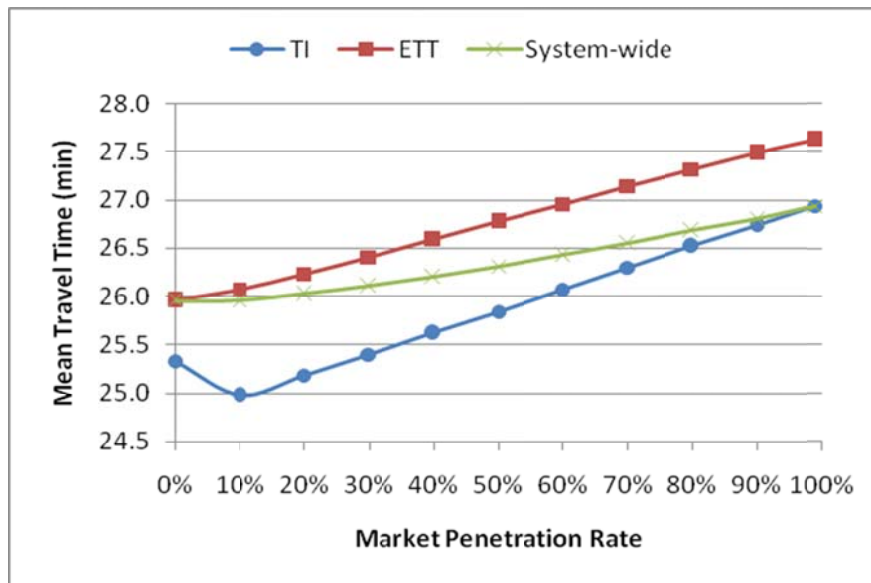
Figure 4.4- Histogram of 100 stochastic demand flow rate samples.

The stochastic distribution has a sample average of 1600 vehicles/hour/lane and standard deviation 214 vehicles/hour/lane, which reveals the inherent randomness in traffic flow. The stochastic capacity data used in the following analysis were obtained from a recent research effort by Jia et al. (2010).

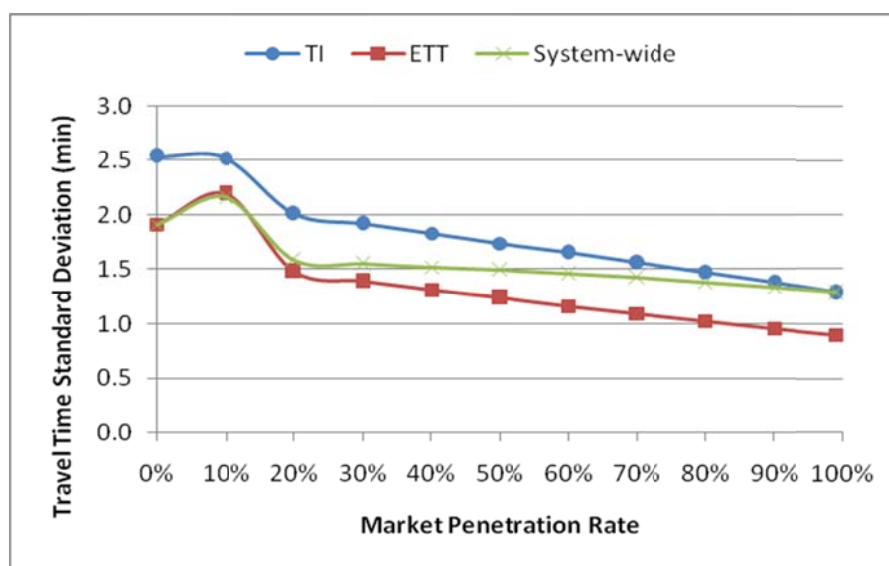
As shown in Figure 4.5(a), with a very small market penetration ($\gamma \leq 10\%$), the mean travel time is improved due to the introduction of traveler information services. As the market penetration rate gradually increases, the mean travel time jumps considerably. This result suggests that that average travel time saving is obtainable by maintaining the market penetration at a low level. Shown in Figure 4.5 (b), the system-wide travel time variability is consistently reduced as more users access traveler information, but TI users do not necessarily have a lower travel time variability compared to ETT users, as the assumed objection function of TI users aim to reduce day-dependent travel time.

4.6 Summary

Conventional network analysis models typically focus on finding a single-day steady-state equilibrium solution by assuming fixed demand and constant capacity. To systematically quantify the system-wide mobility and reliability impact of traveler information provision strategies, this chapter presents a multiday multiclass (in terms of information use) equilibrium model with stochastic capacity and stochastic demand. This study offers a powerful modeling approach to evaluate how travelers with different information accessibility adjust their route choice patterns when various sources of travel time uncertainty, e.g., stochastic demand fluctuations and different levels of information quality, are altered.



(a)



(b)

Figure 4.5- Effectiveness of information provision under stochastic capacity with different market penetration rate.

$$(\rho^{\text{TI}} = 1 \text{ min } \rho^{\text{ETT}} = 5 \text{ min})$$

Our future research will focus on the calibration of stochastic capacity and demand distributions under both recurring and nonrecurring congestion conditions. The proposed model can be also enhanced to consider more realistic route choice utility functions involving both expected travel time and travel time reliability. In this case, new path finding algorithm using multiday samples should be also developed to account for the potential link travel time correlations due to stochastic variations in origin-to-destination demand patterns.

CHAPTER 5

DAY-TO-DAY TRAVELER LEARNING FRAMEWORK

5.1 Introduction

Over the last three decades, the majority of the research interest in the field of DTA were concentrated on how to improve the realism of traveler behavior representation and demand modeling. Examples of DTA modeling innovations include incorporating within-day and day-to-day varying demand patterns, modeling departure time and mode choice, as well as simulating different levels of information availability.

A key foundation for development of strategies aimed at improving the efficiency and reliability of urban transportation network is identifying the location and impact of system bottlenecks. Although free flow capacity and queue discharge rates at system bottlenecks have been traditionally modeled as fixed values, they are in fact random processes. Therefore, assessing the operational impact of network bottlenecks requires reliable and realistic tools that account for stochasticity in prebreakdown flow rates and queue discharge rates.

Focusing on methodological and analytic enhancements to existing dynamic traffic assignment models, this chapter presents a method to seamlessly incorporate stochastic capacity models at freeway bottlenecks and signalized intersections, and

develops adaptive day-to-day traveler learning and route choice behavioral models under the travel time variability introduced by random capacity variations.

To account for different levels of information availability and cognitive limitations of individual travelers, a set of “bounded rationality” rules are adapted to describe route choice rules for a traffic system with inherent process noise and different information provision strategies. Based on a mesoscopic dynamic traffic simulator, namely DYNASMART-P (Mahmassani, 2001), this research enhances a number of key modeling components to meet the above challenges. The enhancements include a new set of day-to-day learning and route choice rules under the resulting stochastic travel time variations.

This chapter is organized as follows. The second section and the third section first introduce the conceptual route choice mechanism designed to respond to the stochastic travel time variations. This is followed by a detailed simulation implementation procedure in the fourth section. This chapter concludes with a case study for the real-world network in the fifth section and overall summaries in the last section.

5.2 Overall Modeling Framework

As illustrated in Figure 5-1, a simulation-based evaluation framework is used in this study to estimate the system performance for a multiday planning horizon under stochastic road capacity.

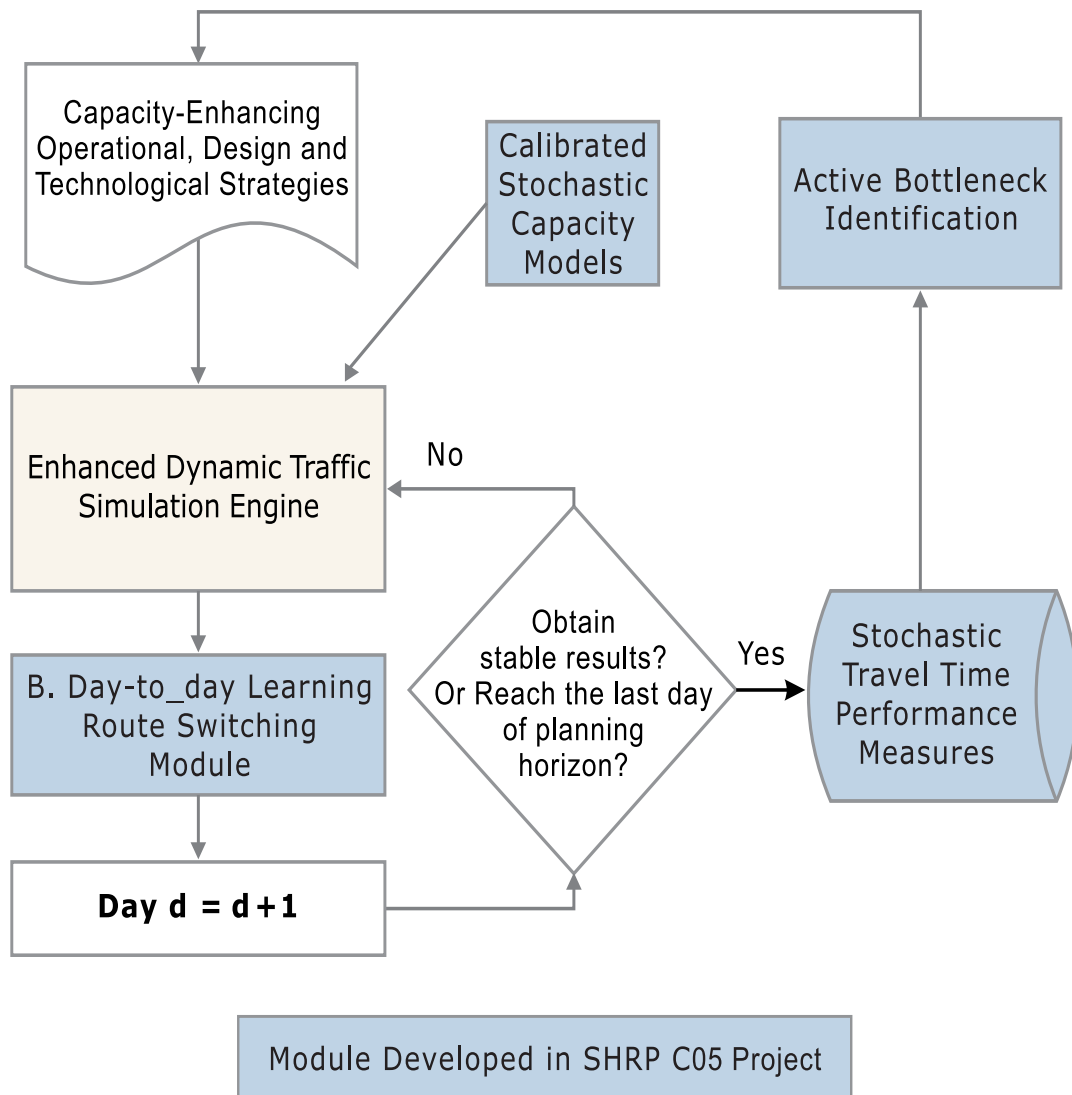


Figure 5.1- Capacity-Enhancing Strategy Evaluation Framework.

Source: SHRP2 C05 Report (2010)

A simulation-based evaluation framework is used to estimate the system performance for a multiday planning horizon under stochastic road capacity. The existing version of DYNASMART-P can be deployed in three distinct modes. These modes differ mainly in the assignment component applied. The first mode represents a one-step simulation-assignment procedure in which vehicles are assigned to the current-best-path, random path or any number of predetermined paths (e.g., historical paths). The second mode represents an iterative user equilibrium (UE) procedure. The third mode is a day-to-day system evolution modeling framework that interfaces the within-day simulation assignment with day-to-day behavior adjustment rules. Because this day-to-day system evolution-modeling framework was not fully developed at the outset of this project, DYNASMART-P was enhanced to model realistic traveler response mechanisms from multiple information classes.

In a day-to-day learning framework, users with pretrip and en-route information always start from a habitual path. If pretrip/en-route information becomes available, they will rely solely on the pretrip or en-route information to make route switching decisions. If a driver does not acquire any traveler information, he or she will rely on the historical experiences and starts the trip following the habitual (historical) path.

5.3 Day-To-Day Traveler Learning and Route Choice Model

As has been stated previously, conventional traffic assignment methods assume static, deterministic road capacity. Therefore, the travel time of a path only depends on the flow pattern on that path. In other words, for a fixed network-wide path flow pattern, the corresponding path travel times do not change. However, real-world road capacities

vary with time over a certain range, and a driver's travelling experience on a single day can be dramatically affected by the underlying realized capacity values on that particular day. In other words, travelers will experience different travel times on the same path over different days even for the same path flow pattern because of the inherent travel time variability introduced by stochastic capacity. As a result, conventional "within-day" or iterative route choice methods for reaching user equilibrium, such as the method of successive averaging (MSA), may not enable drivers to recognize and appropriately respond to the travel time variability/unreliability resulting from capacity fluctuation. A theoretically rigorous and practically useful traveler route choice model is crucially needed in order to adaptively capture the stochastic day-to-day travel time evolution process and also to maintain robustness under disruptions due to stochastic capacity reductions. To this end, a new route choice mechanism is proposed to simulate the drivers' route choice behavior under stochastic traffic process noise. By comparison, conventional stochastic assignment models focus on traveler perception errors under a deterministic traffic environment. The proposed mechanism includes two key components: a route choice learning module and a route choice decision module. In addition, different user classes, which receive and perceive different types of traffic information at different decision points along trips, are further investigated in this study.

5.3.1 Conceptual framework

The day-to-day learning framework proposed by Hu and Mahmassani (1997) and Jha et al. (1998) provides a promising path for seamlessly integrating stochastic capacity models in the DTA simulator for large-scale networks. Generally speaking, the learning

behavior in such a day-to-day learning framework is determined by each vehicle's historical traveling experiences, the traveler information obtained before and during the trip, as well as newly experienced travel times on the current day.

Conceptually, our proposed model includes three components:

Traffic flow assignment model:

$$f^{d+1} = A(f^d, T^d, w^d) \quad (5.1)$$

Stochastic traffic system simulation process:

$$t^d = S(f^d) + w^d \quad (5.2)$$

$$\text{Travel time perception model: } T^d = t^d + \varepsilon^d \quad (5.3)$$

where

f^d = assigned route flow pattern on day d , determined by traffic assignment model/function $A(\cdot)$,

t^d = true travel time on day d , determined by dynamic assignment/simulation function $S(\cdot)$,

w^d = the system noise introduced by the stochastic capacity,

T^d = the observed travel time by a traveler,

ε^d = the traveler perception error associated with perceived travel time in the network, introduced by the sampling error associated with personal experience and quality of information.

It should be remarked that most existing day-to-day learning models are implemented with stable road capacity, which assume no system noise, i.e., $w^d = 0$, so the travel time t^d is a deterministic vector for a given set of route flows, f^d in equation (5.2). Accordingly, the focus in the previous research has been on how to reach the deterministic steady-state conditions, and how to construct realistic learning/updating models for the travel time perception error term ε^d related to equation (5.3).

In this study, we enhance a dynamic traffic flow simulator, namely DYNASMART-P, to describe a traffic simulation process with day-to-day varying system noise, w^d in equation (5.2). Corresponding to the traffic flow assignment model, Equation (5.4), a day-to-day learning module is presented to describe adaptive traveler behavior across multiple days in a stochastic traffic evolution environment. The essential idea for the learning module is to enable certain users to use their historical traveling experiences to construct their estimates and make decisions under uncertain system travel times (introduced by the system noise w^d). To simplify the route choice rules, we assume $\varepsilon^d = 0$ in our following discussion. As a result, the proposed model does not involve the use of a Probit or Logit model to assign traffic flows and does not require a travel perception error updating process.

5.3.2 Route choice utility function and simplified route switching rule

Jia, Zhou, Li, Roupail and Williams (2010) adapted a behaviorally sound route choice utility function, proposed and calibrated by Brownstone and Small (2004) and Lam and Small (2001), to consider the stochastic nature of traffic systems.

$$GT = T + \frac{VOR}{VOT} \times TSD + \frac{TOLL}{VOT} = T + \beta \times TSD + \frac{TOLL}{VOT} \quad (5.4)$$

where

GT = the generalized travel time,

T = the expected travel time for traveler,

TSD = perceived travel time variability.

β = reliability ratio (computed as the ratio of Value of Reliability (VOR) and Value of Time (VOT)).

Toll = road toll charge, and it is assumed to be zero in the following discussions as no toll-related strategies will be evaluated in this paper.

It has been well recognized that travel time variability and reliability are important measures of service quality for travelers. In the above utility function, equation (5.4), the travel time standard deviation (TSD) is used to measure system travel time variability associated with the underlying stochastic traffic process. This contrasts with the perception error variance in a deterministic assignment model. For a single traveler v , the route choice decision is made by comparing the generalized travel time of habitual path, GT_v^h , and that of alternate path, GT_v^a .

$$GT_v^h > GT_v^a \quad (5.5)$$

where

v = traveler index,

h =index for habitual path, and

a =index for potential alternative path.

According to Equation (5.4), if the generalized travel time of the habitual path, GT_v^h , is greater than that of alternate path, GT_v^a , as shown in Equation 8, a vehicle should switch his route from the habitual path to the alternative path. The resulting decision rule could be derived as:

$$T_v^h - T_v^a > \beta(TSD_v^a - TSD_v^h) \quad (5.6)$$

In this study, T_v^h is equal to $\bar{T}_v^{d-K, d-1}$ as calculated in equation (5.7). In order to take a traveler's multiday travel time experience into account. T_v^a is calculated using the estimated travel time on the shortest path. It should be noted that the calculation of T_v^a varies for different user classes, which will be discussed in section 5.3.3.

$$\bar{T}_v^{d-K, d-1} = \frac{T(P_v^{d-K}) + T(P_v^{d-K+1}) + \dots + T(P_v^{d-1})}{K} \quad (5.7)$$

where d = day index

K = number of days in the learning memory window

$\bar{T}_v^{d-K,d-1}$ = traveling experience (i.e., average travel time) for traveler v from day $d-K$ to day $d-1$, on a particular path,

$T(P_v^{d-1})$ = travel time on path P_v^{d-1} , and P_v^{d-1} is the path traveled by vehicle v on day $d-1$.

The right side of equation (5.6) can be viewed as the minimum acceptable absolute tolerance needed for a route switch decision. This value arises from three components: the reliability ratio β , the standard deviation of travel time on the habitual path TSD_v^h , and the standard deviation of travel time on the alternative path TSD_v^a . The calibration study from Noland et al. (1998) indicated a reliability ratio value of $\beta = 1.27$ based on survey data from more than 700 commuters in the Los Angeles region. The setting of parameter K depends on the signal-to-noise ratio in the traffic system. Specifically, the more stable the travel time process, the smaller K can be and still yield a reliable mean travel time estimate. In general, K must be large enough to filter out the process noise from the stochastic traffic system.

The travel time variability measure, TSD_v^h , for the habitual path can be calculated from multiday travel times experienced by the traveler. The remaining challenge is how to estimate the standard deviation of travel time on the alternative path, TSD_v^a , where the traveler has little or no experience on this path. When there is no external pretrip or en-route information available, TSD_v^a needs to be calculated from the traveler's prior experience. To our knowledge, there is no widely accepted method to calibrate the standard deviation of perceived travel times on alternative paths for travelers without access to advanced traveler information systems and relying on prior knowledge only. In this research, we assume TSD_v^a is significantly larger than TSD_v^h due to the lack of

precise information and the high level of uncertainty associated with the perceived alternative travel time. The calibration of the minimum acceptable absolute tolerance was beyond the scope of this study. Therefore, this research uses a simplified, single term model, $\beta(TSD_v^a - TSD_v^h)$, to represent the minimum acceptable absolute tolerance needed for a route switch decision. This simple model is intuitively sound, and using it eliminates the need for extensive calibration efforts.

In this study, a bounded rationality model, which states that a driver's decision depends on their desired satisfaction level, is adapted to make the route choice comparison. The bounded rationality concept is employed because there has been growing attention (starting from the early work by Mahmassani and Herman (1990) to bounded rationality since Herbert Simon (1995) pointed out that perfectly rational decisions are often not feasible given the limits of human cognition.

Based on the minimum acceptable absolute tolerance and the relative acceptable tolerance, a set of bounded rationality rules, shown in Equation (5.11), are used to describe users' route switching behavior. As opposed to the optimization theory in which users select the best option from *all possible* decisions, in the bounded rationality approach, users perform limited searches, accepting the first satisfactory decision.

$$\delta = \begin{cases} 1 & \text{if } \bar{T}_v^{d-K, d-1} - T_v^a > \text{MAX}[\alpha, \lambda \times T_v^h] \\ 0 & \text{otherwise} \end{cases} \quad (5.8)$$

where

$\delta = 1$, switch to an alternative path; 0 , remain on the habitual/ current path,

α = Minimum acceptable absolute tolerance needed for a switch *and* $\alpha = \beta(TSD_v^a - TSD_v^h)$,

λ = Relative acceptable tolerance (i.e., relative improvement threshold).

5.4 Conceptual Simulation Framework and System Implementation

The system evolution-modeling simulation framework for the enhanced version of DYNASMART-P is illustrated in Figure 5.2. In the proposed modeling framework, static demand (i.e., the same number of vehicles with fixed departure times) is simulated over different days.

In the above conceptual simulation framework, three critical inputs (illustrated in the input boxes in Figure 5.2) should be prespecified by users, which are listed as follows:

- Time-dependent traffic demand,
- Bottleneck locations,
- Percentage of unequipped, pretrip and en-route users,
- Parameters of the bounded rationality rule.

The following day-to-day learning procedure is developed in this study to realistically model the incremental adaptation of traveler route selection behavior to the implementation of targeted strategies for improving sustainable flow rates within the network.

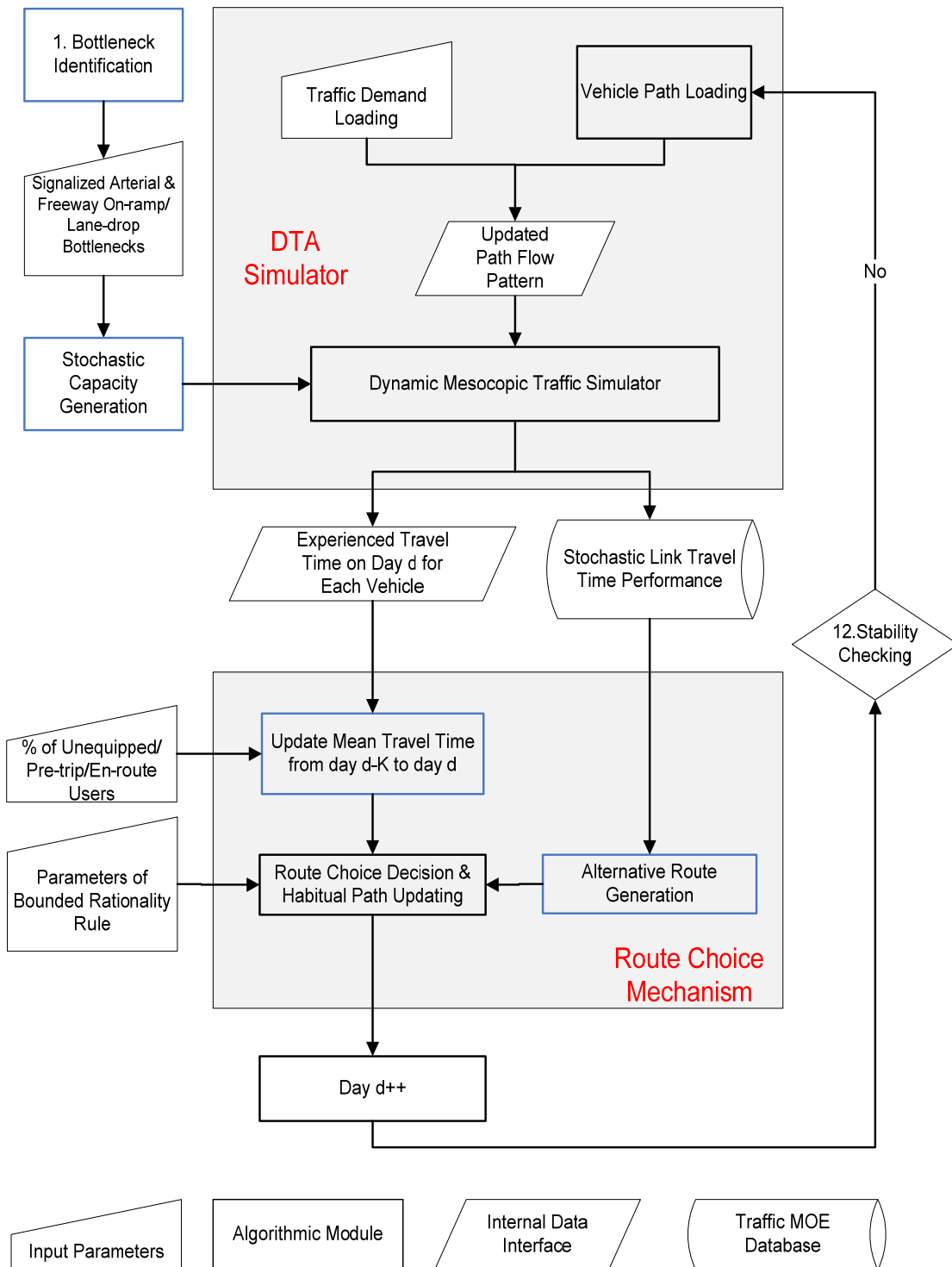


Figure 5.2- Comprehensive conceptual simulation framework.

Given the stochastic nature of the improved traffic models, changes in preferred paths are made based on running averages with a fixed look-back period and a minimum travel time improvement threshold. The number of travelers that are willing to change planned routes is limited to ensure a stable route switching response. The route choice model enables driver classes with access to pretrip or en-route information to select alternate routes in response to random queues on their preferred routes. Minimum travel time improvement thresholds are also used for the dynamic route choice model.

Notations

d = day index

K = number of days in the learning memory window

i = origin index

j = destination index

v = traveler index

τ = departure time interval

$p_{i,j,\tau}^d$ = least travel time path for OD pair (i, j, τ) on day d

$\pi_{i,j,\tau}^d$ = least travel time for path $p_{i,j,\tau}^d$

p_v^d = path traveled by vehicle v on day d

$\bar{T}_v^{d-K,d}$ = average travel time for traveler v traveling on the path p_v^d from day $d-K$ to day d

α = absolute improvement threshold bound for bounded rationality rule

β = relative improvement threshold for bounded rationality rule

The day-to-day learning simulation algorithm is detailed as follows.

Initialization Set the iteration counter of outermost loop $d=0$.

0. Generate information user class for each vehicle according to prespecified market penetration rates.

1. Identify traffic bottleneck locations in the network according to the network topology and number of lanes, and then output freeway merge/diverge/weaving bottleneck locations to input data block A.

Day-to-day Traffic Simulation

2. Generate random capacity input for each freeway bottleneck every 15 minutes, according to calibrated stochastic headway models for merge, diverge and weaving links.

3. Generate random capacity input for each arterial link at the beginning of each signal cycle, according to a calibrated stochastic headway model for arterial streets.

4. According to network-wide prevailing travel time, generate pretrip and en-route shortest paths for each origin-destination pair.

5. Load vehicles into the network with their habitual paths p_v^d .

6. For each vehicle equipped with ATIS information (pretrip or en-route), compare the prevailing travel time between the habitual path and the suggested path from ATIS strategy, fetch bounded rationality rule parameters for different information classes from input data blocks *B* and *C*, and change the vehicle's path to suggested path from the pretrip or en-route information provision services if the relative and incremental improvement thresholds are satisfied.

7. Given updated flow pattern from the route switching module, perform a dynamic network assignment under stochastic capacity for the entire planning horizon.

Post-trip Traveler Learning and Route Switching Decision

8. Obtain the percentage of travelers willing to learn from data input block *D*.

9. For each vehicle v willing to switch, obtain its current path on day d . calculate the mean travel time $\bar{T}_v^{d-K,d}$ from day $d - K$ to current day d .

10. Based on the time-dependent network-wide travel time database, generate the least travel time path $p_{i,j,\tau}^d$ as a post-trip alternative route for OD pair (i,j) and departure time τ , and calculate the corresponding travel time $\pi_{i,j,\tau}^d$.

11. Update habitual paths according to the bounded rationality rules and the parameters are specified in data input block E .

$$\text{If } (\pi_{i,j,\tau}^d + \alpha) \leq \bar{T}_v^{d-K,d} \quad \text{Or} \quad \pi_{i,j,\tau}^d \leq \bar{T}_v^{d-K,d} \times (1 - \beta)$$

then switch route to the shortest travel time path; that is, set $p_v^d = p_{i,j,\tau}^d$. Otherwise, remain on the current habitual route on day d .

12. Stability checking: if the current flow pattern is stable or the network-wide traveler switching rate is close to steady-state conditions, then stop. Otherwise, continue.

5.5 Case Study

The proposed simulation frameworks are applied to a real-world subarea network within the Portland, Oregon metropolitan area in order to demonstrate the model applicability and usefulness. The subarea network selected for this purposes is illustrated in Figure 5.3. It is relatively large in size and therefore represents a good opportunity to test scaling issues associated with the method applications. The network (Figure 5.3) includes 858 nodes, 2000 links, and 208 origin-destination zones. Among the 858 nodes, 169 of them are modeled as signalized intersections with actuated control and the remaining are modeled at uncontrolled nodes with capacity constraints.

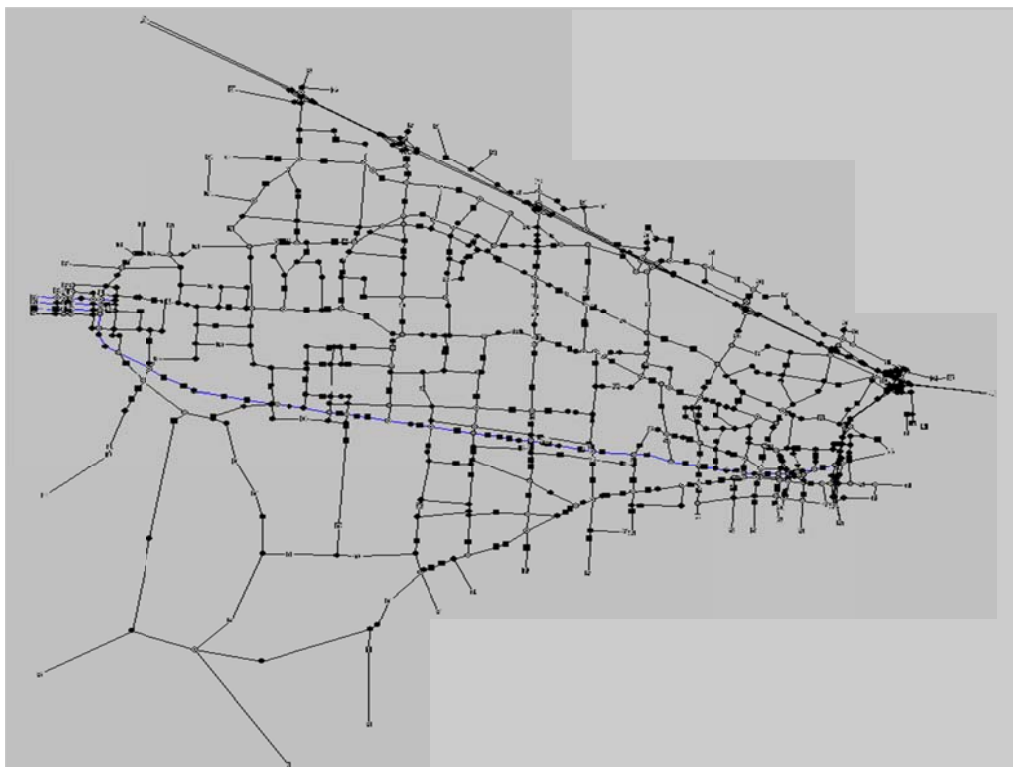


Figure 5.3- Portland network study area.

Source:SHRP2 C05 Final Report (2010)

In this case study, the percentage of vehicles assigned to each of three available user classes was as follows: 98% of drivers were assumed to have no access to real-time information about network conditions (referred to as the “unequipped” user class); 1% were assumed to access pretrip information only (referred to as the “pretrip” user class); and 1% were assumed to have access to continuous en-route information (referred to as the “en-route” user class). Among the unequipped users, the percentage of drivers who are willing to make a route change in any given day was set to 15%. The number of days in the learning window was set to $K = 5$. Therefore the mean travel time was calculated from the experience of day $d-5$ to day $d-1$. This mean travel time represents each driver's

historical traveling experience. The calibrated parameters of the stochastic models described in section 3 were applied to generate stochastic capacity and queue discharge flow rates for freeway bottlenecks (i.e., on-ramp and lane drop segments) and saturation flow rates for signalized arterials. For simplicity, the minimum acceptable absolute tolerances used in bounded rationality rule are 5 minutes for unequipped users and 2 minutes for pretrip/en-route users. The default value of the relative switching threshold is set to 20% in this study.

In the case study by Jia, Zhou, Li, Rouphail and Williams (2011), the simulation run is performed over 100 days of simulated time in order to effectively generate realistic results. Figure 5.4 shows the network-wide average travel time and route switching rate of total vehicles segmented in three time regimes.

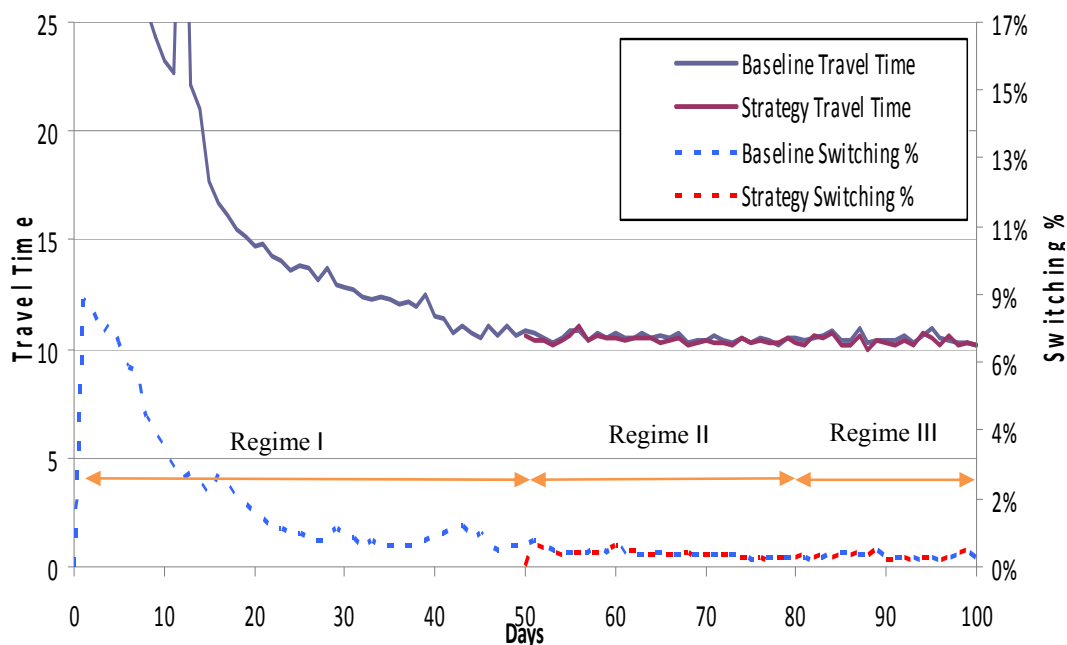


Figure 5.4- Network-wide simulation results.

Source: SHRP2 C05 Final Report (2010)

In this study, for example, during the baseline stabilization period (Regime I in Figure 5.4) 50 days are simulated to achieve a stable baseline scenario. The average travel time diminishes significantly during the first 40 days and stabilizes afterwards.

After the baseline stabilization period was completed, the operational and/or construction strategies to be evaluated were introduced into the network, and we carried out the simulation process for an additional 30 days to allow driver adjustments and achieve stable conditions under the new scenario. This is referred to as the strategy stabilization period and is illustrated as Regime II. Following immediately upon this 30-day period was a simulation of an additional 20 days (Regime III in Figure 5.4) that formed the basis for the summary results output associated with the particular strategy being investigated. In regime III, although the average travel time or switching rate is relatively stable, there are still obvious day-to-day fluctuations, because the travel time experience on a single day can be dramatically affected by the underlying stochastic capacity features. Therefore, evaluation of network performance only based on the last simulation day (last iteration) is not recommended and new reliability-oriented system performance measures should be applied to take multiple days into account. In this study, for example, the simulation results from the last 20 days were used to report the network performance.

5.6 Summary

In this study, methodological and analytic enhancements to existing dynamic traffic simulation models have been proposed for the purpose of increasing the realism and sensitivity of the models in simulating real-world network and the effects of strategy

applications. The particular focus is on how to seamlessly integrate stochastic capacity models and compatible route choice models within a stochastic capacity environment. These enhancements have been prototyped and tested through a mesoscopic DTA simulator, DYNASMART-P, and could be easily incorporated into other dynamic traffic simulation/analysis models as well. The study described in this paper provides the following contributions to the existing DTA models:

- An innovative simulation platform incorporating stochastic road capacity for both freeway and arterial links, which enables reasonable and realistic modeling of travel time.
- A new set of day-to-day learning and route choice models which enables a realistic representation of drivers' route selection process and effectively stabilizes overall network flow under stochastic capacity conditions.
- Practical modeling guidelines which are effective for the enhanced DTA model to simulate various capacity-enhancing design, operational, and technological strategies.

CHAPTER 6

ANALYTICAL MODELS ON DERIVING TRAVEL TIME VARIABILITY DISTRIBUTIONS FROM STOCHASTIC CAPACITY DISTRIBUTIONS

6.1 Introduction

Travel time reliability has been widely recognized as an important element of a traveler's route choice and departure time scheduling decision. In recent years, operating agencies have begun to shift more focus toward monitoring and improving the reliability of transportation systems, in addition to ensuring the mobility performance measures. With a growing trend of incorporating trip time variability into traveler information provision systems, many ongoing Intelligent Transportation Systems (ITS) development efforts are devoted to establishing probe-based data collection systems.

As an essential attribute in travelers' route and departure time decision, travel time reliability serves as an important quality-of-service measure for dynamic transportation systems. Dong and Mahmassani (2009) recently developed a statistical approach to calibrate the travel time reliability measure as a function of flow rates, and the resulting regression models were used to predict trip reliability costs and user benefits for a given set of flow rates obtained from dynamic traffic assignment/simulation results.

Another approach for systematically estimating travel time variability in a traffic network is to perform a day-to-day dynamic traffic assignment module, where the travel time patterns evolve depending on a number of variability sources, e.g., stochastic capacity, stochastic demand and random route choice behavior. Although this approach provides a fully dynamic and stochastic modeling environment for studying various uncertainty sources and assessing the benefits of traffic management strategies, it still requires considerable data collection, calibration and computational efforts to perform realistic day-to-day assignment results.

This chapter investigates a fundamental problem of quantifying travel time variability from its root sources: stochastic capacity and demand variations that follow commonly used log-normal distributions. A volume-to-capacity ratio-based travel time function and a point queue model are used to demonstrate how day-to-day travel time variability can be explained from the underlying stochastic demand and capacity distributions.

This chapter also uses simplified peak-hour demand profiles to estimate time-of-day or time-dependent travel time variability functions at traffic bottlenecks. The proposed models provide theoretically rigorous and practically usefully tools to understand the causes of travel time unreliability and evaluate the system-wide benefit of reducing demand and capacity variability.

Given a set of observed or simulated traffic conditions, e.g., traffic flow and queue profiles on a link or a corridor, this study aims to provide efficient analytical approximation methods to specify the PDF of travel time distributions as a result of stochastic capacity and demand distributions. Focusing on planning-level applications,

the goal of our proposed research is to enable a quick characterization of travel time reliability statistics without resorting to the comprehensive but computationally challenging day-to-day simulation or numerical approximation approaches. We also envision that an efficient travel time variability estimation module can be extremely useful in a real-time traffic information provision system where travel time reliability information needs to be rapidly predicted based on a set of predicted traffic conditions (e.g., for the next 30 minutes). In this case, travel time reliability statistics calibrated from the archived travel time database are insufficient or difficult to predict future system performance variations, which are highly dependent on the dynamic states of prevailing and future traffic conditions, rather than the steady-state historical pattern.

In addition, we are interested in estimating the time-dependent travel time variability for a traffic bottleneck. Congestion caused by bottlenecks contributes about 40% of the nationwide urban congestion. As a bottleneck is activated when the provided capacity is insufficient for and restricts the incoming traffic flow, it is critical to achieve a better understanding on how the travel time variability at bottlenecks are contributed by variations of its incoming flow and queue discharge flow. To this end, we will derive and construct analytical relationship between the capacity change and the waiting time change on a bottleneck, by extending theoretical results from the link cost marginal analysis for traffic queuing systems.

This chapter is organized as the following sequence.

- (1) Several key statistical properties of log-normal distribution are reviewed, which is a state-of-practice distribution used in many empirical studies for describing travel time variability.

(2) By assuming log-normal distributions for stochastic demand and capacity, and in the context of the BPR function as travel time performance functions, this chapter aims to prove that the resulting travel time follows a log-normal distribution, so the travel time variability can be analytically derived from the variation parameters in demand and capacity.

(3) Furthermore, a more realistic point queue model is considered, and under an assumption of log-normal distributions for stochastic capacity variations, the corresponding total waiting time can be characterized through log-normal distributions.

(4) This chapter then uses simplified peak-hour demand profiles to derive time-of-day travel time variability functions at a traffic bottleneck.

(5) A simple case study with real-world data from the I880 corridor in the Bay Area, CA is conducted to demonstrate and verify the proposed analytical methods.

6.2 Review of Statistical Properties of Log-Normal Distribution

There are a wide range of probability distributions available, such as Weibull and normal distributions, to describe travel time variability and its sources of randomness. The reason for selecting the log-normal distribution in the proposed analytical framework is based on (1) its goodness-of-fit on empirical data, and (2) its attractive mathematical properties for multiplicative functions of log-normally distributed random variables, which are particularly useful for conceptualization, formalization, and abstraction in travel time variability study.

In general, the Gaussian (normal) distribution has been widely used to characterize symmetrical random variations. For many skewed variations, for example,

mean values are low but variances are large, the log-normal distribution can achieve a desirable fit. More importantly, what we should recognize the major difference between normal and log-normal distributions is their additive vs. multiplicative effects. Specially, if $X_j \sim N(\mu_j, \sigma_j^2)$, then $Y = \sum_j X_j$ is also normally distributed.

For functions of log-normally distributed random variables, there are the following properties (Aitchison and Brown, 1957).

Property 1: If $X \sim LN(\mu, \sigma^2)$, then variable $Y = \frac{1}{X}$ is also log-normally distributed, $Y \sim LN(-\mu, \sigma^2)$.

Property 2: If $X_j \sim LN(\mu_j, \sigma_j^2)$ are n independent log-normally distributed variables, then product $Y = \prod_{j=1}^n X_j$ is also log-normally distributed as $Y \sim LN(\sum_{j=1}^n \mu_j, \sum_{j=1}^n \sigma_j^2)$.

Property 3: If $X \sim LN(\mu, \sigma^2)$ and $a \neq 0$, then $Y = X^a$ is also log-normally distributed as $Y \sim LN(a\mu, a^2\sigma^2)$.

Property 4: If $X \sim LN(\mu, \sigma^2)$, then $Y = aX$ is also log-normally distributed as , $Y \sim LN(\ln a + \mu, \sigma^2)$

Property 5: If $X \sim LN(\mu, \sigma^2)$, then $X + c$ becomes a shifted log-normal distribution with $E[X + c] = E[X] + c$ and $\text{Var}[X + c] = \text{Var}[X]$.

$$E[X] = e^{\mu + \frac{1}{2}\sigma^2},$$

$$\text{Var}[X] = (e^{\sigma^2} - 1)e^{2\mu + \sigma^2}$$

$$SD[X] = \sqrt{Var[X]} = e^{\frac{\mu + \frac{1}{2}\sigma^2}{2}} \sqrt{(e^{\sigma^2} - 1)}$$

Property 6: Sum of lognormal

Consider $Y = \sum_{j=1}^n X_j$, where $X_j \sim LN(\mu_j, \sigma_j^2)$ are independent log-normally distributed variables. There is no closed-form expression available to describe the stochastic distribution of Y , but random variable Y can be numerically approximated by another log-normal distribution Z at the right tail.

6.3 Deriving Travel Time Variability Distribution Based on BPR Function

Consider the following BPR function on a single link or corridor,

$$T = FFTT \times \left(1 + \alpha \times \left[\frac{V}{C} \right]^\beta \right) = FFTT + FFTT \times \alpha \times \left[\frac{V}{C} \right]^\beta \quad (6.1)$$

where T = travel time

$FFTT$ = Free-flow travel time,

V = link volume,

C = link capacity

Coefficients α and β can be set to commonly used default values 0.15 and 4, respectively.

Proposition 1: If incoming demand and capacity are assumed to be log-normal variables, that is, $V \sim LN(\mu_V, \sigma_V^2)$ and $C \sim LN(\mu_C, \sigma_C^2)$, then

$$T \sim LN\left(\ln(FFTT \times \alpha) + \beta \times (\mu_V - \mu_C), \beta^2 \times (\sigma_V^2 + \sigma_C^2)\right) + FFTT \quad (6.2)$$

Proof:

According to property 1, since the link capacity c is a log-normal variable,

$$\frac{1}{C} \sim LN(-\mu_C, \sigma_C^2).$$

According to property 2, since the demand V and $\frac{1}{C}$ are log-normal variables,

$$\frac{V}{C} = V \times \frac{1}{C} \sim LN(\mu_V - \mu_C, \sigma_V^2 + \sigma_C^2)$$

According to property 3, $\left(\frac{V}{C}\right)^\beta \sim LN\left(\beta \times (\mu_V - \mu_C), \beta^2 \times (\sigma_V^2 + \sigma_C^2)\right).$

According to property 4,

$$FFT T \times \alpha \times \left(\frac{V}{C}\right)^\beta \sim LN\left(\ln(FFT T \times \alpha) + \beta \times (\mu_V - \mu_C), \beta^2 \times (\sigma_V^2 + \sigma_C^2)\right).$$

According to properties 5 and 6,

$$T \sim LN\left(\ln(FFT T \times \alpha) + \beta \times (\mu_V - \mu_C), \beta^2 \times (\sigma_V^2 + \sigma_C^2)\right) + FFT T$$

and $E(T) = \exp(\ln(FFT T \times \alpha) + \beta \times (\mu_V - \mu_C) + \frac{1}{2} \times \beta^2 \times (\sigma_V^2 + \sigma_C^2)).$

The coefficient of variations $=SD(T)/E(T) = \sqrt{\exp\left[\beta^2 \times (\sigma_V^2 + \sigma_C^2)\right] - 1}$, where

$SD(T)$ can be derived from Property 5.

End of proof.

In summary, if both road demand and capacity are log-normally distributed, then the resulting travel time is a shifted log-normal variable with analytical form for the

expected value and variance. Using those properties, one can quantify how reducing variations in the source of randomness affects the overall travel time variability.

6.4 Deriving Travel Time Variability Distribution

Based on Point Queue Model

In this section, we consider a bottleneck with a study time horizon from 0 to time H . The stochastic capacity, more precisely, queue discharge rate Q for a point queue model at the bottleneck can be described as a shifted log-normal function $Q \sim LN(Q^{\max}, \mu_Q, \sigma_Q^2)$, where shift = the maximum queue discharge rate Q^{\max} . That is, $Q = Q^{\max} - \Delta Q$, where ΔQ is the deviation of queue discharge rates and $\Delta Q \sim LN(\mu_Q, \sigma_Q^2)$. Note that we assume a constant queue discharge rate for each congestion period in this study, where the actual queue discharge rates can slowly evolve as a time-varying parameter within the same congestion peak period. As the theoretical development in this chapter involves both static V/C-based BPR function and point queue model, it is important to highlight two key differences between these two models. First, the point queue model assumes zero delay unless $V > C$, while a BPR-type function still produces delays when $V < C$.

In addition, a traffic queuing model needs to clearly distinguish prebreakdown flow rates (that triggers the change of traffic states from uncongested to congestion) and queue discharge flows (after a breakdown occurs), and these two types of flow rates are time-dependent. A travel time performance function like BPR functions, on the other hand, simply uses hourly capacity to characterize the overall congestion level.

For simplicity, we first assume constant demand in this example. Using a known (time-dependent) demand pattern, and the maximum queue discharge rate Q^{\max} , we can use the point queue model to calculate the queue profile, characterized in the input-output queuing diagram shown as Figure 6.1, where curves A and D represent vehicle upstream arrival pattern and downstream departure pattern, respectively. All the curves are expressed in terms of cumulative numbers of vehicles, where the slope of a departure curve indicates the queue discharge rates of vehicles at the bottleneck.

In the point-queue model, the horizontal distance between curves A and D shows the waiting time of a vehicle, and the total waiting time is denoted as W . The vertical distance between curves A and D shows the number of vehicles accumulated in the queue starting from time s to dissipating at time e . The area between two curves, A and D in Figure 6.1, represents the total queuing delays of all vehicles. The following discussion aims to construct a probability distribution function of the total waiting time W .

To evaluate the impact of flow switching strategies in the dynamic traffic assignment process, a variety of studies have been conducted for computing local link marginals due to adding or deleting a vehicle from a link. Ghali and Smith (1995) used a deterministic point queue model to describe traffic flows and gave analytical formula to quantify the marginal impact of total link travel time due to a small change in incoming flow. In particular, the marginal improvement with respect to adding or deleting a vehicle is approximately proportional to the time interval from a vehicle entering time t to the end of congestion e , that is, the system-wide marginal travel time change is $m = (e-t)$.

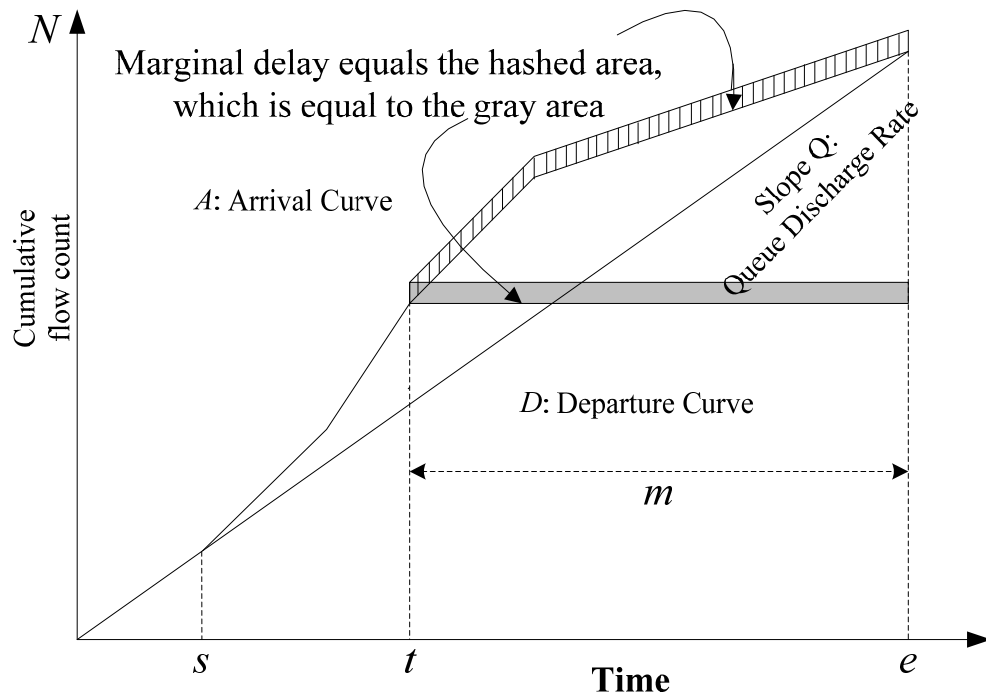


Figure 6.1- Local link marginal delay evaluation method for vehicle entering at time t .
(based on figure by Ghali and Smith (1955))

In Figure 6.2, we can derive the impact to the total waiting time due to one unit of departure flow change at time t . If we consider the queue discharge rate is changed by one unit for the congested period from time s to e simultaneously, then the total system-wide waiting time change ΔW is

$$\int_s^e \Delta Q(e-x)dx = \frac{1}{2} \Delta Q \times (e-s)^2 = \frac{1}{2} \Delta Q \times M^2, \quad (6.3)$$

where ΔQ is the capacity change rate and M is the queue duration.

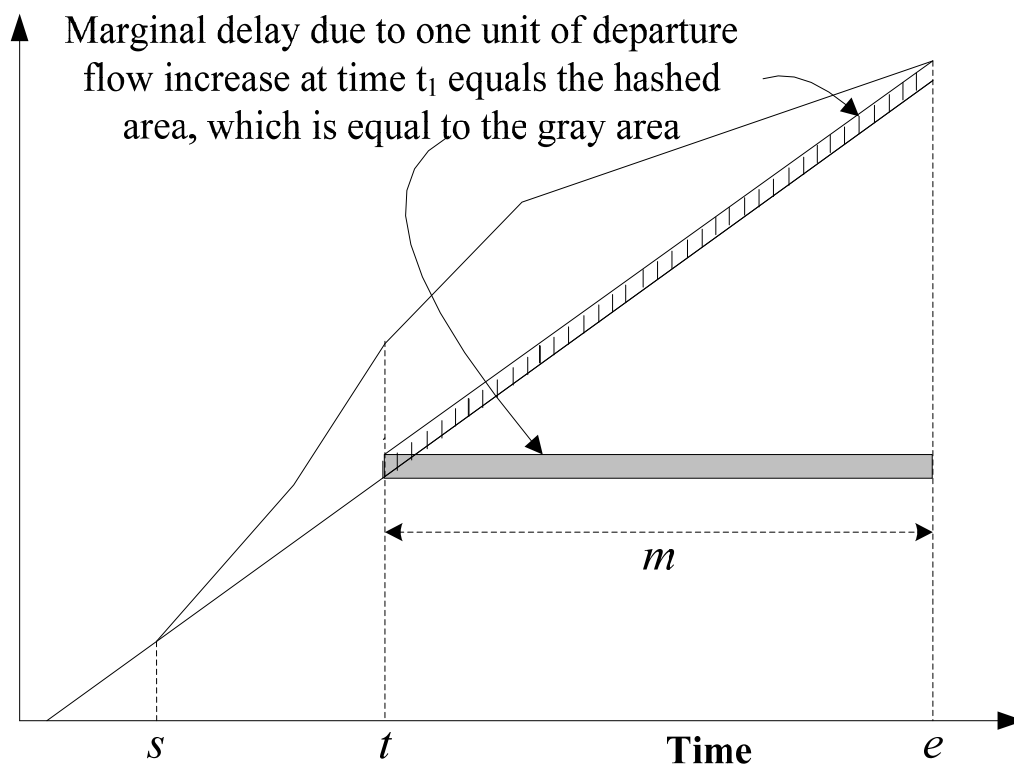


Figure 6.2- Local marginal delay evaluation method for one unit of departure flow change at time t .

Shown in Figure 6.3, we can have the following geometric interpretation for the key formula used in this study

$$\Delta W = \frac{1}{2} \times (\Delta Q) \times M^2 \quad (6.4)$$

where ΔQ is the capacity change rate and M is the queue duration.

Note that the total system-wide waiting time is the area between the cumulative curves A and D .

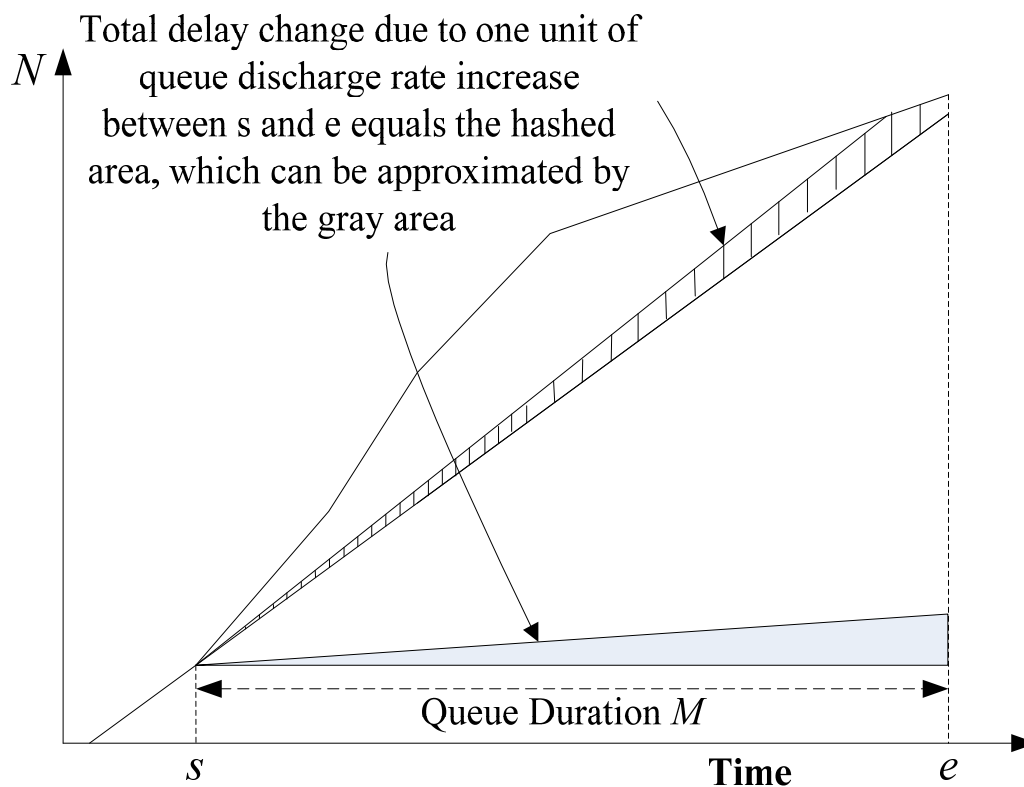


Figure 6.3- Total delay change for one unit of discharge rate change for the entire congestion duration.

The change of total waiting time (a change in queue discharging rate) can be approximated by

$$\frac{1}{2} \times [D'(e) - D(e)] \times (e - s) \approx \frac{1}{2} \times (\Delta Q) \times (e - s) \times (e - s) = \frac{1}{2} \times (\Delta Q) \times M^2 \quad (6.5)$$

where $D'(e) - D(e)$ is the height of the “change” hashed triangular, which can be roughly approximated by $(\Delta Q) \times (e - s)$.

$M = e - s$ corresponds to the width of the “change” triangular.

Proposition 2: If the variations of queue discharge rate Q is assumed to be a log-normal variable, that is, $\Delta Q \sim LN(\mu_Q, \sigma_Q^2)$, then the total waiting time variability can be described by

$$\Delta W \sim LN\left(\ln\left(\frac{1}{2}M^2\right) + \mu_Q, \sigma_Q^2\right) \quad (6.6)$$

Proof:

According to property 4, since ΔQ is a log-normal variable,

$\Delta W = \frac{1}{2} \times (\Delta Q) \times M^2$ also follows a log-normal distribution

$$\Delta W \sim LN\left(\ln\left(\frac{1}{2}M^2\right) + \mu_Q, \sigma_Q^2\right).$$

End of Proof.

A useful implication from proposition 2 is that the entire congestion duration of a queue is the leading factor that determines delay variability, and a longer queue duration

leads to higher variability. In other words, travel time reliability is more sensitive to *queue duration* than *mean queue length*. As illustrated in Figure 6.4(a), two congestion periods have the same duration length ($M_1 = M_2$) but different total waiting times ($W_1 < W_2$), the derived analytical formula in equation (6.6) indicate that their waiting time variability has the same magnitude if the queue discharge rates follow the same distribution. On the other hand, even the first congestion period in Figure 6.4 (b) has a smaller waiting time than the second congestion period ($W_1 < W_2$), and the travel time unreliability associated with the first period is higher because $M_1 > M_2$.

Recently, many research efforts (i.e., Bates et al., 2003) are devoted to using empirical data to calibrate the relationships between Coefficient of Variation (CV) and Congestion Index (CI) as equation (6.7). As shown in our analytical derivation, congestion duration M should have a stronger correlation with the coefficient of variation, compared to the average travel time.

$$CV = \gamma CI^\theta \quad (6.7)$$

where CV = Standard deviation / mean of travel time

CI = Mean travel time / Free-flow travel time.

γ = Constant or scale factor

θ = elasticity coefficient for congestion index

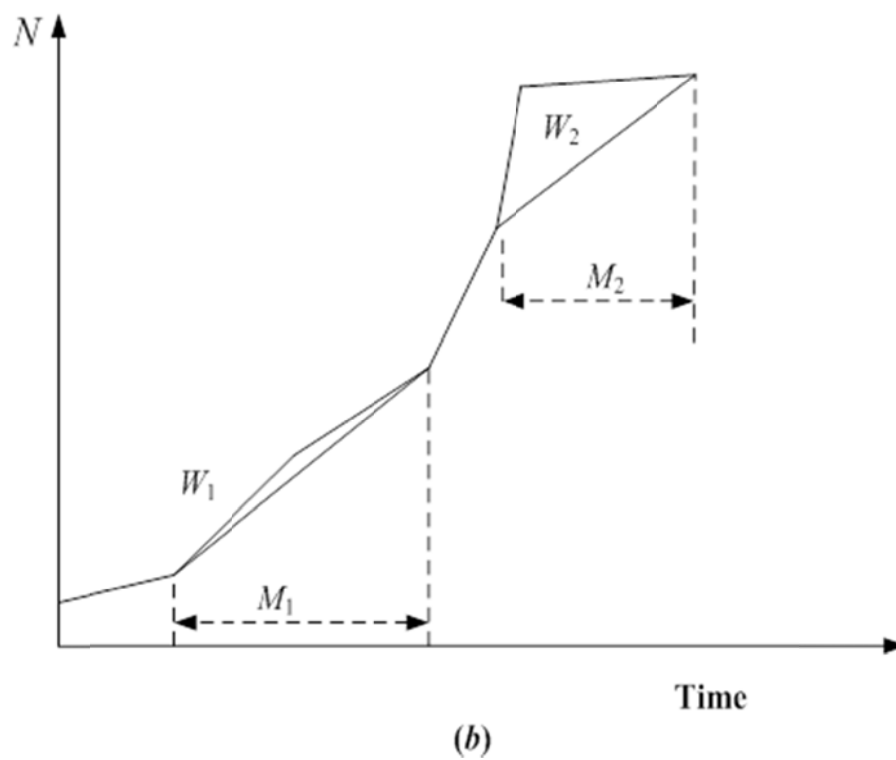
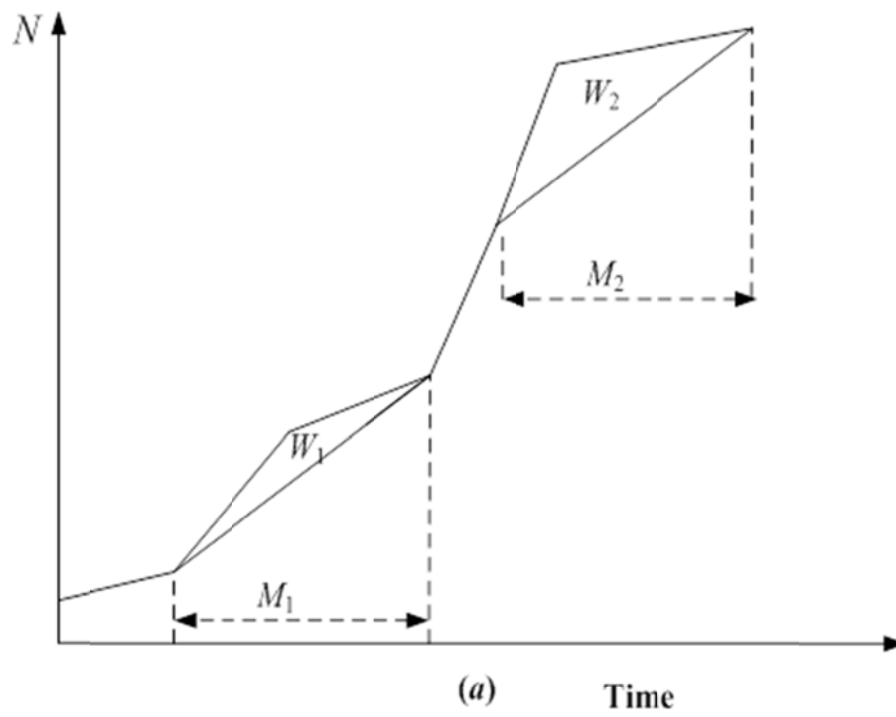


Figure 6.4- Waiting time variability in different queue duration cases.

Considering both stochastic incoming flow and queue discharge rates, a nature extension is to incorporate stochastic demand into the above framework using the following generalized flow change formula.

$$\Delta W = \frac{1}{2} \times (\Delta Q + \Delta R) \times M^2 \quad (6.8)$$

where ΔR is the change of incoming demand/flow.

Although there are approximation models available for representing the sum of two log-normal variables as a single log-normal variable, according to property 6, the random distribution $\Delta Q + \Delta R$ does not have a closed-form formula for the resulting μ and σ .

6.5 Deriving Time-Dependent Delay Variability Distribution

The above analysis calculates the waiting time variability for the entire congestion period over a long analysis horizon, and it is also desirable to quantify the time-dependent delay variability for any given timestamp within the congestion period, in order to estimate and further control the travel time variability under a dynamic and stochastic environment in a finer time resolution.

In the following discussion, we consider a point queue system with a time-dependent demand profile as shown in Figure 6.5.

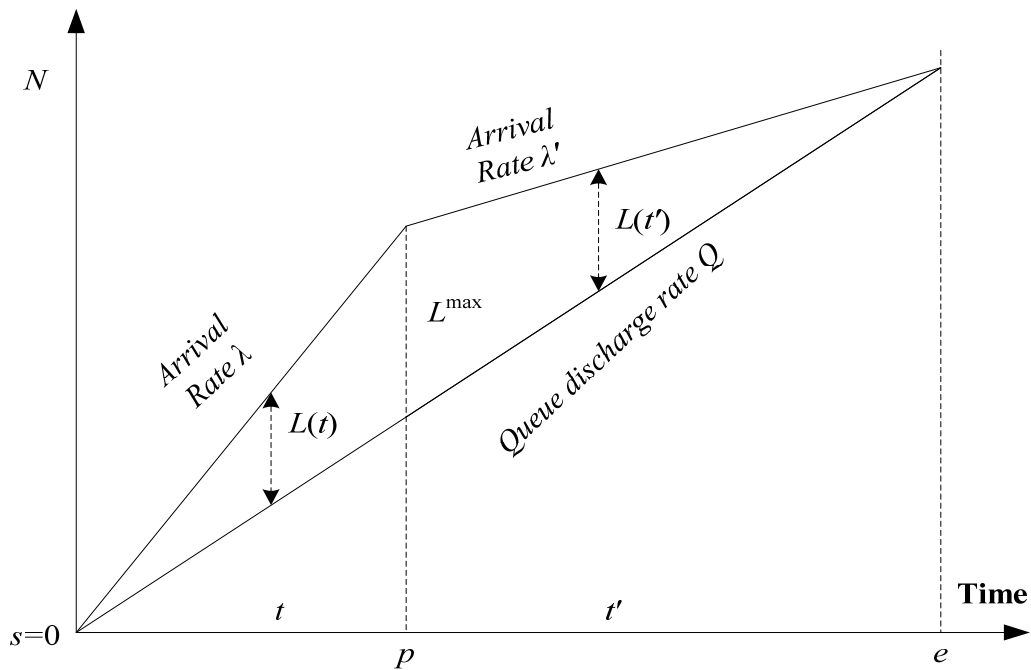


Figure 6.5- Time-dependent queuing evolution diagram.

From time 0 to time e , each realization of stochastic queue discharge rates remains as constant Q . From time 0 to time p , the arrival rate λ is higher than outgoing flow rate Q , leading to an increasing queue length profile up to L^{\max} .

In this first congestion building up period, the queue length at time t is

$$L(t) = (\lambda - Q) \times t \quad (6.8)$$

The time-dependent waiting time for vehicles arriving at the stop bar of the queue system is the prevailing queue length $L(t)$ divided by the (constant) queue discharge rate Q :

$$W(t) = \frac{L(t)}{Q} = \frac{(\lambda - Q)}{Q} \times t = \left(\frac{\lambda}{Q} - 1\right) \times t = \frac{\lambda}{Q} \times t - t \quad (6.9)$$

Proposition 3: If incoming flow rate λ and queue discharge rates Q are assumed to be log-normal variables, then delay $W(t)$ at time t is a shifted lognormal distributed variable.

Proof: If both λ and Q are log-normally distributed, then their ratio is also a log-normal variable, according to Properties 1 and 2, $\frac{\lambda}{Q} \sim LN(\mu_\lambda - \mu_Q, \sigma_\lambda^2 + \sigma_Q^2)$.

By further considering the multiplier of time index t ,

$$W(t) \sim LN(\ln t + \mu_\lambda - \mu_Q, \sigma_\lambda^2 + \sigma_Q^2) - t.$$

End of Proof.

Based on the above proposition, the time-varying or time-of-day delay variability $W(t)$ is still determined by the underlying demand and capacity randomness, and one can analytically estimate the mean and variance of $W(t)$ for given stochastic demand and flow distributions. Furthermore, as the parameter μ for random variable $W(t)$ increases as congestion time t advances (that is, through function of $\ln(t)$), the time-dependent delay variability rises when traffic congestion gets worse.

In this congestion dissipation period from time p to time e , the arrival rate λ' is lower than queue discharge flow rate Q , so the queue length is gradually reduced from L^{\max} to 0. The corresponding queue length at time t' is

$$L(t') = L^{\max} + (\lambda' - Q) \times (t' - p) \quad (6.10)$$

and the delay at time t' is

$$\begin{aligned} W(t') &= \frac{L(t')}{Q} = \frac{L^{Max}}{Q} + \frac{\lambda' - Q}{Q} \times (t' - p) = \frac{\lambda - Q}{Q} p + \frac{\lambda' - Q}{Q} \times (t' - p) \\ &= \frac{\lambda}{Q} p + \frac{\lambda'}{Q} \times (t' - p) - p - (t' - p) \end{aligned} \quad (6.11)$$

There are three elements in equation (6.11), it is easy to show that random variables $\frac{\lambda}{Q} p$ and $\frac{\lambda'}{Q} \times (t' - p)$ are log-normally distributed, but $W(t')$ does not have a closed-form expression as the sum of log-normal variables. As $\frac{\lambda}{Q} p$ and $\frac{\lambda'}{Q} \times (t' - p)$ share the same random variable Q in the denominator, these two variables is more likely to be statistically correlated. As a result, the numerical approximation formulas suitable for Property 6 are not applicable here due to the violation of independence assumption.

6.6 Calibrating Probability Distributions

Recent empirical research (Brilon et al., 2005; Jia et al., 2010) indicates that highway capacity can be characterized as a random variable. In this section, we use a data set for a bottleneck at the I880 freeway corridor, San Francisco Bay Area to calibrate statistical distributions of capacity (long-term capacity C in the static traffic assignment model and queue charge rate Q in the point-queue model) and incoming demand flow rates. To calibrate queue discharge rates, the volume, speed and occupancy data are extracted from the PeMS database covering from 01/01/2007 to 09/30/2008. To verify the travel time variability prediction results, the flow volume and travel time index

measures are collected and processed from 03/01/2009 to 07/30/2009 between 8AM and 9AM (morning peak hour).

The 15-minute queue discharge rate after the breakdown (Figure 6.6) is provided by Jia et al. (2010). We can obtain a shifted log-normal distribution with the following probability density function (Figure 6.7). Figure 6.8 shows the log-normal probability density function for demand flow rate distributions. The detailed definitions of prebreakdown flow rates and queue discharge rates are provided in the paper by Jia et al. (2010).

$$f_X = (r; \mu, \sigma) = \frac{1}{(x-\gamma)\sigma\sqrt{2\pi}} e^{-\frac{[\ln(x-\gamma)-\mu]^2}{2\sigma^2}}, \quad x > 0 \quad (6.12)$$

where

x = random variable

γ = the shift parameter

μ = the mean of the variable's natural logarithm, and

σ = the standard deviation of the variable's natural logarithm.

In the last row of Table 6.1, the measure of travel time index (TTI) is defined as a ratio of travel time /FFTT, as FFTT is a constant, according to Property 4, TTI can be shown as a log-normally distributed random variable. Many empirical studies (Emam and Al-Deek, 2006; Oh and Chung, 2006) shows that the log-normal distribution is a good representation of travel time variations.

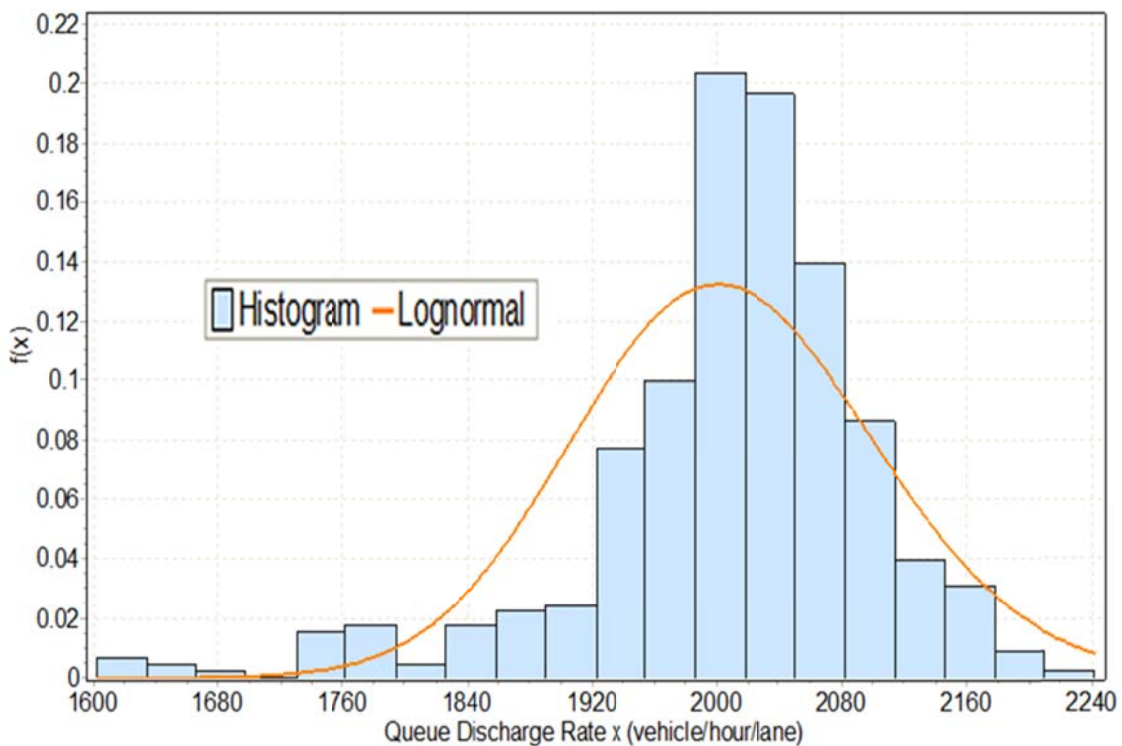


Figure 6.6- Log-normal probability density function for queue discharge rate.

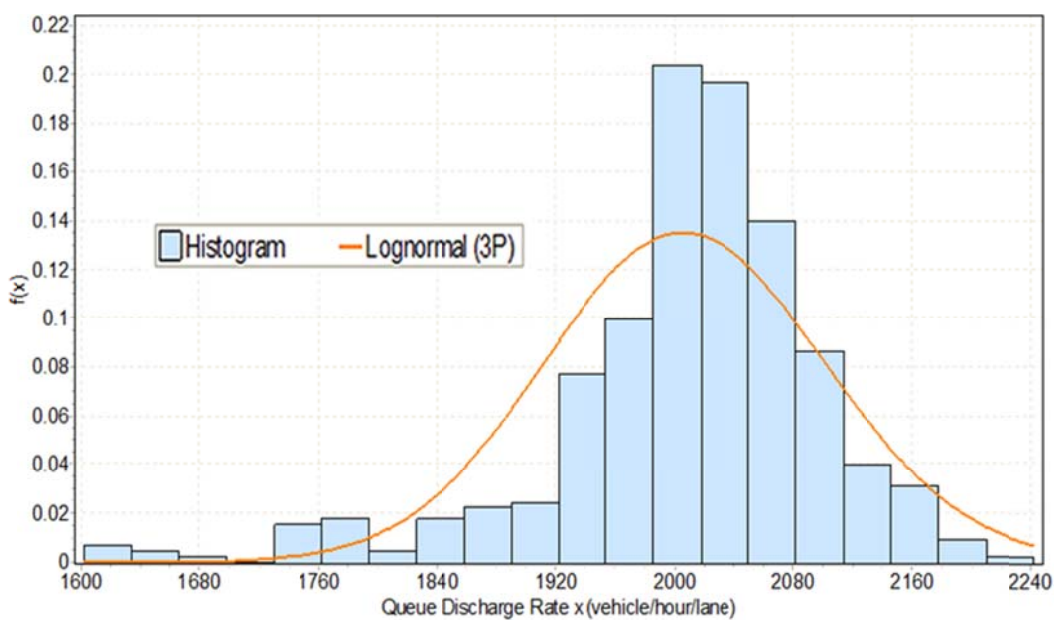


Figure 6.7- Shifted Log-normal probability density function for queue discharge rate.

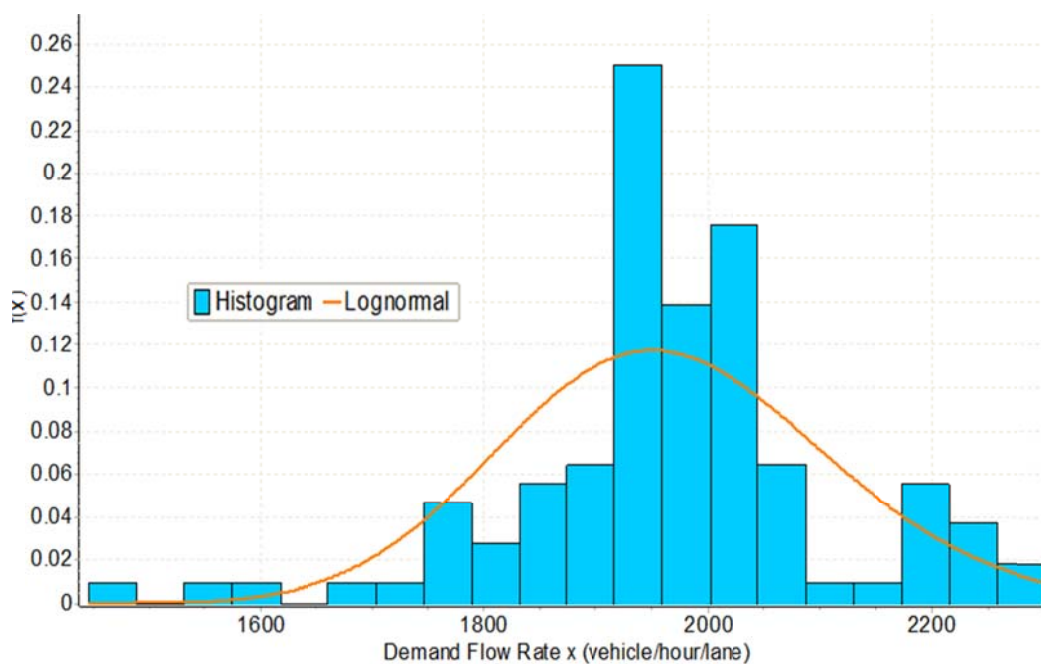


Figure 6.8- Log-normal probability density function for demand flow rate distributions.

Table 6.1- Summary of calibration results.

	μ	σ	Shift γ	Kolmogorov Smirnov statistics
Log-normal distribution for 15-min queue discharge rate (veh/h/ln)	7.603	0.048	0	0.133
Shifted log-normal distribution for 15-min queue discharge rate (veh/h/ln)	8.356	0.022	-2250	0.127
Shifted log-normal distribution for hourly demand (veh/h/ln)	7.581	0.074	0	0.143
Log-normal distribution for travel time index	0.081	0.116	0	0.102

Shown in Figure 6.9, the overall travel time distribution can be viewed as a mixture of two modes of traffic conditions: free-flow traveling state ($TTI < 1.16$) vs. congested state ($TTI > 1.16$). A multistate travel time reliability model is recently proposed by Guo et al. (2010) to represent the travel time variability pattern through a mixture of two normally distributed components.

In the following discussion, we focus on how to construct a travel time distribution for the congested state. When the incoming demand does not exceed the likely lower bound of normal capacity (e.g., less than [mean travel time – 2 standard deviations]), vehicles can still drive at a free-flow speed without encountering any delays. To capture the demand variations under congested conditions, Figure 6.10 extracts the high-demand region from Figure 6.8, and then estimates the corresponding parameters of a log-normal model.

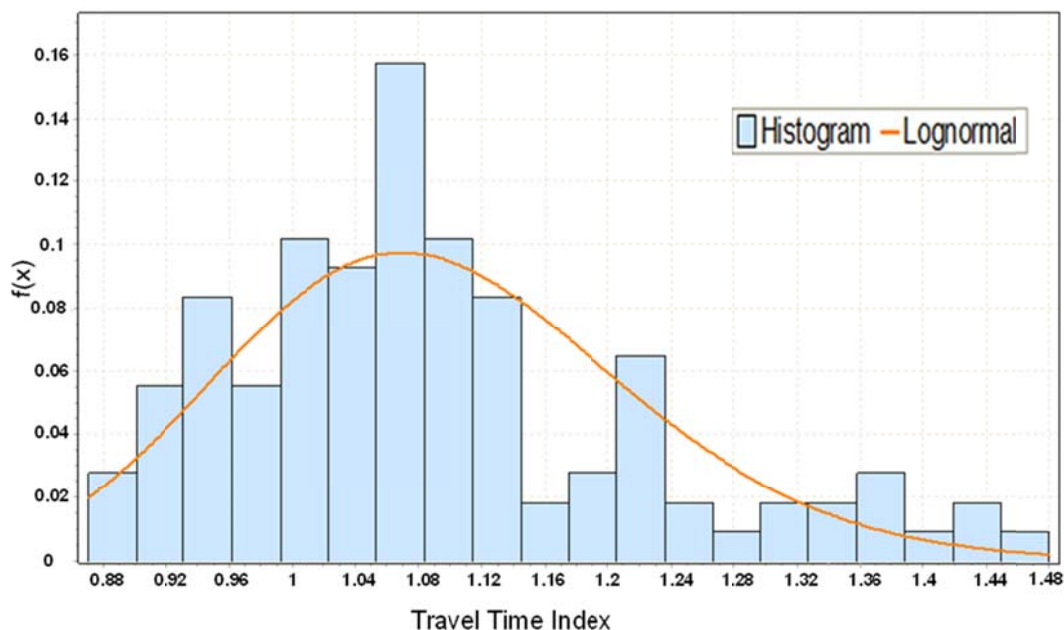


Figure 6.9- Log-normal probability density function for travel time index distribution.

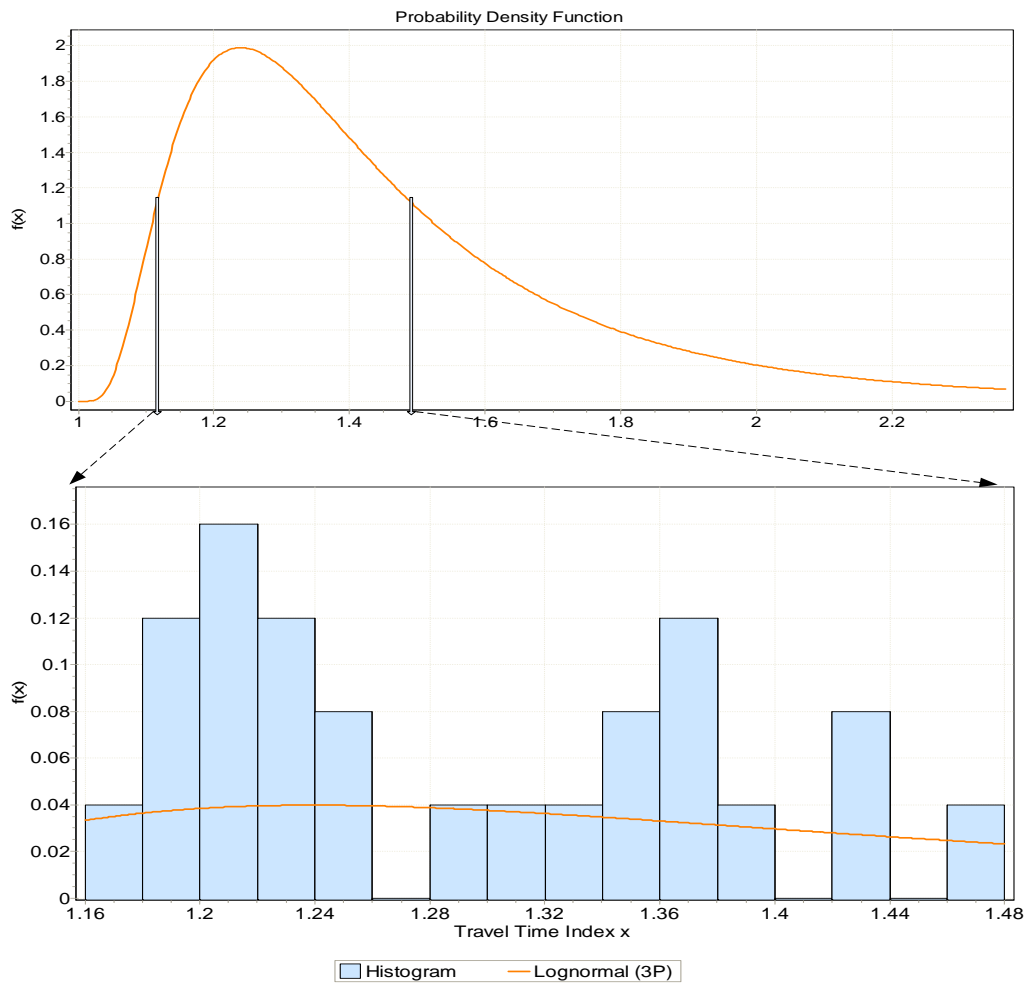


Figure 6.10- Complete PDF for predicted travel time variations.

mode = 1.24, mean = 1.47, standard deviation = 0.35, coefficient of variation = 0.24.

Furthermore, according to the recommended BPR parameters in Highway Capacity Manual, we select $\alpha = 0.39$, $\beta = 6.3$ for Interstate 880, which is a freeway facility with a free-flow speed of 75 miles per hour (or 120 km per hour).

By using $TTI \sim LN(\ln(\alpha) + \beta \times (\mu_v - \mu_c), \beta^2 \times (\sigma_v^2 + \sigma_c^2)) + 1$, which is adapted from equation (6.2), we can analytically derive the following parameters for the resulting log-normal distribution for congested traffic conditions. $\mu = -0.983$, $\sigma = 0.67$, shift $\gamma = 1$.

The corresponding PDF over the entire possible region of TTI (from 1.0 to 2.2) is plotted in the top graph of Figure 6.10. The bottom plot specifically compares the observed TTI and derived TTI from our proposed model in the congestion region (TTI from 1.16 to 1.48).

We have a few remarks based on the above preliminary estimation results. First, the analytically derived log-normal distribution can reasonably resemble the variability trend in travel time distributions. On the other hand, the real-world travel time variations might come from other sources such as weather conditions, work zones and special events, while our proposed model only focuses on the randomness sources in terms of capacity and demand fluctuations. It should be also noticed that the theoretical travel time index distribution has a shift parameter of 1.0 (according to the underlying BPR function), which cannot reproduce “speeding” travel time index < 1 .

6.7 Summary

This chapter investigates a fundamental problem of quantifying travel time variability from its root sources: stochastic capacity and demand variations that follow commonly used log-normal distributions. A volume-to-capacity ratio-based travel time function and a point queue model are used to demonstrate how day-to-day travel time variability can be explained from the underlying stochastic demand and capacity distributions. This chapter also uses simplified peak-hour demand profiles to estimate time-of-day or time-dependent travel time variability functions at traffic bottlenecks. The proposed models provide theoretically rigorous and practically useful tools to understand

the causes of travel time unreliability and evaluate the system-wide benefit of reducing demand and capacity variability.

In summary, this chapter now provides a method to derive reliability in travel demand models that use BPR functions, based on distributions of demand and capacity. Our future research plans to characterize those distributions based on facility type and FTTT, and we also need to test the bottleneck theory with point queue and validate it with empirical data. Additionally, it is necessary to find appropriate approximate solutions when closed form ones do not exist.

CHAPTER 7

CONCLUSIONS AND FUTURE RESEARCH NEEDS

7.1 Overall Conclusions

This dissertation presents several methodological advances addressing a series of important research questions for modeling traveler behavior under stochastic supply and demand and quantifying travel time variability from stochastic capacity distributions.

This dissertation addresses a series of critical and challenging issues in evaluating the benefits of Advanced Traveler Information Strategies under different uncertainty sources. In particular, three major modeling approaches are integrated in this dissertation, namely: mathematical programming, dynamic simulation and analytical approximation. The proposed models can: (1) represent static-state network user equilibrium conditions, while considering knowledge quality and accessibility of traveler information systems under both stochastic capacity and stochastic demand distributions; (2) characterize day-to-day learning behavior with different information groups under stochastic capacity; and (3) quantify travel time variability from stochastic capacity distribution functions on critical bottlenecks.

In the **planning-level methodology for evaluating traveler information provision strategies** under stochastic capacity conditions, a new nonlinear optimization-

based analysis method is proposed for incorporating modeling components on stochastic capacity, travel time performance functions and different degrees of traveler knowledge in an ATIS environment. The proposed method categorizes commuters into two classes: (1) those with access to perfect traffic information every day, and (2) those with knowledge of the expected traffic conditions across different days. Using a gap function framework (for describing the user equilibrium under different information availability), a mathematical programming model is formulated to describe the route choice behavior of the perfect information (PI) and expected travel time (ETT) user classes under stochastic day-dependent travel time. Driven by an operational algorithm suitable for large-scale networks, the model was applied to a simple corridor and medium-scale networks to illustrate the effectiveness of traveler information under stochastic capacity conditions.

A multiday multiclass traffic equilibrium analysis model is further presented for quantifying traffic information provision benefits under stochastic demand and capacity conditions. This study offers a powerful modeling option to evaluate how travelers with different information accessibility adjust their route choice patterns when various sources of travel time uncertainty, e.g., stochastic demand fluctuations and different levels of information quality, are altered.

The **day-to-day traffic simulation and traveler learning framework** focuses on how to seamlessly integrate stochastic capacity models and compatible route choice models within a stochastic capacity environment. These enhancements have been prototyped and tested through a mesoscopic DTA simulator and could be easily incorporated into other dynamic traffic simulation/analysis models as well.

This dissertation also investigates a fundamental problem of **quantifying travel time variability from its root sources**: stochastic capacity and demand variations that follow commonly used log-normal distributions. A set of analytical models are proposed for quantifying travel time variability from its root sources: stochastic capacity and demand variations. A volume-to-capacity ratio-based travel time function and a point queue model are used to demonstrate how day-to-day travel time variability can be explained and approximated from the underlying stochastic demand and capacity distributions.

From this dissertation, **the key findings related to ATIS strategy evaluation** are summarized below.

1. Under stochastic link capacity, users equipped with ATIS can reduce both their mean travel time and travel time variability across different days, compared to travelers who rely only on knowledge of average traffic conditions.

2. Equipping a small percentage of users with access to travel information can help the system better balance flow between congested and uncongested routes, and fully utilize available unused capacity.

3. Better system-wide benefits regarding travel time saving and reliability are achieved compared to the no information or limited information cases until reaching a saturated market penetration rate.

4. An appropriate tolling or real-time information service scheme may encourage travelers to switch from a congested to a less congested route under stochastic link capacity conditions, and it can improve both travel time and its reliability. On the other

hand, the generalized travel time for users is increased due to an inclusion of equivalent travel time and user cost associated with charged toll.

5. In terms of reducing travel time variability, demand smoothing strategies produce the most effective variability reductions, followed by traveler information accessibility enhancement strategies.

7.2 Research Contributions

7.2.1 Theoretical Contributions

Conventional network analysis models typically focus on finding a single-day steady-state equilibrium solution by assuming fixed demand and constant capacity. To systematically quantify the system-wide mobility and reliability impact of traveler information provision strategies, this study presents a novel multiday multiclass (in terms of information use) equilibrium model with stochastic capacity and stochastic demand.

The proposed methodology can: (1) model complexity and uncertainty in the dynamic traveler adaptive learning behavior; (2) provide an effective and efficient quick-response tool to decision-makers to understand the uncertainty by using advanced modeling tools with minimal data requirements to perform; and (3) generate new knowledge to address the fundamental research challenges in traffic congestion mitigation application domains.

The proposed approach can use peak-hour demand and demand profiles to analytically estimate time-of-day or time-dependent travel time variability functions at traffic bottlenecks. These models provide theoretically rigorous and practically usefully

tools to understand the causes of travel time unreliability and evaluate the system-wide benefit of reducing demand and capacity variability.

7.2.2 Practical Contributions

In addition to providing investigation results to the above theoretical questions, this study will contribute to the current state of practice in the following aspects.

It will help traffic planners to systematically quantify the impact of traffic mitigation strategies (such as pretrip and en-route information) under stochastic capacity. It will model predictive information and day-to-day evolution which result from user decision and network dynamics.

In particular, the study described in this dissertation provides the following contributions to the existing DTA models:

- A new set of day-to-day learning and route choice models which enables a realistic representation of drivers' route selection process and effectively stabilizes overall network flow under stochastic capacity conditions.
- Practical modeling guidelines which are effective for the enhanced DTA model to simulate various capacity-enhancing design, operational, and technological strategies.

In this study, methodological and analytic enhancements to existing dynamic traffic simulation models have been proposed and implemented for the purpose of increasing the realism and sensitivity of the models in simulating real-world network and the effects of strategy applications.

7.3 Future Research Needs

With enhanced traffic modeling formulations under stochastic capacity and demand, this dissertation illustrates considerable potential for generalizing the modeling framework into the field of traffic state estimation and large-scale planning applications. On the other hand, these innovative methods still require further investigation into numerous issues, especially in the following dimensions:

1) **Modeling nonrecurring congestion conditions.** Quantifying benefits of traveler information provision strategies in a stochastic environment creates a great need for rigorous formulations and practical solution procedures for the traffic network assignment problem. It is desirable to further enhance the proposed model to systemically evaluate the value of information and reliability associated with stochastic demand fluctuations and different levels of information quality, under both recurring and nonrecurring congestion conditions. Without considering the impact of nonrecurring delay sources, the benefits of ATIS strategies can be significantly underestimated.

2) **Efficient variance reduction methods.** The computational challenges introduced by the proposed method stem from the sampling-based representation of stochastic capacity distributions. Future research plans to use variance reduction techniques, such as importance sample, to reduce the required sample size, and apply distributed computing techniques, e.g., cloud computing, to improve the computational efficiency within a nonshared memory environment.

3) **Incorporating reliability-related route choice models.** The proposed model can also be enhanced to consider more realistic route choice utility functions involving both expected travel time and travel time reliability. In this case, a new path finding

algorithm using multiday samples should also be developed to account for the potential link travel time correlations due to stochastic variations in origin-to-destination demand patterns.

4) Quantifying facility-dependent and state-dependent travel time variability distributions. Regarding identification of the location and impact of system bottlenecks, one future research plans to characterize the travel time distributions based on facility type and different travel conditions (e.g., free-flow vs. congested). In particular, a multistate travel time reliability model should be suitable to represent the travel time variability pattern through a mixture of multiple normally or log-normally distributed components (in terms of stochastic capacity and demand). Additionally, it is necessary to find appropriate approximate solutions when closed form ones do not exist.

APPENDIX

LIST OF TERMS

ATIS	Advanced Traveler Information Systems
ATMS	Advanced Traffic Management Systems
BPR	Bureau Of Public Roads
DTA	Dynamic Traffic Assignment
ETT	Expected Travel Time
EV	Expected Value
FFTT	Free-Flow Travel Time
ITS	Intelligent Transportation Systems
KKT	Karush-Kuhn-Tucker
LETP	Least Expected Travel Time Path
LTP	Least Travel Time Path
MOE	Measure Of Effectiveness
MP	Market Penetration
MSA	Method Of Successive Averages
OD	Origin-Destination
PDF	Probability Density Function

PI	Perfect Information
SD	Standard Deviation
SUE	Stochastic User Equilibrium
TI	Traveler Information
<i>TSD</i>	Travel Time Standard Deviation
TTF	Travel Time Function
TTI	Travel Time Index
UE	User Equilibrium
VMS	Variable Message Signs
VOT	Value Of Time

REFERENCES

- Aitchison, J., and Brown, J.A.C. (1957). *The Lognormal Distribution*, Cambridge University Press, Cambridge UK.
- Ban, X., Li, Y., and Margulici, J.D. (2009). "Optimal Use of Changeable Message Signs for Displaying Travel Times." PATH Research Report ITS-PRR-2009, Institute of Transportation studies, University of California, Berkeley.
- Bar-Gera, H. (2001). "Transportation Network Test Problems." Ben-Gurion University of Negev.
- Bates, J., Black, I., and Fearnon, J. (2003). "Frameworks for Modelling the Variability of Highway Journey Times." Report to the Department for Transport, United Kingdom.
- Bonneson, J., Nevers, B., Zegeer, J., Nguyen T., and Fong T. (2005). "Guidelines for Quantifying the Influence of Area Type and Other Factors on Saturation Flow Rate." Final Report, Florida Department of Transportation.
- Brilon W., Geistefeldt J., and Regler M. (2005). "Reliability of Freeway Traffic Flow: A Stochastic Concept of Capacity." *Proceedings of the 16th International Symposium on Transportation and Traffic Theory*, College Park, Maryland, 125-144.
- Brownstone, D., and Small, K.A. (2004). "Valuing Time and Reliability: Assessing the Evidence from Road Pricing Demonstrations." *Transportation Research, PartA*, Vol. 39, pp. 279–293.
- Brilon W., Geistefeldt J., and Zurlinden, H. (2007). "Implementing the Concept of Reliability for Highway Capacity Analysis." *Transportation Research Record: Journal of the Transportation Research Board*, 2027: 1-8.
- Cambridge Systematics (2005). "Traffic Congestion and Reliability: Trends and Advanced Strategies for Congestion Mitigation." Federal Highway Administration.
- Chang, G-L., Mahmassani, H.S., and Herman, R. (1985). "Macroparticle Traffic Simulation Model to Investigate Peak-Period Commuter Decision Dynamics."

- Transportation Research Record: Journal of the Transportation Research Board*, No. 1005, pp. 107- 121.
- Chen, A., Yang, H., Lo, H.K., and Tang, W.H. (2002). "Capacity Reliability of a Road Network: An Assessment Methodology and Numerical Results." *Transportation Research*, 36B, 225-252.
- Chen, R. B., and Mahmassani, H.S. (2004). "Travel Time Perception and Learning Mechanisms in Traffic Networks." *Transportation Research Record: Journal of the Transportation Research Board*, No. 1894, Transportation Research Board of the National Academies, Washington D.C., pp. 209-221.
- Chorus, C.G., Molin, E.J.E., and van Wee, G.P. (2006). "Use and Effects of Advanced Traveler Information Services (ATIS) - a Review of the Literature." *Transport Reviews*. 26. no. 2.127-149.
- Clark, S.D., and Watling, D.P. (2005). "Modelling Network Travel Time Reliability Under Stochastic Demand." *Transportation Research Part B* 39 (2), 119–140.
- de Palma, A., and Picard, N. (2005). "Route Choice Decision Under Travel Time Uncertainty." *Transportation Research Part A* 39A, 295-324.
- Dong, J., and Mahmassani, H.S. (2009). "Flow Breakdown, Travel Reliability and Real-time Information in Route Choice Behavior." *Proceedings of the 18th International Symposium on Transportation and Traffic Theory*.
- Elefteriadou, L., Roess, R.P., and Mcshane, W.R. (1995). "Probabilistic Nature of Breakdown at Freeway Merge Junctions." *Transportation Research Record: Journal of the Transportation Research Board*, No. 1484, Transportation Research Board of the National Academies, Washington D.C.
- Emam, E., and Al-Deek, H. (2006). "Using Real-Life Dual-Loop Detector Data to Develop New Methodology for Estimating Freeway Travel Time Reliability." *Transportation Research Record*, 1959, pp.140-150.
- Ghali, M., and Smith, M. (1995). "A Model for the Dynamic System Optimum Traffic Assignment Problem." *Transportation Research* 29B, 155-170.
- Guo, F., Park, S., and Rakha, H. (2010). "A Multi-state Travel Time Reliability Model." *Transportation Research Record: Journal of the Transportation Research Board*, Transportation Research Board of the National Academies, Washington D.C.
- HCM (Highway Capacity Manual) (2000). *Transportation Research Board*, National Research Council, Washington, D.C.

- Hu, T., and Mahmassani, H. S. (1997). "Day-to-Day Evolution of Network Flows Under Real-time Information and Reactive Signal Control." *Transportation Research, Part C*, Vol. 5, No. 1, pp. 51-69.
- Jha, M., Madanat S., and Peeta, S. (1998). "Perception Updating and Day-to-Day Travel Choice Dynamics in Traffic Networks with Information Provision." *Transportation Research, Part C*, Vol. 6, No. 3, pp. 189-212.
- Jia, A., Williams, B.M., and Roupail, N.M. (2010). "Identification and Calibration of Site Specific Stochastic Freeway Breakdown and Queue Discharge." *Transportation Research Record: Journal of the Transportation Research Board*, Transportation Research Board of the National Academies, Washington D.C.
- Jia, A., Zhou, X., Li, M., Roupail, N.M., and Williams, B.M. (2010). "Incorporating Stochastic Road Capacity into a Day-to-Day Traffic Simulation and Traveler Learning Framework: Model Development and Case Study." Accepted for Presentation and Publication in the *Transportation Research Record: Journal of the Transportation Research Board and 90th Annual Meeting*.
- Kuehne, R.D., and Anstett, N. (1999). "Stochastic Methods for Analysis of Traffic Pattern Formation." *Proceedings of the 14th International Symposium on Transportation and Traffic Theory*, Jerusalem.
- Lam, T., and Small, K.A. (2001). "The Value of Time and Reliability: Measurement from a Value Pricing Experiment." *Transportation Research Part E*, Vol. 37, pp. 231–251.
- Lam, W.H.K., Shao, H., and Sumalee, A. (2008). "Modeling Impacts of Adverse Weather Conditions on a Road Network with Uncertainties in Demand and Supply." *Transportation Research Part B* 42(10), 890-910.
- Lighthill, M.J., and Whitham, G.B. (1955). "On Kinematic Waves II: A Theory of Traffic Flow on Long Crowded Roads." *Proceedings of the Royal Society*, London Ser. A., Vol. 229, No. 1178, 1955, pp.317-345.
- Lo, H. K., and Chen, A. (2000). "Reformulating the General Traffic Equilibrium Problem via a Smooth Gap Function." *Mathematical and Computer Modeling* 31(2/3), 179-195.
- Lo, H K., Luo, X. W., and Siu, W. Y. (2006). "Degradable Transport Network: Travel Time Budget of Travelers with Heterogeneous Risk Aversion." *Transportation Research Part B*, 40(9):792–806.
- Lo, H. K., and Tung, Y. K. (2003). "Network with Degradable Links: Capacity Analysis and Design." *Transportation Research Part B*, 37(4): 345–363.

- Lorenz, M., and Elefteriadou, L. (2000). "A Probabilistic Approach to Defining Freeway Capacity and Breakdown." *Proceedings of the 4th International Symposium on Highway Capacity*, pp. 84-95, TRB-Circular E-C018, Transportation Research Board, Washington D.C.
- Lu, C-C., Mahmassani, H.S., and Zhou, X. (2009). "Equivalent Gap Function-Based Reformulation and Solution Algorithm for the Dynamic User Equilibrium Problem." *Transportation Research Part B*. 43, No. 3, pp. 345-364.
- Mahmassani, H. S. (1984). "Uncertainty in Transportation Systems Evaluation: Issues and Approaches." *Transportation Planning and Technology*, 9, pp. 1-12.
- Mahmassani, H. S. (2001). "Dynamic Network Traffic Assignment and Simulation Methodology for Advanced System Management Application." *Networks and Spatial Economics*, Vol. 1, pp. 267-292.
- Mahmassani, H.S., and Herman, R. (1990). "Interactive Experiments for the Study of Trip Maker Behaviour Dynamics in Congested Commuting Systems." *Developments in Dynamic and Activity-Based Approaches to Travel Analysis*, Gower, Aldershot, England, pp. 272-298.
- Minderhoud, M.M., Botma, H., and Bovy, P.H.L. (1997). "Roadway Capacity Estimation Methods Explained and Assessed." *Transportation Research Record: Journal of the Transportation Research Board*, No. 1572, Transportation Research Board of the National Academies, Washington D.C.
- Nakayama, S. (2007). "Stochastic Network Equilibrium Model Under Uncertain Demand." *Proceedings of the 6th Triennial Conference on Transportation Analysis*, Phuket, Thailand.
- Ng, M.W., and Waler, S.T. (2010). "A Computationally Efficient Methodology to Characterize Travel Time Reliability Using the Fast Fourier Transform." *Transportation Research Part B: Methodological*, In Press.
- Noland, R. B., and Polak, J. W. (2002). "Travel Time Variability: A Review of Theoretical and Empirical Issues." *Transport Reviews*, 22 (1), pp. 39-54.
- Noland R.B., Small, K.A., Koskenoja, P.M., and Chu X. (1998). "Simulating Travel Reliability." *Regional Science and Urban Economics*, Vol. 28, Issue 5, pp. 535-564.
- Okamura, H., Watanabe, S., and Watanabe, T. (2000). "An Empirical Study on the Capacity of Bottlenecks on the Basic Suburban Expressway Sections in Japan." *Proceedings of the 4th International Symposium on Highway Capacity*, pp. 120-129, TRB Circular E-C018, Transportation Research Board, Washington D.C.

- Oh, J. S., and Chung, Y. (2006). "Calculation of Travel Time Variability from Loop Detector Data." *Transportation Research Record: Journal of the Transportation Research Board*, 1945, 12-23.
- Peeta, S., and Ziliaskopoulos, A. (2001). "Foundations of Dynamic Traffic Assignment: The Past, the Present, and the Future." *Networks and Spatial Economics*, Vol.1, pp. 233-265.
- PeMS (2009). <<https://pems.eecs.berkeley.edu>> (January 10, 2009).
- Persaud, B., Yagar, S., and Brownlee, R. (1998). "Exploration of the Breakdown Phenomenon in Freeway Traffic." *Transportation Research Record: Journal of the Transportation Research Board*, No. 1634, Transportation Research Board of the National Academies, Washington D.C.
- Ramming, M.S. (2002). "Network Knowledge and Route Choice." PhD thesis, Department of Civil and Environmental Engineering, Massachusetts Institute of Technology.
- Richards, P. I. (1956). "Shock Waves on the Highway." *Operation Research*, Vol. 4, pp. 42-51.
- Sheffi, Y. (1985). *Urban Transportation Networks: Equilibrium Analysis with Mathematical Programming Methods*, NJ: Prentice-Hall.
- Shrinivasan, K.K., and Guo, Z. (2004). "Day-to-Day Evolution of Network Flows Under Route Choice Dynamics in Commuter Decisions." *Transportation Research Record: Journal of the Transportation Research Board*, No. 1894, Transportation Research Board of the National Academies, Washington D.C., pp. 198-208.
- SHRP 2 C05 Final Report. (2010). "Understanding the Contributions of Operations, Technology, and Design to Meeting Highway Capacity Needs." Strategic Highway Research Program (SHRP 2) Transportation Research Board National Research Council.
- Simon, H. A. (1995). "A Behavioral Model of Rational Choice." *Quarterly Journal of Economics*, Vol. 69, pp. 99-118.
- Smith, M. J. (1993). "A New Dynamic Traffic Model and the Existence and Calculation of Dynamic User Equilibrium on Congested Capacity-Constrained Road Networks." *Transportation Research Part B* 27(1), pp. 49-63.
- Sumalee, A., Connors, R.D., and Luathep, P. (2009). "Network Equilibrium Under Cumulative Prospect Theory and Endogenous Stochastic Demand and Supply." *Transportation and Traffic Theory: Golden Jubilee*, Springer, pp. 19-38.

- TransGuide (2009). <<http://www.transguide.dot.state.tx.us>> (January 10, 2009).
- Weijermars, W.A.M. (2007). "Analysis of Urban Traffic Patterns Using Clustering." T2007/3, TRAIL Thesis Series, The Netherlands.
- Yang, H. (1998). "Multiple Equilibrium Behavior and Advanced Traveler Information Systems with Endogenous Market Penetration." *Transportation Research Part B*, 32, pp. 205-218.
- Yang, H., Kitamura, R., Jovanis, P., Vaughn, K.M., and Abdel-Aty, M.A. (1993). "Exploration of Route Choice Behavior with Advanced Travel Information Using Neural Network Concept." *Transportation* 20, 199–223.
- Yang, H., Ma, O.S., and Wong, S.C. (1999). "New Observations on the Benefit Evaluation of Advanced Traveler Information Systems." *ITS Journal* 5, 251–274.
- Yang, H., and Meng, Q. (2001). "Modeling User Adoption of Advanced Traveler Information Systems: Dynamic Evolution and Stationary Equilibrium." *Transportation Research Part A: Policy and Practice*, Elsevier, 35(10), pages 895-912.
- Yin, Y., and Yang, H. (2003). "Simultaneous Determination of the Equilibrium Market Penetration and Compliance Rate of Advanced Traveler Information Systems." *Transportation Research, Part A*, 37, No.2, 165-181.
- Zhou, X., Mahmassani, H.S., and Zhang, K. (2008). "Dynamic Micro-assignment Modeling Approach for Integrated Multimodal Urban Corridor Management." Accepted for publication in *Transportation Research Part C*. 16, No. 2, pp. 167-186.
- Zhou, Z., and Chen, A. (2008). "Comparative Analysis of Three User Equilibrium Models Under Stochastic Demand." *Journal of Advanced Transportation*, 42(3), 239-263.